AD–A202 665

DTIC
SELECTED
19 JAN 1989
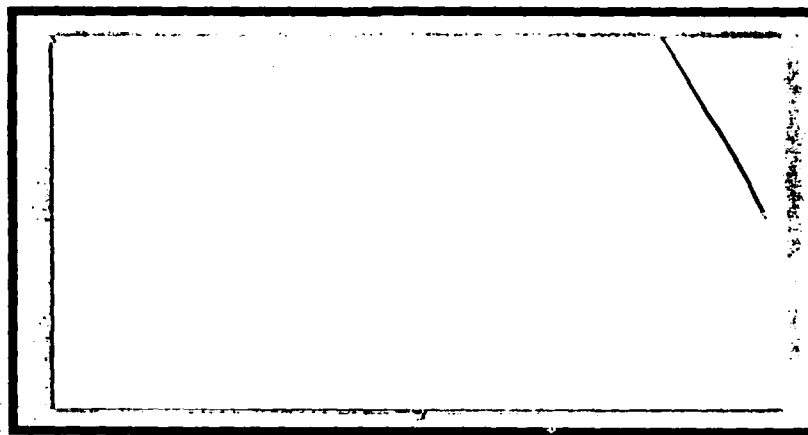E
D

DEPARTMENT OF THE AIR FORCE

AIR UNIVERSITY

# AIR FORCE INSTITUTE OF TECHNOLOGY

Wright-Patterson Air Force Base, Ohio

89    1  17  105

AFIT/GSO/ENP/88D-5

ANALYSIS OF SPACE-BASED LIDAR

FOR AIRCRAFT TRACKING

THESIS

Scott P. Simmons
Captain, USAF

AFIT/GSO/ENP/88D-5

DTIC
ELECTE
1 9 JAN 1989
E

AFIT/GSO/ENP/88D-5

ANALYSIS OF SPACE-BASED LIDAR

FOR AIRCRAFT TRACKING

THESIS

Presented to the Faculty of the School of Engineering

of the Air Force Institute of Technology

Air University

In Partial Fulfillment of the

Requirements for the Degree of

Master of Science in Space Operations

Scott P. Simmons, B.S.E.E.

Captain, USAF

November 1988

Approved for public release; distribution unlimited

## PREFACE

The purpose of this study was to examine the feasibility of using a laser radar or lidar to track aircraft from space. As a first step to a complete analysis, this thesis investigated the laser energy propagation as defined by the lidar range equation. The results, generated from a computer model, indicate that aircraft could potentially be tracked from a satellite in low-earth orbit. Further study is necessary to analyze more atmospheric conditions and specific hardware configurations.

I had a great deal of help from a number of people. I wish to thank Mr. Frank Jenks, Mr. Ron Rodney, Major Bob Hughes, and Mrs. Kris Larsen for their time, insight and patience in getting FASCODE to operate. Also, I wish to thank Captain Steve Spence for his superb insight and help on making the computer model "user-friendly". Also, many thanks go out to Captain Don Holland and Dr. Paul McManamon for their assistance and insights which added immeasurably to this thesis. I am indebted to and wish to thank Major T.S. Kelso (my reader) and Major David Stone (my advisor) for their assistance, corrections, suggestions and patience. Above all, I wish to thank my wife Pattie and my children, John, Becky, and Amanda for their understanding and sacrifice during the many months of work on this thesis.

<div align="right">Scott P. Simmons</div>

## Table of Contents

## List of Figures

# ABSTRACT

This study is a general analysis of the feasibility of tracking aircraft from space using a laser radar or lidar. The basis for the analysis is the lidar range equation. Specific hardware is not discussed.

A computer program was written to model the different parameters involved with the analysis. Atmospheric attenuation equations, which were developed from FASCODE data, define the atmospheric losses for two type of atmospheres (clear and haze). Other lidar range equation variables are either computed from input data or are directly inserted into the program for analysis. Four different types of lasers were investigated. The output data from the model was plotted to show the relationship of various input parameters with the power available at the receiver. The results indicate that lidar systems carried on low-earth orbiting satellites may have the potential to track aircraft. Further analysis is required to develop complete feasibility windows over a wider range of conditions.

# ANALYSIS OF SPACE-BASED
# LIDAR FOR AIRCRAFT TRACKING

## I.  Introduction

### Topic

This thesis is a study of the feasibility of using laser
radar or lidar to track aircraft from space.  For this
study, the term lidar will refer to an active sensor system
in which a laser is used to illuminate a target and the
reflection of the laser energy from that target is collected
and analyzed.  The analytical portion of this study is
centered around computer modeling of several key design
parameters of a lidar system.

### Background & Justification

The news in the United States during the 1980's has been
replete with stories about aircraft accidents.  Many of
these accidents occurred due to the lack of proper or
sufficient tracking and monitoring of the aircraft.  As the
number of aircraft flights around the globe continues to
increase, so will the need for tracking.

Agencies interested in tracking aircraft in the United
States include the Department of Defense and the Federal
Aviation Administration.  Whether in the Persian Gulf or on
the Atlantic coast, the Department of Defense is concerned
with maintaining a watchful eye on aircraft that may

threaten the United States or U.S. interests and forces abroad. The Federal Aviation Administration meanwhile, monitors the skies of the United States to provide for the safety of air travelers and the general populous on the ground. This monitoring function is heavily dependent on precise knowledge of aircraft positions.

Internationally, airline travel over the broad expanses of ocean poses challenges to aircraft traffic control. The lack of precise position data by an international airliner could result in a catastrophe such as an errant aircraft wandering into hostile airspace.

Radar has been the classical answer to the tracking problem in the past. However, radar has several limitations. Depending on height of the antennas and the local terrain, ground-based radar can only detect and track aircraft in the region of the radar site. Low flying aircraft are more difficult to detect due to terrain and line-of-sight limitations. Ground-based radar systems are therefore very dependent on geography, both physical and political.

As man's quest for space and his use of satellites grows, new ideas for space-based sensors have arisen. One such idea involves the use of passive infrared detection technology (15:1). Another space-borne sensor concept also found in the literature is a space-based radar (5:47). Space-based sensors have the significant advantage of un-

precedented geographical access, with some orbits providing worldwide coverage.

The function of tracking aircraft from space poses a multitude of problems. The tracking system must be able to first detect the aircraft and then to acquire data on that aircraft over a period of time so as to establish its position and heading.

As one analysis showed, passive IR detection is limited in position accuracy on the order of 1.67 km of resolution, and therefore subject to spatial ambiguities (15:50). Conventional radar, operating in the microwave frequency range, has a broad beamwidth (dependent on antenna size) and is therefore also susceptible to spatial ambiguities at long ranges (8). To provide accurate position data at long ranges, such as from space, one would like to have a narrow beam system, such as lidar.

## Scope

This thesis is limited to the study of lidar to track aircraft from space. Although other tracking systems and techniques may be feasible, this analysis investigates *only* the lidar option.

Further, this analysis is general in nature. Specific details on laser physics, signal processing and atmospheric attenuation are omitted. Detail in these areas is the subject of books and would drive this analysis into unreasonable length and complexity. Therefore, broad but

3

realistic categorizations of the laser, the processing and the atmosphere are used.

Finally, this thesis is *not* an attempt to develop hardware nor new technologies. Technological capabilities in hardware are assumed and/or speculated. The model is founded on general orbital, optical and lidar principles and should remain useful even as the technology advances.

## II.  Literature Review

### THE LIDAR SYSTEM

All lidar systems can broken down into three major components: the laser, the detector and the processor.  When designing a lidar system, the choice of specifics for these three major subcomponents is a function of the mission and tasking of the lidar system (i.e., what it is supposed to detect).  To track aircraft, the laser must operate at a wavelength that can be propagated through the atmosphere. Once a suitable wavelength is chosen, a detector and appropriate processing technique must be selected to obtain the required information from the signal return.

When choosing the laser for a lidar system, two important characteristics must be considered: 1) the atmospheric attenuation at the operating wavelength and 2) the potential eye hazard associated with lasers operating at that wavelength.

Atmospheric attenuation is a function of the aerosols in the optical path as well as the type and density of the gases encountered along the path.  Certain gases absorb at certain wavelengths while they are relatively transparent at other wavelengths.  Likewise, certain aerosols absorb or scatter stronger at some wavelengths than others.  In combination, the gases and aerosols in the atmosphere create spectral pockets of high attenuation and spectral windows of

high transmittance. To maximize the range of a lidar system, a designer would chose a laser that operates at a wavelength that corresponds to one of the atmospheric windows. This study looks at four such laser wavelengths, all of which happen to operate in an atmospheric window in the infrared portion of the spectrum.

The eye-safe issue for laser operation is again dependent on the wavelength of operation. Sliney and Wolbarsht, adapting from the American Conference of Governmental Industrial Hygienists, break the IR laser wavelengths into three categories (25:261,262,267). The first category, 700 nm to 1049 nm, has the most restrictive exposure limits while the 1.4 $\mu$m to $10^3$ $\mu$m band has the least restrictive limits (25:262). Essentially, the closer the wavelength is to the visible wavelengths, the more restrictive the exposure limits become.

Dr. Paul McManamon from the Air Force Wright Aeronautical Laboratories, has written on two type of lasers for potential use in space, $CO_2$ and Neodymium (17:3). Both operate in an atmospheric window, however Neodymium could be an eye hazard with an operating wavelength around 1.06 $\mu$m. $CO_2$, operating at 10.6 $\mu$m, has an exposure limit rating more than 1000 times higher than neodymium (25:262).

In light of the eye hazards of neodymium, Dr. McManamon suggested two other lasers with longer wavelengths, for investigation: Holmium, operating at 2.1 $\mu$m, and $C^{13}O_2^{16}$,

operating at 11.1 $\mu$m (18). The designation $C^{13}O_2^{16}$ refers to carbon dioxide ($CO_2$) distinguished by the use of carbon-13 instead of carbon-12 in the molecule. Since the attenuation from atmospheric gases is a function of the density of the absorbing gas, one wishes to avoid operating the laser at a wavelength that corresponds to the absorption bands of any of the prevalent atmospheric gases. The atmosphere contains very little carbon-13 based carbon dioxide. Hence, atmospheric attenuation is lower when using a carbon-13 based $CO_2$ laser than a carbon-12 based $CO_2$ laser.

The other major portions of a lidar system are the detector and the associated processing subsection. The actual choice of detector material is wavelength dependent and often effective over only a small bandwidth. For example, Kane, Zhou and Byer recommend a silicon detector for their Nd:YAG lidar system (13:2481). Silicon has a cutoff wavelength at 1.1 $\mu$m (4:191). Therefore, a silicon detector would be sufficient for Nd:YAG but not for $CO_2$.

The processing involved with lidar systems is another factor that would be an integral design consideration and a function of the mission of the lidar system. Since the system under study here would be required to track low altitude aircraft, ground returns must be differentiated from targets. The targets could be differentiated from the ground by their doppler signature. An aircraft, unless

traveling with no relative motion with respect to the ground, would impart a doppler shift on the laser energy which is different than the ground's doppler shift. This difference, if large enough, could then be detected.

One way to accomplish the doppler detection is by heterodyning. Heterodyning is a procedure in which a signal is mixed with a stable frequency source and the difference between the two frequency sources is extracted. Fluckiger, Keyes and Shapiro describe this process as occurring on the photodetector itself (10:318).

Kane, Zhou and Byer propose heterodyne detection in their design of a doppler wind velocity lidar. (13:2481) Their implementation of heterodyning references the frequency shifting of a Nd:YAG signal by "acoustooptical or electrooptic modulation." (13:2480) They also state:

> Pulsed reference beam coherent lidar systems put two principal requirements on the laser technology: first, the 'ow-power oscillator must be stabilized so that the frequency drift during the pulse round trip time contributes only a small fraction of the allowable frequency error; second, a high-energy pulse must be transmitted at a known offset frequency from the oscillator to well within the allowable frequency error. (13:2480)

They further state, with two references listed, that such frequency stability is achievable in Nd:YAG lasers operating at low powers (13:2480).

Another method of extracting doppler information from a returned signal is with autodyne detection, as proposed by Fluckiger, Keyes and Shapiro (10:318).

8

Autodyne detection employs no local oscillator beam.
It is a direct detection scheme involving self-beating
between the various frequency components of the
received signal beam. (10:318)

Such a technique obviates the necessity for the extreme
pulse-to-pulse frequency stability as discussed by Kane,
Zhou and Byer above (10:318). This specific point is very
important with space-based lidar systems since the range to
target is long, resulting in a longer time base in which
pulse-to-pulse frequency stability is required. Fluckiger,
Keyes and Shapiro further explain that autodyne detection
can be used for doppler processing, "can be as sensitive as
heterodyne detection" (10:325) and "is far less sensitive to
receiver optics quality" (10:325) than heterodyne detection
(10:325).

THE ENVIRONMENT

In addition to the components of the lidar system, a
designer would need to consider the sources of attenuation
that the system would be likely to encounter. For this
thesis, the atmosphere poses the largest single source of
attenuation. The effects of attenuation can be mathemat-
ically modeled with the lidar range equation. The partic-
ular version of the lidar range equation used for this study
is taken from Dr. McManamon (17:1):

$$P_r = P_t G_t \left[\frac{\sigma_t}{4\pi R^2}\right]\left[\frac{A_e}{4\pi R^2}\right] (\tau^2) \qquad\qquad (1)$$

where

$P_r$ = power received on the detector

$P_t$ = power transmitted

$G_t$ = transmitter gain

$\sigma_t$ = target cross-section

$R$ = range from the lidar to the target

$A_e$ = area of the receiving optics and

$\tau$ = total (one-way) attenuation from all sources

(17:1)

Several atmospheric attenuation models are available

for calculating the atmospheric attenuation.  Two atmos-

pheric attenuation models were investigated for this thesis.

LOWTRAN and FASCODE.  Both software packages are products of

the Air Force Geophysics Laboratories.  FASCOD2 is the

particular version of FASCODE that was available at the time

of this thesis (20) and the terms are used interchangeably

throughout this document.

> The LOWTRAN code calculates atmospheric transmit-
> tance and radiance, averaged over 20-cm$^{-1}$ intervals
> in steps of 5 cm$^{-1}$ from 350 to 40,000 cm (0.25 to
> 28.5 $\mu$m).  The code uses a single-parameter band
> model for molecular absorption, and includes the
> effects of continuum absorption, molecular scatter-
> ing, and aerosol extinction. (14:10)

FASCOD2 on the contrary, "is a model and computer code for

the accelerated line by line calculation of spectral

transmittance and radiance for atmospheric problems...".

(6:1)  In other words, FASCODE is narrowband.  Since a laser

10

operates at such a narrow linewidth or narrowband. FASCODE
appears to be more appropriate than LOWTRAN for laser
attenuation modeling (12;16).

To illustrate this point, consider the atmospheric
attenuation for a $CO_2$ laser. The laser energy would be
absorbed by the atmospheric $CO_2$ at a very specific wave-
length. This specific absorption is modeled in FASCODE in
its line-by-line calculations. In LOWTRAN however, the
narrow band laser energy attenuation would be approximated
by the broadband average over a wide bandwidth. Because of
LOWTRAN's bandwidth mismatching and the corresponding
errors, FASCODE was deemed more appropriate for laser
attenuation modeling.

## III.  The Model

The main objective of this study was to determine the general feasibility of using a lidar system on a satellite to track aircraft.  The prime tool in accomplishing this task was a computer model. This chapter explains the computer model and many assumptions behind the model.  The code was written in Microsoft@ QuickBASIC on an IBM. PC/XT compatible machine.  The name given to the model is the Optical Aircraft Tracking System (OATS) model.  The actual computer code for the model is listed in Appendix A.

The OATS model was written to be a flexible engineering and research tool to investigate various design alternatives.  The model does not include all alternatives available to a designer nor does it delve into the specifics of individual subsystem operations.  For example, the laser subsystem is modeled with four inputs: 1) the laser pulse power, 2) the wavelength of operation 3) the laser pulse width and 4) the beam divergence angle for the post-optics beam.  Specific laser mechanics such as the lasing medium and the pulsing mechanism are not discussed.  A similar level of generalization was used for the other subsystem models as well.

Equation 1, the lidar range equation, is the core of the model.  The variables for the equation are either given as inputs or calculated from input data.  Subprograms or functions are used for much of the variable manipulation and

generation. Output data is selectable from a variety of options available to the modeler. For example, the modeler may need the available target track time per satellite orbit. This is based on the zenith angle at which a target is first detected. To calculate an initial detection zenith angle, the model uses multiple iterations of the lidar range equation to compute certain parameters and match them with the initial detection criterion. Once this angle is found, a separate function computes the track time available during a single pass of the satellite.

The OATS model can be broken into seven major subsets:

1) Orbital Mechanics

2) The Ranging Algorithm

3) The Transmittance Algorithm

4) The Target Lidar Cross Section Algorithm

5) The Lidar Range Equation

6) The Inputs

7) The Output Data and Calculations

Each of the seven blocks involve several major assumptions and core concepts. These assumptions and concepts will be discussed in the following sub-chapters. Appendix B contains the master list of all variables, an explanation of each variable and the name given to that variable in the code.

## Orbital Mechanics

Because the lidar system under discussion will be carried on a satellite, orbital mechanics plays an important role in the OATS model. The reference for the analysis of the geometry will be the target. The zenith angle (from the target to the satellite) will be used to vary the location of the satellite. To simplify the problem , only circular orbits are discussed and explored. Elliptical, parabolic, hyperbolic, or ballistic trajectories are also possible but will not be addressed in this analysis.

Another simplification in the orbital mechanics of this modeling effort is that the earth is a perfect sphere. Actually, the earth's equatorial radius is 6378.145 km and the polar radius is 6356.785 km (3:94). However, in lieu of a more complex model of the earth, the OATS model uses a spherical approximation. The OATS model concentrates on midlatitude targets only and therefore uses the Midlatitude Winter default value found in FASCODE of 6371.230 km (19:5) for the earth's radius. This value is assumed to be the constant radius of the earth for all computations. The errors induced by this approximation are very small, causing a variation in the signal power received at the satellite of less than one percent.

To define the length of time that the satellite takes to complete one orbit of the earth (the orbital period), the speed of the satellite must first be known. The speed or

14

velocity of a satellite is a function of its altitude. The scalar representation of this relationship (taken from Bate, Mueller and White) is given in Equation 2 as follows:

$$V_s = \left[ \frac{\mu}{r} \right]^{\frac{1}{2}} \qquad (2)$$

where $\mu = 3.986012 \times 10^5 \dfrac{km^3}{sec^2}$

$\quad$ r = radius of the orbit and

$\quad V_s$ = velocity of the satellite in km/sec (3:34,429).

The radius of orbit is the distance from the center of mass of the earth to the center of mass of the satellite and approximated here to be the sum of the radius of the earth and the satellite altitude. Therefore,

$$r = R_e + h \qquad (3)$$

where $R_e$ is the radius of the earth (6371.23 km) and h is the altitude of the satellite from the earth's surface.

Using Equation 2, one can readily calculate the orbital period of a satellite. The circular distance in one orbit is simply the circumference of the orbit or $2\pi( r )$. The orbital period therefore, is the circumference of the orbit divided by the velocity or

15

$$P = \frac{2\pi r}{v_s} = \frac{2\pi r}{\sqrt{\dfrac{\mu}{r}}} \qquad (4)$$

$$P = \frac{2\pi r \sqrt{r}}{\sqrt{\mu}} \qquad \text{where} \qquad \frac{2\pi}{\sqrt{\mu}} = K1 \qquad (5)$$

such that $K1 = 0.009952$ when $r$ is in km and $P$ is in seconds. Therefore, the orbital period in seconds is expressed as

$$P = K1 \left[ r \right]^{\frac{3}{2}} \qquad (6)$$

From this relation, one can easily calculate the angular revolution rate of the satellite. The rate, $\omega$, in radians per second is simply expressed as:

$$\omega = \frac{2\pi}{P} \quad \text{or} \quad \omega = 631.349 \left[ r \right]^{-1.5} \qquad (7)$$

Given a zenith angle $\theta$ and the corresponding geocentric angle $\phi$, defined in Figure 1, the geocentric angular rate or $\dfrac{d\phi}{dt}$ is equivalent to $\omega$.

The geometry in Figure 1 yields a triangle for which Equation 8 applies (9:8).
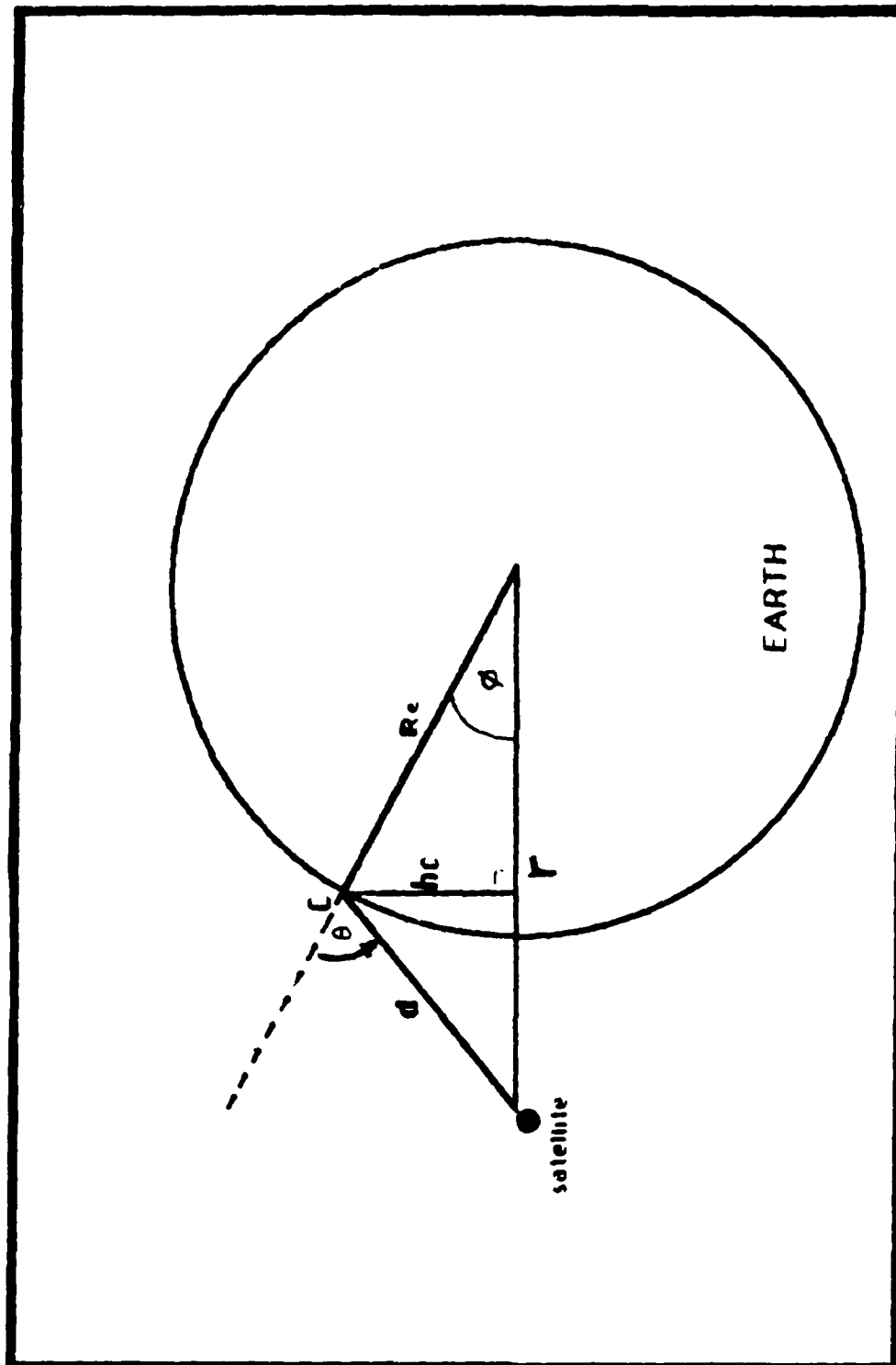
**FIGURE 1 ORBITAL GEOMETRY**

17

$$\frac{1}{2} h_c r = \frac{1}{2} R_e d \sin(C) \qquad (8)$$

From Figure 1 and Equation 8, one can calculate the transit time from a given zenith angle inbound to the same zenith angle outbound (i.e. symmetrical about the normal to the earth's surface) for a circular orbiting satellite at any given altitude (assuming that the satellite passes through the normal vector). In Figure 1, d is the distance from the satellite to a point or target on earth while $R_o$ is the radius of the earth (assumes that the target is on the earth's surface). Also, the angle $\theta$ defines the angle C since $(C + \theta)$ must equal $\pi$. Therefore, Equation 8 can be simplified as:

$$h_c r = R_e d \sin(C) \qquad (9)$$

or

$$h_c = \frac{R_e d}{r} \sin(C) \qquad (10)$$

However, from the given geometry, $h_c$ is also defined as

$$h_c = R_e \sin(\phi) \qquad (11)$$

which yields:

$$R_e \sin(\phi) = \frac{R_e d}{r} \sin(C) \qquad (12)$$

18

$$\sin(\phi) = \frac{d}{r} \sin(C) \qquad (13)$$

$$\phi = \sin^{-1}\left[ \frac{d}{r} \sin(C) \right] \qquad (14)$$

Given the geocentric angle $\phi$ which is defined by d, r and $\theta$ (where $\theta = \pi - C$, and d, r, and $\theta$ are entering arguments), the rate of change of $\phi$ is simply the satellite's revolution rate $\omega$. Given the two dimensional case (when the satellite passes directly overhead of the target) and given that $\theta_1$ is the zenith angle where tracking begins, the time from $\theta_1$ to when the satellite is directly overhead ($\theta = 0$) is simply $\phi/\omega$. Therefore, if tracking is symmetric about the $\theta = 0$ point, then the time of potential track $\psi$ is $2\phi/\omega$. Note that this assumes that the track will not be lost through the doppler null (directly overhead) or for any other reason such as fluctuating Lidar Cross Section (LCS), which is a function of aspect angle.

## The Ranging Algorithm

To calculate range one must first establish a reference. In Figure 2, the origin of the three axes is the location of the target and therefore the central reference point. The target here is assumed to be at low level ( 10 meters from the surface for the OATS model). Also, the target is assumed to be stationary (i.e. the change in

19
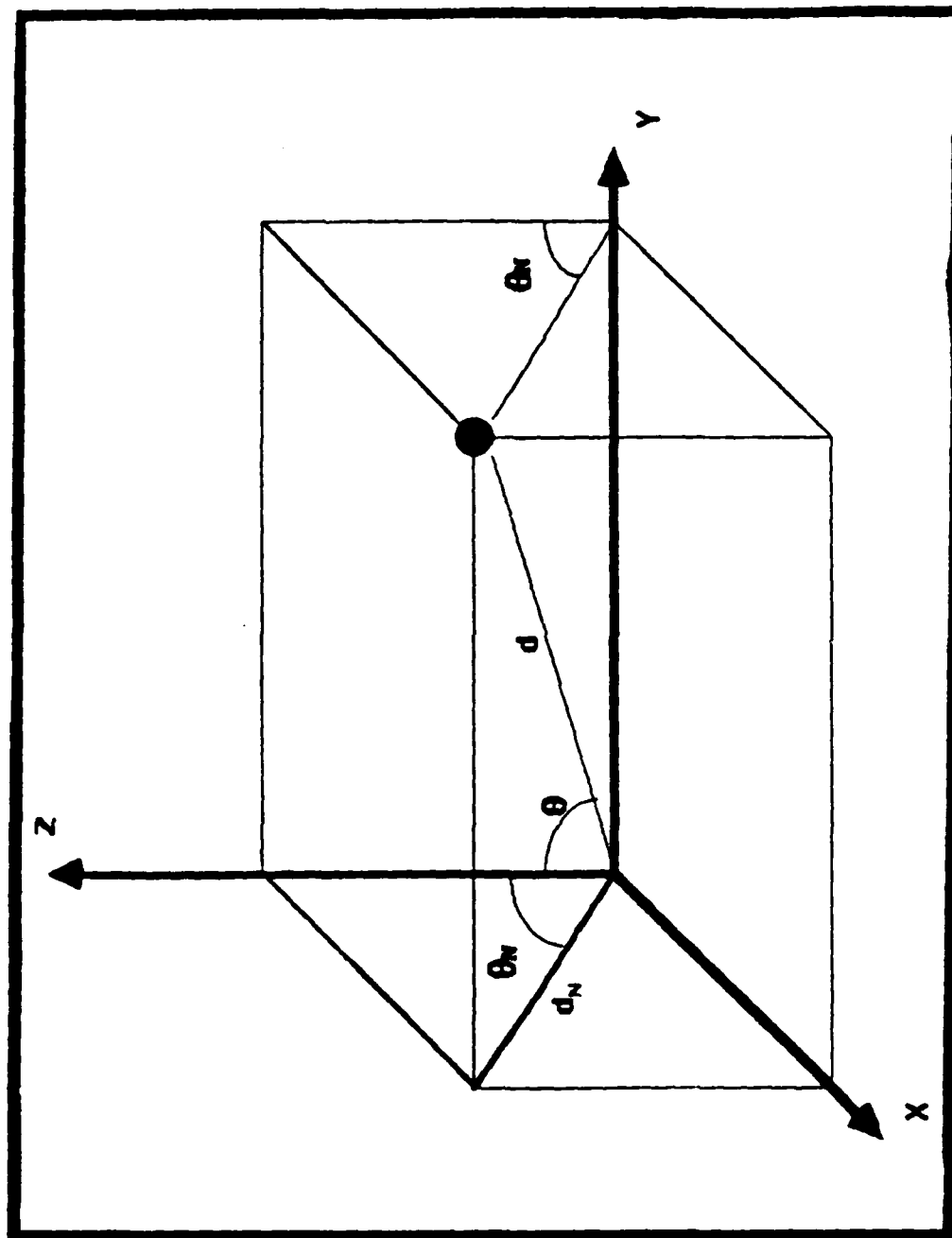
FIGURE 2 RANGING GEOMETRY

distance from the target to the satellite is due *only* to the velocity of the satellite). The satellite is set in a circular orbit of some selectable altitude and some selectable offset. The offset is simply the distance that the target is from the satellite's ground track at its closest point of approach. The offset is along the Y axis and the satellite ground track is parallel with the X axis. The X-Y plane intersects the earth's surface at the origin only and therefore the Z axis represents a normal to the earth. Expanding on Figure 2, the following terms apply:

d - distance from the target to the satellite

y - shortest distance from the target to the satellite's ground track

h - altitude of the satellite above the earth's surface

$d_N$ - the "no-offset range"; defined as the distance from the target to the satellite's projection on the X-Z plane; this is the shortest distance from the satellite to the Y axis.

$\theta$ - zenith angle of the satellite measured from the Z axis

$\theta_N$ - the "no-offset zenith angle" defined as the angle from Z-axis to $d_N$ vector

The known data entries into the OATS model are satellite altitude, h, the offset, y, and the no-offset zenith angle, $\theta_N$. To calculate d, the following equation can be used (9:385):

$$d = \sqrt{x^2 + y^2 + z^2}$$

(15)

21

To solve for d, the terms x, y and z must be defined. The satellite, if in a perfect circular orbit over a perfect spherical earth, has a constant altitude, h. In Equation 15, z is the apparent height of the satellite above the x-y plane. In the OATS model, z must always be positive since the no-offset zenith angle, $\theta_N$ is limited from $80°$ to $-80°$. The value for z reaches its maximum when $\theta_N$ is zero and it reaches its minimum when $\theta_N$ is $\pm 80$ degrees. The value for z in Equation 15 is a function of $\theta_N$ such that

$$z = d_N \cos(\theta_N) \tag{16}$$

where $d_N$ is the no-offset range. The apparent satellite altitude is now a function of the no-offset range.

The value for y is not straightforward. Since the earth is curved, y does not exactly equal the ground range of the offset. If $y = d_0$ is the "direct orthogonal range", then let D be the ground range. Figure 3 describes the geometry. From the figure.

$$\sin \phi = \frac{d_0}{R_e} \tag{17}$$

and the circumference of the earth is $2\pi R_e$. The portion of the circumference that forms the angle $\phi$ is

22
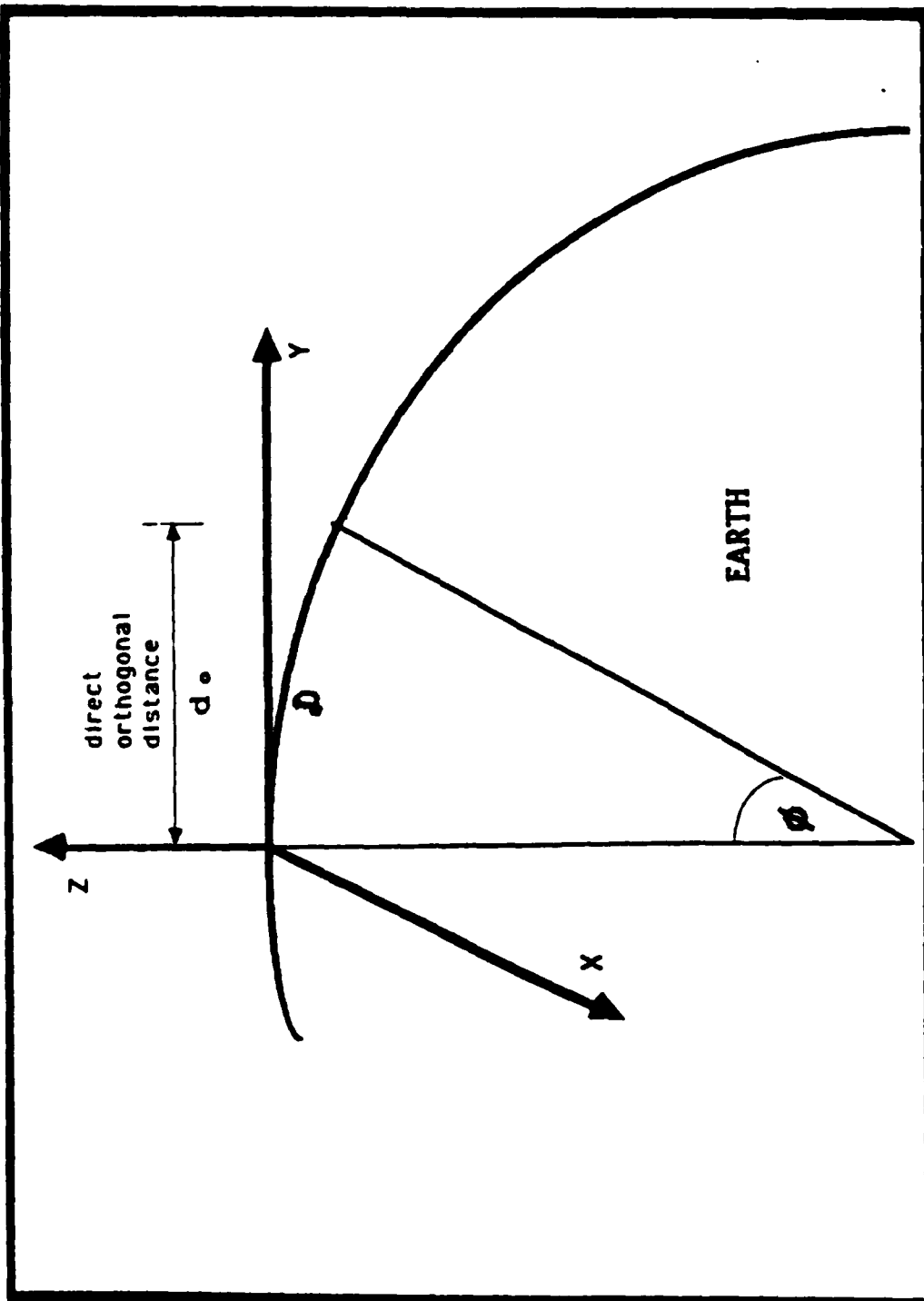
**FIGURE 3 OFFSET GEOMETRY**

$$\frac{\phi}{2\pi}\left[2\pi R_e\right] \quad \text{or} \quad \phi R_e \qquad (18)$$

In the figure therefore, $D = \phi R_e$. Still assuming that the zenith angle is $\pm 80°$ then the distance $d_o$ is strictly a function of $D$ such that

$$d_o = R_e(\sin\phi) = R_e\left[\sin\frac{D}{R_e}\right] \qquad (19)$$

For small offset distances, $d_0 \approx D$. The error in this approximation is given in percentage by

$$\%\varepsilon = \left|\frac{d_0 - D}{D}\right| \times 100 \qquad (20)$$

Figure 4 graphically portrays this error. Since the error is so small out to 500 km, the model uses the approximation $d_o = D$, the direct orthogonal range is approximated by the ground range. For Equation 15 then, $y = d_0$ and the OATS model is limited to offsets of 500 km or less. Beyond 500 km, the user must accept the offset error or compensate with some other means.

The final term in Equation 15 that must be identified is x. Using the same logic that formed the basis for Equation 16, the value for x, the distance out the X axis is

$$x = d_N \cos(\theta_N) \qquad (21)$$

24

# OFFSET ERROR

## (% ERROR FROM APPROXIMATION)
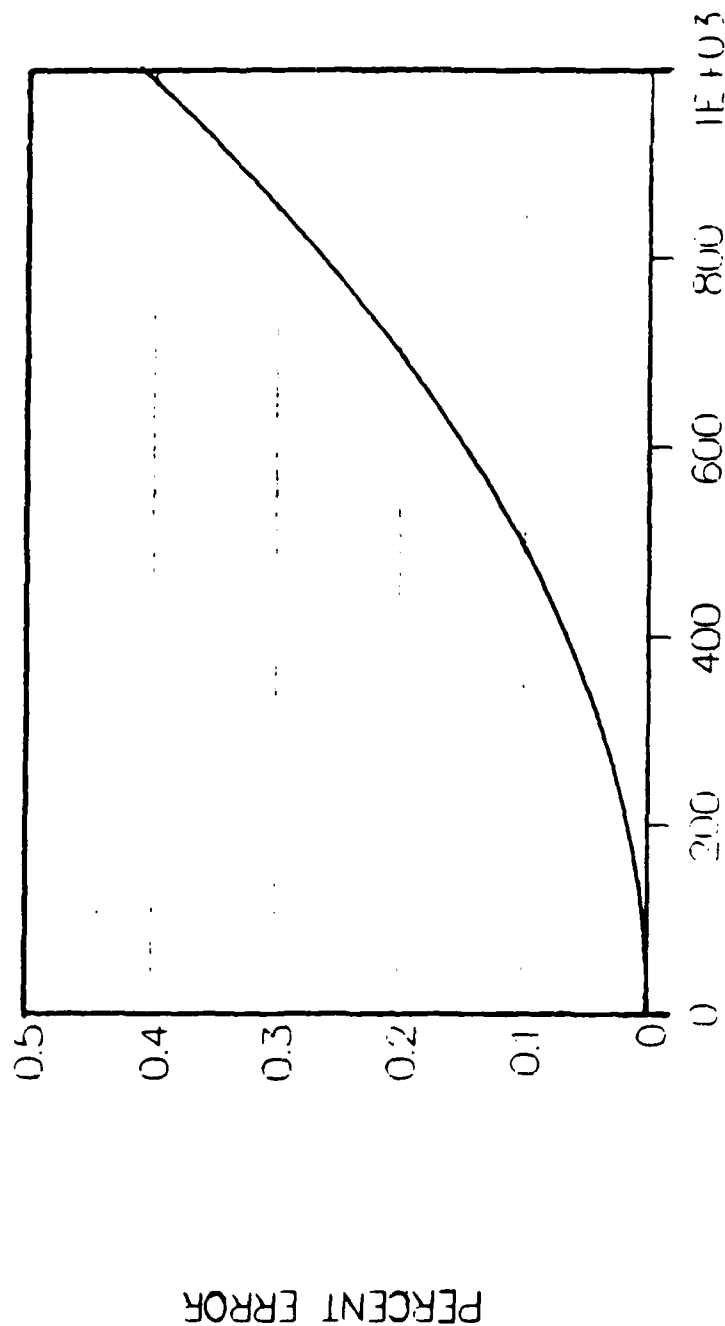


**FIGURE 4 OFFSET ERROR**

25

Equation 21 shows that x is a function of the zero offset range, $d_N$. The planar geometry for this case (i.e. $d = d_N$ since $y = 0$) is shown in Figure 5. The range from the target to the satellite can be approximated with Equation 22 shown below.

$$\cos \theta_N \approx \frac{h}{d_N} \qquad (22)$$

Therefore,

$$d_N \approx \frac{h}{\cos \theta_N} \qquad (23)$$

This approximation is only good for small angles $\theta_N$ because it assumes no curvature in the satellite's path.

To be more precise and take curvature into account, the law of cosines can be used to precisely calculate $d_N$. This algorithm for the computation of the distance $d_N$, was developed with Don Holland and a version of it is listed below (11). A general form of the law of cosines is listed in Equation 24 (9,8).

$$c^2 = a^2 + b^2 - 2\, a\, b\, \cos(C) \qquad (24)$$

Applying Equation 24 to Figure 5 yields

$$r^2 = R_e^2 + d_N^2 - 2\, R_e d_N \cos(\pi - \theta_N) \qquad (25)$$

26
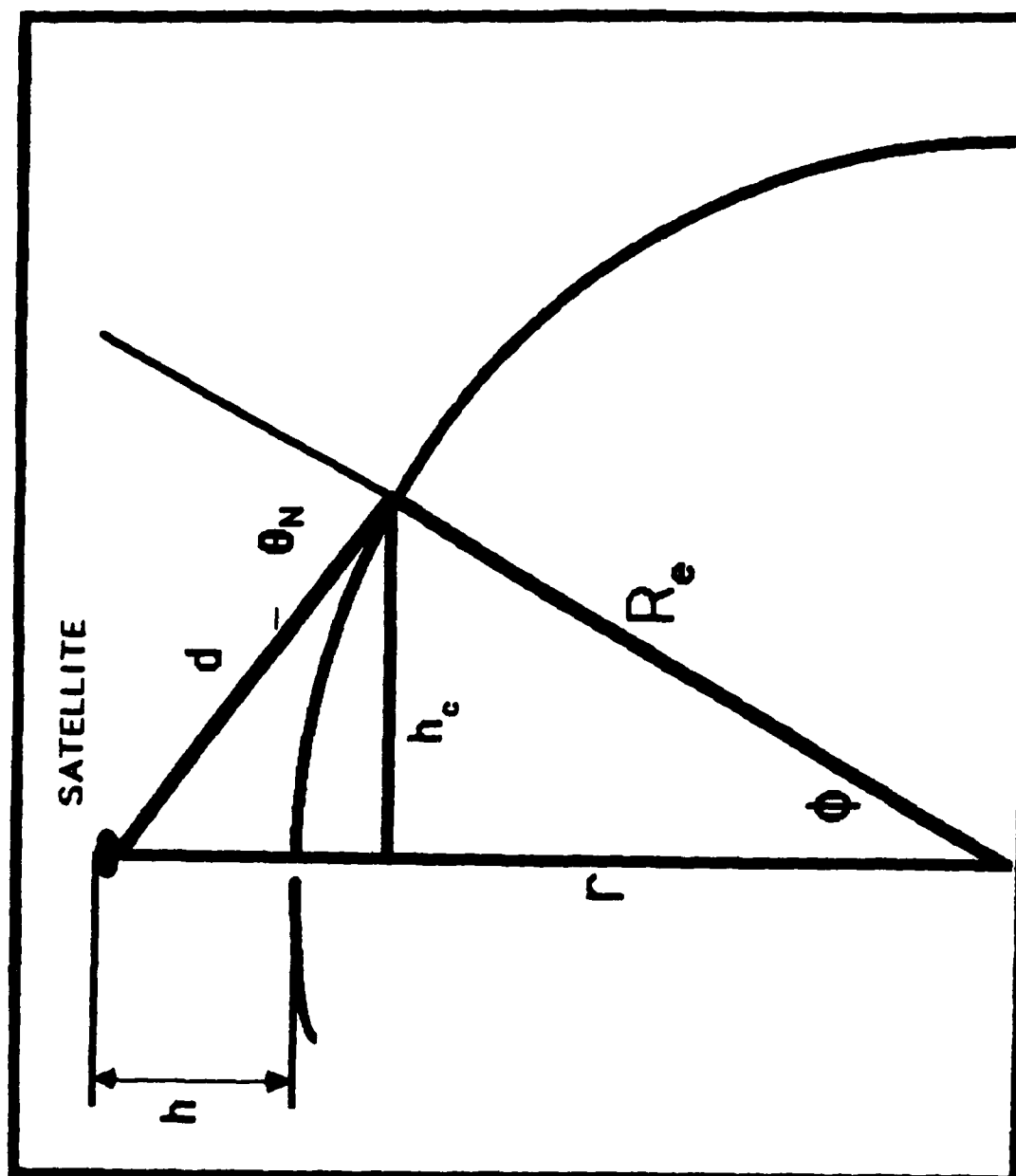
FIGURE 5 NO OFFSET PLANAR GEOMETRY

Since $r = R_e + h$ and $R_e$, h and $\theta_N$ are entering arguments.
Equation 25 can be rewritten as

$$d_N^2 - 2 R_e d_N \cos(\pi - \theta_N) + R_e^2 - (R_e + h)^2 = 0 \qquad (26)$$

letting

$$K_3 = -2 R_e \cos(\pi - \theta_N) \qquad (27)$$

and

$$K_4 = R_e^2 - (R_e + h)^2 \qquad (28)$$

then

$$d_N^2 + K_3 d_N + K_4 = 0 \qquad (29)$$

Solving for $d_N$ with the quadratic equation

$$d_N = \frac{-K_3 \pm \sqrt{K_3^2 - 4 K_4}}{2} \qquad (30)$$

Since $\theta_N$ can range from $0°$ to $90°$ (lower than the horizontal
is not allowed in the OATS model), the term $K_3$ will always
be positive. For all satellites with a positive altitude,
the term $K_4$ will always be negative. Therefore, the term
under the radical will always be a positive quantity.
Equation 30 can be rewritten as

$$d_N = \frac{-K_3 + \sqrt{K_3^2 - 4 K_4}}{2} \qquad (31)$$

Therefore, Equation 31 always returns a real and positive value for the range from the target to the satellite. Recall $d_N$ is the zero offset range from satellite to target.

Going back to Figure 2, $d_N$ is now simply a function of satellite altitude, h , radius of the earth, $R_e$, and the no-offset zenith angle, $\theta_N$. The term $\theta_N$ becomes a key component in the OATS model.

The three key terms of Equation 15 $(x,y,z)$ have been defined with Equations 16, 21 and the $y = d_o$ approximation. The distance from the satellite to the target can therefore be computed with good accuracy out to 1000 km offset range and beyond 1000 km offset if Equation 19 is used to correct long range variation in y.

It must be noted however that this range, d, is the geometric range and is not the optical path range. The actual optical path through the atmosphere would be greater than or equal to the direct range, d, due to the refraction of the light through the atmosphere.

## The Transmittance Algorithm

The process of computing the transmittance of the laser energy through the atmosphere was very labor intensive and yet yielded the model's least flexible results. The labor intensive portion of the transmittance calculations was from using FASCOD2 on the Aeronautical Systems Division's CDC Cyber computer system. The lack of flexibility in the results stems from the narrow applicability of the results. Over 120 FASCODE computer runs yielded only two types of very specifically defined atmosphere types.

Transmittance in this model is simply the ratio of the signal that gets through the atmosphere to the signal that was sent from the radiating source. The transmittance, $t$, therefore varies from 0 (no power transferred) to 1 (all power transferred). As previously discussed, transmittance through the atmosphere is a function of wavelength. This wavelength dependence is determined by the composition of the atmosphere.

FASCOD2 is constructed so as to give the modeler a wide combination of atmospheres to simulate. Thousands of combinations are available. These combinations are due to the ability of the FASCOD2 user to define a wide number of constituents in the atmosphere at different altitudes and concentrations. Items that can be selected in various concentrations include, up to 28 molecular species, clouds, rain and even volcanic particles. Six pre-established

atmospheric models are available to define general atmosphere profiles for certain conditions (1:1). One of these pre-established models, the Midlatitude Winter model was used to generate the transmittance data for the OATS model. This model is established for latitudes about $45°$ North Latitude (1:1). It therefore covers much of the United States, Europe and Asia, where aircraft operations are common. The Midlatitude Winter model defines the temperature profile of the atmosphere which is used with a corresponding data base defining the concentrations of gases at different altitudes (1,1-3).

The variable IHAZE was the only variable changed in order to create two types of atmospheres for the OATS model. The first atmosphere had IHAZE held constant at 0, defining no haze in the atmosphere. The second atmosphere had IHAZE held to 2, defining a 5 km rural haze profile. Although further runs were attempted using clouds, unresolved software anomalies on the CDC cyber computer prevented success with cloud models.

Each run of FASCODE was designated at a set zenith angle and resulted in a series of 17 transmittance values corresponding to 17 wavenumbers or wavelengths. The spacing between each increment of wavenumber was approximately $x$ where $x = (2.4 \times 10^{-7} * \text{wavenumber})$, an *extremely narrow* section of the electromagnetic spectrum at laser frequencies. By choosing the center frequency transmittance values

for runs at a variety of zenith angles, a curve was established. Eight curves were developed, one for each atmosphere and laser combination. The curves defined the relationship of transmittance to zenith angle.

In order to be able to generate transmittance values for any zenith angle, an equation for each curve was sought. $SAS_{\circledR}$ (21) software was used for this purpose. Using the General Linear Model (GLM) procedure, coefficients for a fifth-order polynomial equation were computed for each curve. This procedure uses a least squares fitting algorithm in its computations (21:62).

The precision of the curve fit was enhanced through a data transformation. Instead of using the zenith angle as the independent variable, the cosine of the zenith angle was used. The input data for this process is listed in Appendix C for each curve.

The accuracy of the curve fit with the actual data was *very good*. A means to determine the goodness of fit is the $R^2$ value that is automatically generated for each GLM run. "$R^2$ measures how much variation in the dependent variable can be accounted for by the model." (21:64) An $R^2$ value better than .999 was achieved for each of the eight curves. In other words, the fifth-order polynomial equation was almost a perfect fit to the curve in all eight cases.

Data input for the curve fitting were restricted to zenith angle ranges from $0°$ to a maximum of $80°$. Although

some data was generated with FASCODE beyond the limit of $80°$, this data was not used. For example, the $CO_2$ with carbon-12 curve with no haze was developed for zenith angles from $0°$ to $90°$. This particular series showed a transmittance curve that appeared exponential for the first $80°$ but had a tail in the last $10°$ (i.e. from $80°$ to $90°$). In accounting for this tail, the curve fitting algorithm drove the accuracy of the first $80°$ off by a small margin. The data input was subsequently restricted to a maximum of $80°$ and resulted in an improved accuracy in the fit. This increase in accuracy was traded for the extended range ( $80°$ to $90°$) for the OATS model.

The $80°$ upper limit also makes sense in a realistic scenario of a laser radar on a satellite tracking low altitude targets. Further complications to the system arise in $80°$ to $90°$ sector. The additional attenuation in this regime (not modeled with FASCODE here) would be very high from dust, pollen, terrain, etc. for low altitude targets. Also, refraction would be at its worst.

With the coefficients from the polynomial curve fit, one can easily calculate a very accurate transmittance for any zenith angle. However, the underlying assumption here is that FASCODE is a perfect model of the atmospheric transmittance and that the atmosphere exactly matches the atmosphere loaded into FASCODE.

Because the atmospheres modeled by FASCODE ( i.e.,clear

atmosphere with no aerosols or 5 km haze the only aerosol)
yield relatively optimistic values of transmittance, an
additional attenuation capability was built into the OATS
model. Although unsubstantiated for accuracy, an exponen-
tial model was used to simulate the variance of the trans-
mittance, $\tau$, as a function of zenith angle. The value
entered into the model is the additional attenuation desired
for a zenith angle of zero (in dB). For angles beyond 0
degrees, the additional attenuation is computed with the
following equation

$$\tau_\theta = e^{-\alpha L} \qquad (32)$$

where L is the length through the atmosphere. For this
equation, the atmosphere is assumed to end at an altitude of
120 km, the definition of space used for the FASCODE runs.
The value for L is therefore at a minimum when $\theta$ is zero
(L=120 km) and at a maximum when $\theta$ is at 80°, the OATS limit
(L$\approx$557 km). The geometry is therefore the same as that
described in the ranging algorithm. Since L is a function
of $\theta$ only, the value for L is simply the range if h is 120
km for all values of $\theta$. Therefore, the ranging function is
invoked in the OATS model to calculate the value L for any
zenith angle.

The coefficient $\alpha$ is determined from the input
attenuation requirement, $\mathfrak{I}(0)$. The term $\mathfrak{I}$ is the

attenuation input by the modeler and $\mathfrak{I}(0)$ designates the attenuation at a zenith angle of zero degrees. Since $\mathfrak{I}(\theta)$ represents the attenuation in dB, the ratio of received power to transmitted power is,

$$\zeta = \frac{Rx \text{ power}}{Tx \text{ power}} = 10^{\gamma} \quad \text{where } \gamma = \frac{-\mathfrak{I}(0)}{10} \tag{33}$$

so that the attenuation coefficient $\alpha$ can be defined as

$$\alpha = \frac{-\ln \zeta}{120} \tag{34}$$

Therefore, the transmittance factor, $\tau_a$ is defined as

$$\tau_a(\theta) = e^{-\alpha L(\theta)} \tag{35}$$

The transmittance factor, $\tau_a$ is multiplied by the computed transmittance from the fifth-order polynomial for a clear atmosphere to yield the overall model transmittance at a given zenith angle.

The transmittance through the atmosphere can be calculated in the OATS model in three ways:    ·

1) a clear, no-aerosol atmosphere made up of 28 molecular species

2) atmosphere number one with 5 km rural haze

3) atmosphere number one with a selectable additional attenuation factor.

## Lidar Cross Section

One of the more complicated portions of the OATS model is the generation of Lidar Cross Section (LCS) values for the targets that the lidar system is intended to track. The LCS of a target, $\sigma$, is analogous to the Radar Cross Section (RCS) of a target in the microwave frequency range but is merely differentiated in its application to the optical frequency ranges.

Bachman, in his discussion of optical cross sections of targets, starts his analysis with the equation

$$\sigma = \rho \, G \, A \tag{36}$$

"...where

$\rho$ = reflectance of the target surface

G = gain of target

A = projected physical area." (2:35)

He goes on further to define gain, G as

$$G = \frac{4 \, \pi \, A_c}{\lambda^2} = \frac{4 \, \pi}{\Omega_r} \tag{37}$$

"where $A_c$ is defined as area of coherence (equivalent normal incidence flat plate area) of the target and $\Omega_r$ is the backscatter solid beamwidth from the target." (2:35)

Bachman continues his development and says, "...the equivalent specular scatterer is equivalent to

$$\sigma = \frac{4\,\pi}{\lambda^2}\ A^2 \tag{38}$$

which is identical to the radar cross section (RCS) at wavelength $\lambda$." (2:36)  Indeed, Skolnik cites Mentzer and defines the RCS of a "large flat plate of arbitrary shape" (23:43) with the same equation.

However, Bachman further goes on to define the cross section of a diffuse scatterer by defining $\Omega_r = \pi$ and stating that the relationship "assumes backscatter energy over $\pi$ steradians of the $4\pi$ steradians of the isotropic sphere..." (2:36)  With this assumption, he ends up with the cross section of a diffuse reflector defined as

$$\sigma = 4\ \rho\ A\ \cos^2\theta \tag{39}$$

In the OATS model, two types of targets are available, the flying sphere and the flying brick.  The spherical target approximation is the simplest in its derivations and application.  From Skolnik, who cites Mentzer, the cross section of a sphere is $\pi a^2$ where a is the radius of the sphere (23:43).  However, in this treatment of cross section, the target is assumed to be Lambertian or a diffuse reflector.  Therefore, based on Equation 39, one can show

that the ideal diffuse reflecting sphere has a LCS of

$$\frac{8}{3} \pi \rho r^2 \tag{40}$$

where r is the radius of the sphere.

This can be done by integrating over a hemisphere so that

$$\sigma = 4 \rho \int_{\theta=0}^{\pi/2} A \cos^2\theta \, d\theta \tag{41}$$

Following the integration scheme used by Slater to solve a similar problem, the increment of integration is a ring representing a segment of the hemisphere defined by $d\theta$. According to Slater's orientation in this type of integration, the area of the ring (if radius = 1) is

$$A = 2 \pi \sin(\theta) \, d\theta \tag{42}$$

(24:529).

Combining Equations 41 and 42 yields

$$\sigma = 8 \pi \rho r^2 \int_{\theta=0}^{\pi/2} \sin(\theta) \cos^2(\theta) \, d\theta \tag{43}$$

The solution to this equation is

$$\sigma = \frac{8}{3} \pi \rho r^2 \tag{44}$$

The flying brick model uses three orthogonal surfaces oriented in a manner such that no surface overlaps or shadows the other (e.g. a brick). This model was developed to more accurately represent an aircraft. Although most aircraft are not shaped like a brick, most aircraft tend to have a larger projection area (silhouette) from a top perspective than from a frontal perspective. By making the assumption that a larger projection area equates to a larger LCS, one can assume that most aircraft have a larger LCS from a top perspective than from a frontal/rear perspective. Since a satellite-borne lidar system would potentially track a target aircraft over a $160^\circ$ arc (the OATS model limit) through the aircraft's upper hemisphere, a varying LCS would be a reasonable assumption. The original idea for a brick came from a discussion with Lt. Blake and Mr. Weigand (27). The brick model provides the changing LCS that could be expected from a true aircraft as the satellite transits through a full range of zenith angles.

If the aircraft's LCS is known and can be simplified to a sum of three perpendicular cross sections, those data could be put into the OATS model inputs as the area and reflectivity of the target.

The following assumptions form a foundation for the OATS model:

1. The frontal and rear faces of the brick have equal projected areas.

2. The side faces of the brick have equal projected areas.

3. The aircraft (the brick) is in straight and level flight with no crab (i.e. the true heading vector is normal to the frontal face).

4. The skin reflectance, $\rho$, is uniform and the surface is diffuse (or Lambertian).

5. The sum of the cross sections of the three surfaces of the brick is equal to the total cross section.

This geometry can be pictured in Figure 6. The frontal or rear projected areas are depicted with PA1, the top projected area as PA2 and the side projected area as PA3. The satellite ground track and target geometry are further depicted in Figure 7. To maintain a consistent three face object, a geometry transformation was developed. This transformation realigns the target faces so that the normal vector to the frontal face is always parallel with the satellite's geometry (see Figure 8 and 9). From the new configuration, symmetry about the Z axis can be assumed so that the variation in offset zenith angle, $\theta_N$, from $90°$ to $0°$ is symmetrical with the variation from $0°$ to $-90°$.

If a simple projection area transformation is used, the effect is obscured. The simple transformation is

$$A_1' = |A_1 \cos \beta| + A_3 \sin \beta \tag{45}$$

$$A_3' = |A_3 \cos \beta| + A_1 \sin \beta \tag{46}$$

These transformations simply change the projected areas of the target. The top projected area remains the same,
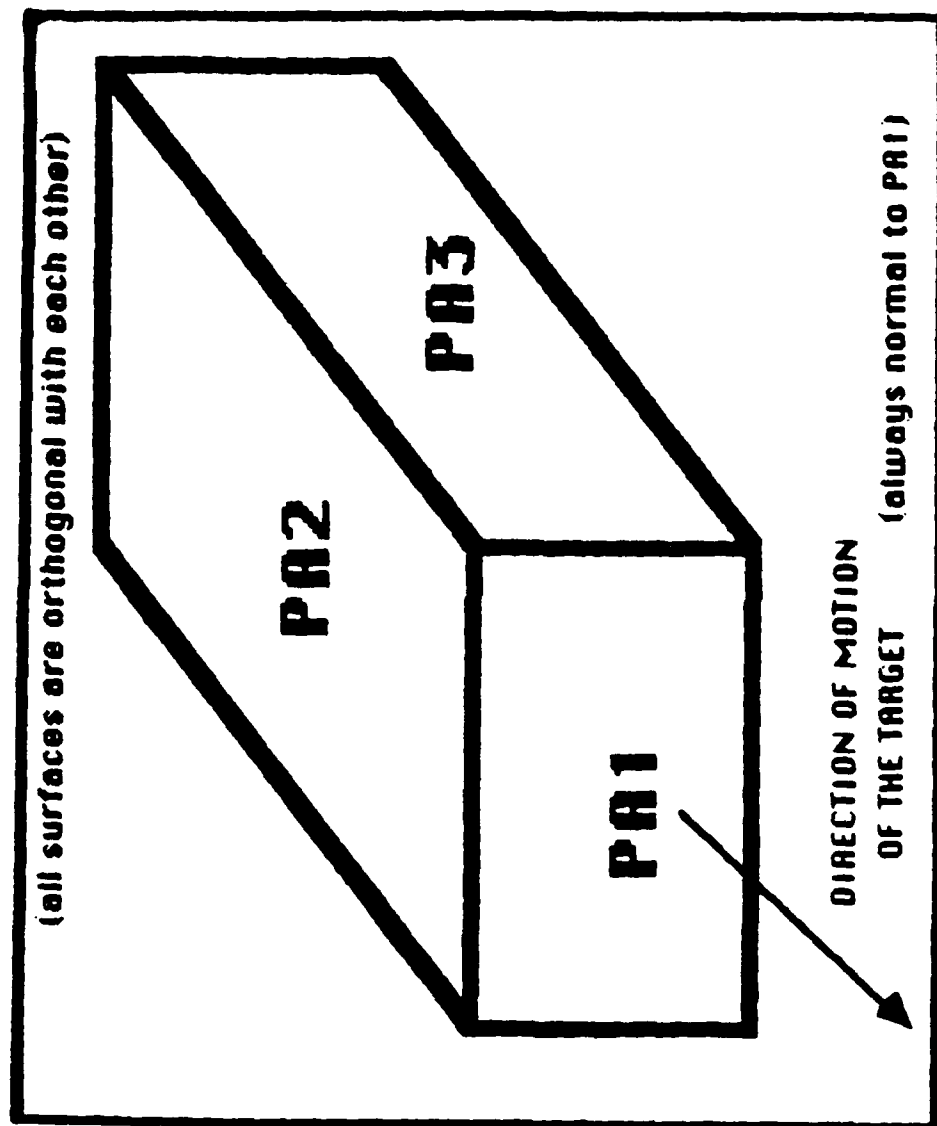
FIGURE 6 PROJECTED AREAS OF THE TARGET

(all surfaces are orthogonal with each other)

PA2

PA3

PA1

DIRECTION OF MOTION
OF THE TARGET    (always normal to PA1)
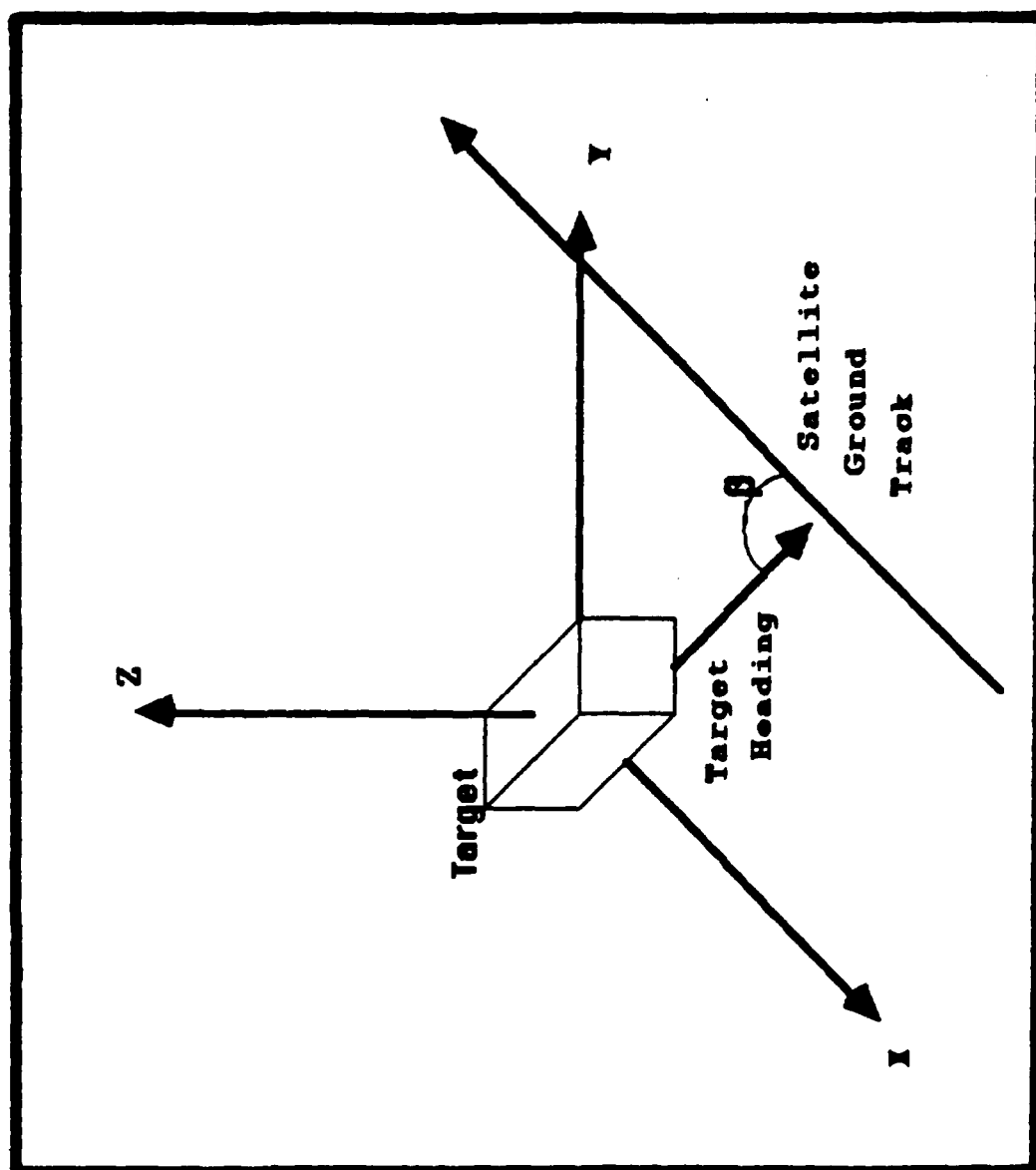
FIGURE 7 ACTUAL TARGET ORIENTATION
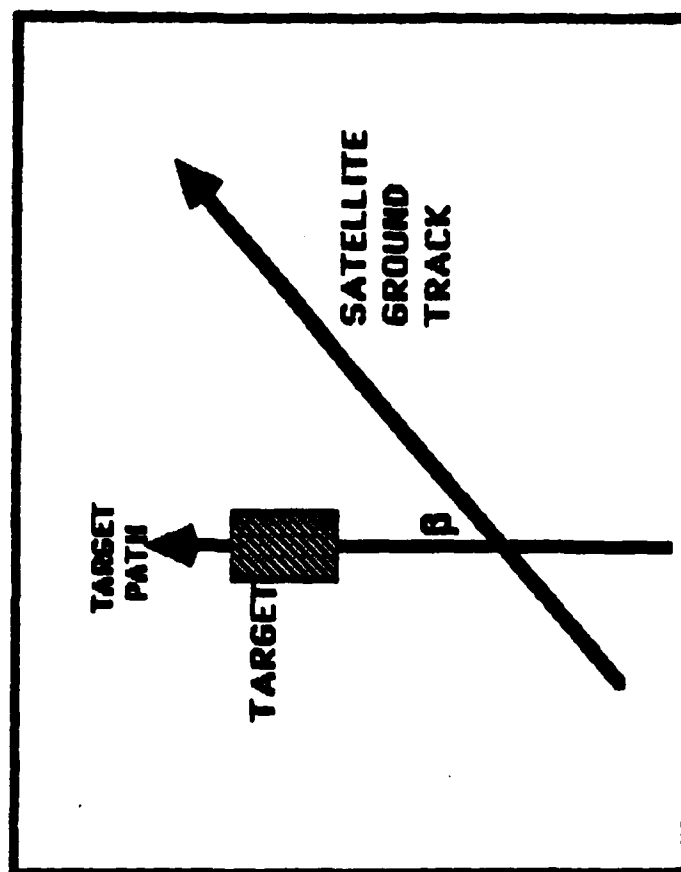
FIGURE 8 ACTUAL TARGET GEOMETRY
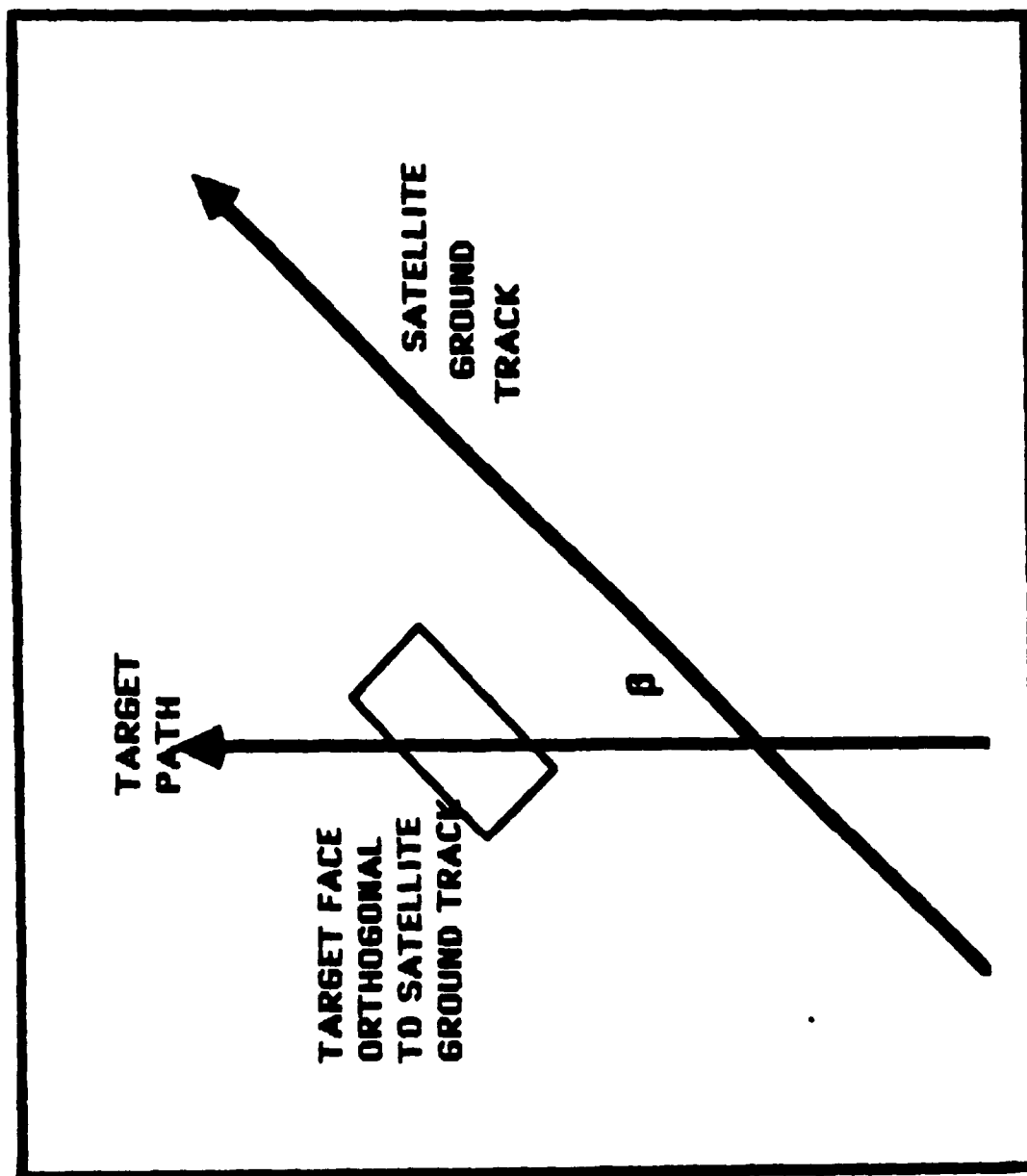
**FIGURE 9 TRANSFORMED TARGET GEOMETRY**

independent of the targets true heading if the target is straight and level. However, the failure of these transformations is found in the fact that the variation in planar LCS is a function of $\cos^2\theta$ (from Equation 39). Therefore the sum of projected areas in Equations 45 and 46, when viewed from an angle $\beta$, *does not* have the same LCS as the transformed areas ($A'_1$ and $A'_3$) due to the $\cos^2\theta$ term.

The following example illustrates this point and the transformation inaccuracies. The true frontal projected area is 5 square meters, the side projected area is 20 square meters. The angle $\beta$ is $30°$. Therefore,

$$A'_1 = |5 \cos \beta| + 20 \sin \beta \approx 14.33 \text{ sq meters} \qquad (47)$$

$$A'_3 = |20 \cos \beta| + 5 \sin \beta \approx 19.82 \text{ sq meters} \qquad (48)$$

To simplify the example, the zenith angle, $\theta$, is set to $90°$. Note, the top surface does not contribute if $\theta = 90°$. The target's untransformed cross section is $\sigma_T = \sigma_1 + \sigma_3$ where

$$\sigma_1 = 4 \rho (5) \cos^2\delta \qquad (49)$$

$$\sigma_3 = 4 \rho (20) \cos^2\delta \qquad (50)$$

If the angle $\delta$ is set to $45°$ for this example (where $\delta$ defines the satellite's position along its path), then

$$\sigma_1 = 10 \rho$$

$$\text{and} \quad \sigma_3 = 40 \rho$$

$$\text{so that} \quad \sigma_T = 50 \rho \ .$$

But the transformed geometry yields

$$\sigma_1 \approx 28.66$$

$$\sigma_3 \approx 39.64$$

$$\overline{\phantom{xxxxxxxxxx}}$$

$$\sigma_T = 68.30 \text{ square meters.}$$

The transformations in Equation 45 and 46 are therefore shown to be imprecise.

To correct for this, the transformation equations were modified to reflect the $\cos^2\theta$ dependence to be

$$A_1' = |A_1 \cos^2\beta| + A_3 \sin^2\beta \tag{51}$$

$$A_3' = |A_3 \cos^2\beta| + A_1 \sin^2\beta \tag{52}$$

These transformation equations will accurately transform the surface areas to pseudo-areas such that the psuedo-areas can be used in the LCS equations for LCS computations. The psuedo-areas *do not* represent true projection areas because of the square terms.

It is important to point out that although the accuracy of the transformation is improved, the entire procedure

rests on the premise that the flying object consists of three orthogonal surfaces. As the three surface approximation varies from reality, so does the accuracy of the model. The three surface model does, however, give the modeler the opportunity to have the target LCS realistically change with aspect angle.

The next step in the construction of the flying brick model was the development of equations to accurately compute the individual surface LCS values. From Equation 39, it is apparent that the off-normal aspect angle needs to be calculated or estimated.

The simplest case involves no offset (see Figure 10). In this case, only two surfaces are involved, PA1 and PA2, when $\beta = 0$ or $\pi$. Even if the targets heading is not parallel with the satellite's ground track (i.e., $\beta \neq 0$, $\beta \neq \pi$), the transformation in Equations 51 and 52 yield an equivalent geometry such that the pseudo-areas $A_1'$ and $A_2$ can be used to keep the geometry simple, i.e., only two side subject to illumination/reflection. With no offset,

$$\sigma_T = \sigma_1 + \sigma_2 \tag{53}$$

where

$$\sigma_1 = 4 \rho A \cos^2 (\frac{\pi}{2} - \theta) \tag{54}$$

$$\sigma_2 = 4 \rho A \cos^2\theta \tag{55}$$

**SATELLITE / TARGET GEOMETRY**

OFFSET = 0    ZENITH ANGLE = $\theta$
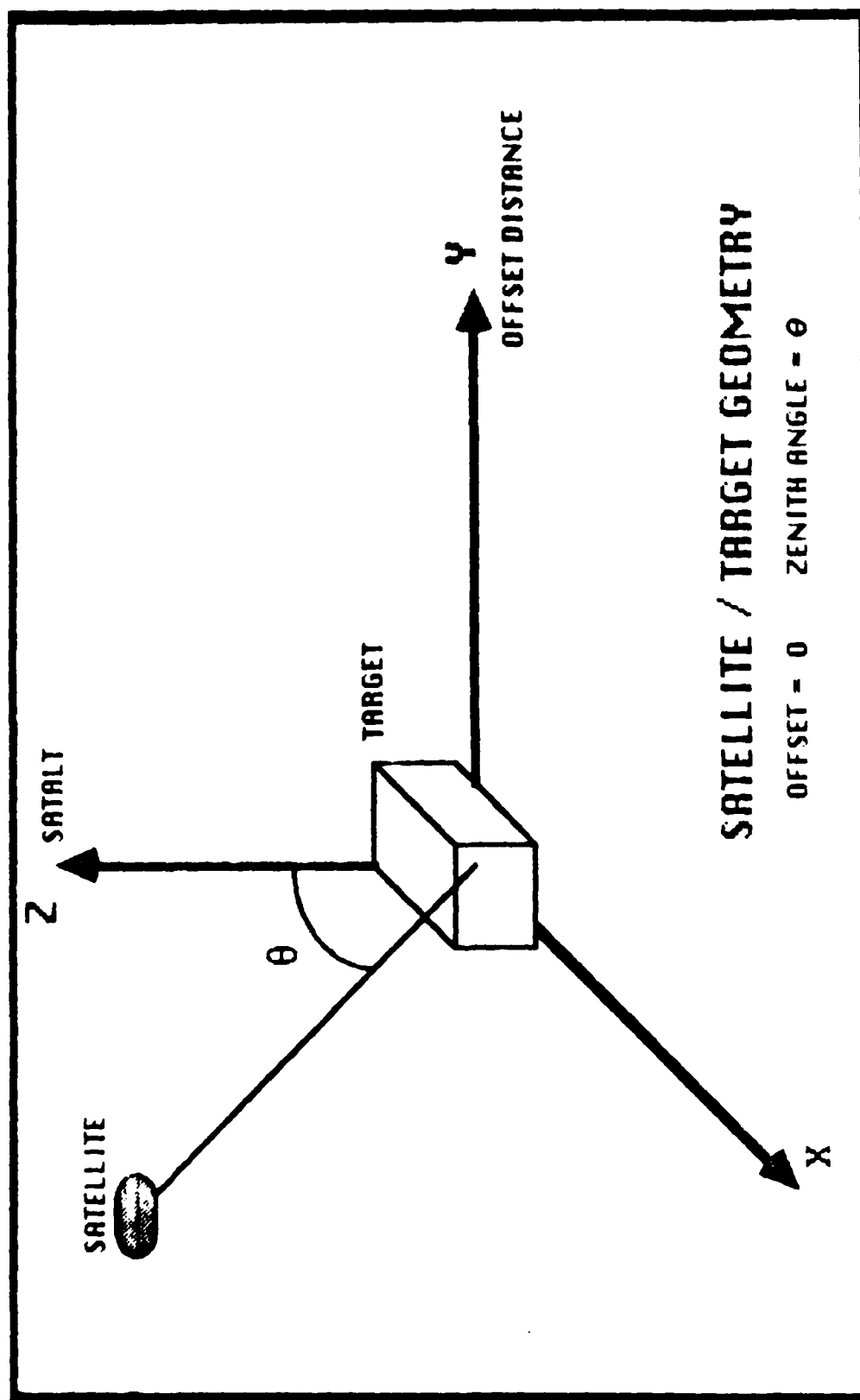
FIGURE 10    ZERO OFFSET GEOMETRY

*HOWEVER*, by including an offset into the geometry, the model switches to the geometry depicted in Figure 11.

Using the angle relationship for spherical coordinates (9:385) and transferring it into the present coordinate system and symbology,

$$\alpha_2 = \cos^{-1}\left[\frac{z}{\sqrt{x^2 + y^2 + z^2}}\right] \qquad (56)$$

where $\alpha_2$ is the angle from the Z axis to the vector formed by the distance from the target to the satellite. This is the off-normal angle for PA2 (or $A_2$) of the brick model. In terms of the no-offset zenith angle, $\theta_N$,

$$\cos\theta = \frac{z}{d_N} \qquad (57)$$

so that

$$z = d_N \cos\theta_N \qquad (58)$$

where $d_N$ is the no-offset range. The value for x is

$$x = d_N \sin\theta_N \qquad (59)$$

Since $d_N$ is already computed during ranging, Equation 58 and 59 are convenient. Using the same relationship as Equation 56, $\alpha_1$ and $\alpha_3$ are given as follows.
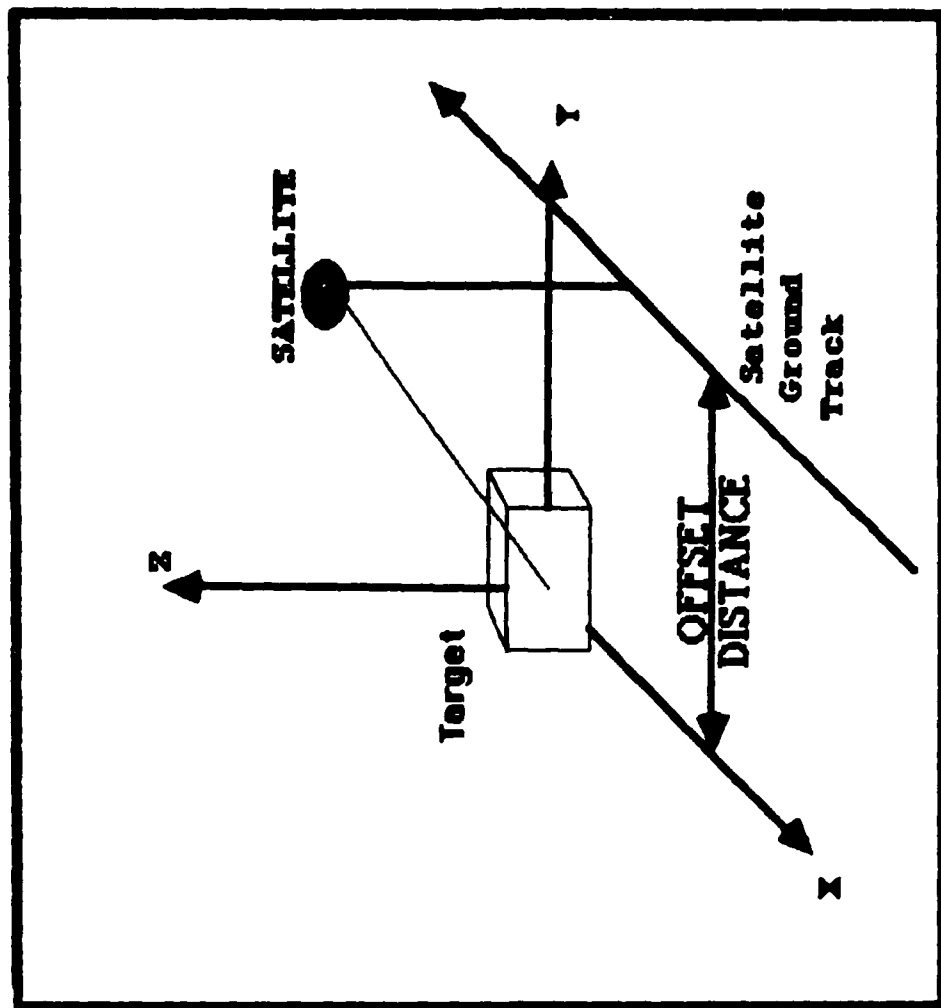
FIGURE 11 OFFSET GEOMETRY

$$\alpha_1 = \cos^{-1}\left[\frac{x}{\sqrt{x^2 + y^2 + z^2}}\right] \qquad (60)$$

$$\alpha_3 = \cos^{-1}\left[\frac{y}{\sqrt{x^2 + y^2 + z^2}}\right] \qquad (61)$$

From these relationships, the individual surface LCS values can be computed. The following equations form the individual LCS values that are necessary.

$$\sigma_1 = 4 \rho A_1' \cos^2\alpha_1 \qquad (62)$$

$$\sigma_2 = 4 \rho A_2 \cos^2\alpha_2 \qquad (63)$$

$$\sigma_3 = 4 \rho A_3' \cos^2\alpha_3 \qquad (64)$$

The total brick LCS from any aspect is therefore

$$\sigma_T = \sum_{x=1}^{3} \sigma_x = \sigma_1 + \sigma_2 + \sigma_3 \qquad (65)$$

51

## The Lidar Range Equation

The fifth major subsection of the OATS model is the lidar range equation, its form, its variables and the underlying assumptions. This equation is the hub of the OATS model.

The particular form of the lidar range equation used in the OATS model is taken from Dr. Paul McManamon's analysis of lidar ranging along with his equations for transmission beam gain, $G_{Tx}$, signal to noise ratio, S/N, and effective aperture, $A_e$ (17:1). These equations are listed below.

$$P_{Rx} = P_{Tx} \ G_{Tx} \left[ \frac{\sigma_t}{4 \ \pi \ R^2} \right] \left[ \frac{A_e}{4 \ \pi \ R^2} \right] \tau^2 \qquad (1)$$

$$A_e = \frac{\pi \ D^2}{4} \qquad (66)$$

$$G_{Tx} = \frac{4 \ \pi}{\theta_B^2} \qquad (67)$$

$$S/N = \frac{P_{Rx} \ \eta}{\hbar \ \nu \ B} \qquad (68)$$

The prior three subsections defined the target's lidar cross section, $\sigma_t$, the atmospheric transmittance, $\tau$, and the range from the target to the satellite, R, for use with Equation 1. The following pages will define the terms from Equation 1 that have not been defined or explained, specifically, $A_e$, $G_{Tx}$, $P_{Rx}$ and $P_{Tx}$.

Equation 66 defines the receiver aperture, $A_e$. This equation is valid for a circular receiving aperture of diameter, D, and the aperture is simply the area defined by a circular optic with a diameter, D. However, Stimson, in his analysis of antenna gain, also uses $A_e$ and says, "Effective area is equal to physical area times aperture efficiency" (26:137) where he later labels aperture efficiency, $\eta$, (hereafter designated $\eta_A$). Combining both concepts, the new equation would be

$$A_e = \frac{\pi D^2 \eta_A}{4} \tag{69}$$

The aperture efficiency here could be less than one for reasons such as: 1) an occlusion from satellite structure, 2) occlusion from optics (like a secondary cassegrain reflector) and 3) less than 100% of the circular optic being used for collection (e.g. structure attachment points on a parabolic dish). However, the OATS model uses Equation 66 as it is written thereby assuming an aperture efficiency of one. The modeler must be cognizant of this and if $\eta_A$ is less than one, the value for D must be altered so to result in a properly proportioned value for $A_e$.

Equation 67 defines transmitter gain from beam directivity. The OATS model deviates from Equation 67 on this term and uses a more precise circular aperture assumption. The new relationship is listed below as Equation 70.

$$G_{Tx} = \frac{16}{\theta_B^2} \qquad (70)$$

In Equations 67 and 70, $\theta_B$ is the "transmit beam angular diameter" (17:1) or the full angle beam divergence measured at the 3 dB points (17:2). The deviation between Equation 67 and Equation 70 results from the basic definition of gain. Stimson defines the gain due to the directivity of an antenna in the following way,

> "The gain of an antenna is the ratio of the power per unit of solid angle radiated in a specific direction to the power per unit solid angle that would nave been radiated had the same total power been radiated uniformly in all direction..." (26:137)

Or rewriting Skolnik's gain definition in present terms,

$$G_{Tx} = \frac{4\pi}{\Omega} \qquad (71)$$

where the term $\Omega$ is defined as the beam area by Skolnik (23,262). However, for a circular antenna, $\Omega$ is a function of $\theta_B$, the beam divergence angle. Using Slater's definition of solid angle, here defined as $\Omega$,

$$\Omega = \frac{A_s}{r_s^2} \qquad (72)$$

where $A_s$ is the projected area on a sphere of radius $r_s$ (24:528). If the radius of the sphere (distance from the

54

beam origin to projected area plane) is 1, then $\Omega = A_c$.

Assuming $r_s = 1$, for small divergence angles, $\theta_B$,

$$\frac{\theta_B}{2} \approx \tan\left[\frac{\theta_B}{2}\right] = \frac{d}{2} \qquad \text{so that} \quad \theta_B \approx d \qquad (73)$$

where $d$ is the diameter of the projected circular area.

Since the projected area is $\pi\, r_s^2$ where $d = 2\, r_c$ , then

$$\Omega_{SA} = \frac{\pi}{4}\, \theta_B^2 \qquad (74)$$

so that the gain of a circular antenna is

$$G_{Tx} = \frac{4\,\pi}{\Omega_{SA}} = \frac{16}{\theta_B^2} \qquad (75)$$

The OATS model uses this relationship and is therefore built on the assumption of a circular beam.

Notice that the gain of the antenna, $G_{Tx}$, is based on the beam divergence, $\theta_B$, of the laser where $\theta_B$ is defined by the 3dB points. This is an optimistic approximation since only one-half of the laser power is within the angle defined by $\theta_B$.

The final terms requiring explanation in Equation 1 are the two power terms, $P_{Tx}$ and $P_{Rx}$. These terms are simply the power transmitted, $P_{Tx}$, and the power received, $P_{Rx}$. The transmitted power is the power in a single laser pulse

and can be calculated by dividing the energy per pulse by the duration of the pulse (pulse width). The received power is the amount of energy per time period that has reflected from the target and is collected in the receiver's optics.

To add more flexibility into the model a processing gain factor, $G$, was included. This factor is nonspecific in the OATS model and can be used to apply the additional increase in the signal from any post reception processing technique. It allows the modeler to include gains in signal strength from such techniques as coherent integration of the returned pulses but is flexible enough that it can be used for any beneficial *or* detrimental designs in the system. The application of this factor is therefore very design dependent.

The final portion of the lidar range equation that must be addressed is the signal-to-noise ratio, S/N. The OATS model assumes a shot noise-limited sensor and a bandwidth-pulsewidth product equal to one (17:2). (For example. assuming a 10 MHz bandwidth for the receiver. the matching pulsewidth would be 100 nanoseconds for a BW-PW product of one.) The assumption of a shot noise-limited sensor in the OATS model greatly simplifies the process of predicting the noise in the system. It is also validated by Boyd from his statement, "...the predominant noise source in a well-designed optical heterodyne detection system is shot noise in the photocurrent." (4,204)

From Equation 68, B is the bandwidth (17,2) or more specifically, the "i-f bandwidth" (4,204) which is the intermediate frequency bandwidth. The term $\eta$ is defined as the detector quantum efficiency (4,128), not to be confused with $\eta_A$, the aperture efficiency.

> The quantum efficiency, $\eta$, of a photoemissive surface measures its performance and is defined as the number of electrons emitted per incident photon. The quantum efficiency varies approximately from $10^{-4}$ to $5 \times 10^{-1}$ for most photocathodes and it varies as a function of the incident radiation wavelength. (22:31)

The OATS model sets the quantum efficiency to 0.1, eliminating the details of individual detectors. However, this is another function that could be combined in the processing gain. $\mathcal{G}$, if the modeler desired to vary the quantum efficiency of the system. For example, if the actual quantum efficiency to be modeled was 0.2, the processing gain, $\mathcal{G}$, could be increased by 3 dB to allow for this better quantum efficiency.

From Equation 68, the term $\nu$, is the frequency, $h$ is Planck's constant and $P_{Rx}$ is the power at the receiver (defined with Equation 1). To achieve a BW-PW product of one, the bandwidth is pre-established in the model once the pulse energy, $E_{Tx}$, and pulsewidth, PW, are set. One can combine Equations 1 and 68 (17:2) which yields the following set of relationships.

$$\frac{E_{Tx}}{PW} = P_{Tx} \qquad\qquad (76)$$

$$S/N = E_{Tx}\left[\frac{16}{\theta_B^2}\right]\left[\frac{\sigma_t}{4\pi R^2}\right]\left[\frac{\pi D^2}{16\pi R^2}\right]\left[\frac{\tau^2\eta}{\hbar\nu B\ PW}\right]\mathfrak{G} \qquad (77)$$

Simplifying with PW*B = 1 and $\eta$ = 0.1 then,

$$S/N = \left[\frac{E_{Tx}\sigma_t}{\pi\ \theta_B^2\ R^2}\right]\left[\frac{D^2}{4\ R^2}\right]\left[\frac{\mathfrak{G}\ \tau^2}{10\ \hbar\ \nu}\right] \qquad (78)$$

which is then simplified to the core lidar range equation
for the OATS model:

$$S/N = \frac{E_{Tx}\ \mathfrak{G}\ \sigma_t\ D^2\ \tau^2\ \lambda}{(2.4979\times10^{-23})\ \theta_B^2\ R^4} \qquad (79)$$

Another feature that was inserted in the computational
equations in the OATS model was for spot size. With a low
flying satellite and a large aircraft, one can conceive of
the scenario when the spot size of the laser is smaller that
the size of the aircraft. If the projected area of the
target is larger than the spotsize, then the lidar range
equation needs to be adjusted. To accommodate this, the
OATS model compares the computed spot size with the target's
projected area. If the projected area of the target is

larger than the spot size, then the spot size to projected area ratio is computed, $\chi$. This ratio is directly inserted into the range equation to correct for small spot size errors induced from the LCS equations. This direct insertion is reasonable and simple. The reasonability stems from the linear effect of projected area on the LCS. The simplicity results from the direct insertion as opposed to recalculation of the LCS for the new areas. It is important to note, however, that the laser energy is assumed to be proportionately spread among all three surfaces of the target (e.g., if the top surface of the brick represents 70% of the projected area of the brick then 70% of the laser irradiance is assumed to fall on the top surface). The actual distribution of the irradiance would be complex and a function of the pointing error probability, brick orientation and spot size.

This analysis and implementation of the spot size correction is also applicable to the sphere. With a sphere, however, as $\chi$ gets small, the equation for LCS of a sphere approaches the equation for LCS of a planar surface with no off normal angle (assuming perfect pointing). The LCS under perfect pointing conditions could be readily calculated by integrating over a partial sphere. But, since there is no such thing as a perfect pointing system (especially at these ranges) $\chi$ is directly inserted into the lidar range equation just as it is for the brick model.

The computation of the spotsize uses $\theta_B$, the 3 dB beam divergence angle. The spotsize is therefore the 3 dB spotsize. This represents only an approximation to the actual irradiance pattern at the target. A specific irradiance pattern would depend on the precise optical configuration of the laser and the perturbations the beam encountered in the atmosphere.

For both the brick and sphere models, the $\chi$ insertion technique is an approximation. Actual observations should validate these assumptions since the beam pointing error and beam jitter would be distributed about the perfect pointing and no jitter points (assuming no bias). These assumptions therefore are built around the mean of naturally occurring random pointing errors.

This spot size correction reveals another significant limitation and assumption of the OATS model. To use either computational method for calculating LCS (i.e., spot greater than projected area or spot less than projected area), the underlying assumption is that the beam is perfectly geometrically coupled (i.e., spot pattern matches target pattern). In other words, the beam spot on the target is such that it completely engulfs the target or it illuminates a portion of the target with no portion of the beam missing the target. This essentially boils down to the idealistic assumption that there is no spillage of the beam energy, even with perfect pointing. For example, if the spot

60

pattern is circular with an area equal to $\pi$ but the target pattern is that of an aircraft but also of area $\pi$, there is no way that 100% of the energy will illuminate the target since their patterns are not matched.

If the pointing is perfect and if the beam spot size is large compared to the size of the target (floodlight), then the geometrically coupled illumination assumption is not bad. If the area of the spot is on the order of the projected area of the aircraft, significant portions of the beam may not be on the target due to pattern mismatching. If the spot size is very small compared to the dimensions of the target aircraft (i.e., extremely small $\theta_B$) then the pointing accuracy will tend be the dominant source of error (either on target or off target).

Equation 79 is therefore rewritten with $\chi$ inserted to form Equation 80.

$$ S/N = \frac{E_{Tx}\ \mathfrak{G}\ \sigma_t\ D^2\ \tau^2\ \lambda\ \chi}{(2.4979 \times 10^{-23})\ \theta_B^2\ R^4} \tag{80} $$

## The Inputs

The portion of the OATS model in which the modeler is most involved is the data input segment. It is in this segment that the modeler describes the scenario for analysis.

Table 1 lists all the cued inputs for the OATS model, some of which are displayed only if the prior data entries require the additional data fields.

Certain fields in the input segment require further description. The BEAMOD field cues the user for the beam model to be used for the analysis. It allows three options. The first option asks for the desired beam width (BMDVG) in radians. With the second option, the beam divergence is assumed to be diffraction limited and uses Equation 81. This equation is used to compute the "3dB full width diffraction limited beam divergence." (17:2) This is defined below.

$$\theta_B = 1.08 \ \frac{\lambda}{D} \tag{81}$$

Therefore, the 3 dB diffraction limited BEAMOD entry cues the model to calculate the beam divergence angle from the selected effective receiver diameter (assumes receiver optics are used for beam transmission also). This likewise assumes that the aperture efficiency, $\eta_\lambda$ is 1.0 for the transmission of the beam.

If BEAMOD option 3 is chosen, the OATS model computes a beam divergence using Equation 82 (taken from 17:2) for a beam that is "not quite diffraction limited". (17:2)

$$\theta_B = 1.30 \ \frac{\lambda}{D} \tag{82}$$

## TABLE 1          INPUT DATA FIELDS

| FIELD | UNITS | DESCIPTION |
|---|---|---|
| SATALT | km | -altitude of the satellite above earth |
| LASER | | -type of laser to be studied |
| | 1 | -CO2 with carbon 12 |
| | 2 | -CO2 with carbon 13 |
| | 3 | -Holmium /YLF at 2.06 $\mu$m |
| | 4 | -Neodynium in silicate glass |
| JOULES | joules | -laser pulse energy |
| PWI | microseconds | -pulsewidth of laser pulse |
| SNdB | dB | -detection threshold S/N |
| RXmicro | microwatts | -receiver sensitivity |
| PGdB | dB | -processing gain |
| RXD | meters | -diameter of effective receiver optics |
| BEAMOD | | -model for beam divergence definition |
| | 1 | -selectable beamwidth |
| | 2 | -3dB diffraction limit |
| | 3 | -wider than diffraction limit |
| ATMOS | | -atmospheric model |
| | 1 | -clear atmosphere (no aerosol) |
| | 2 | -5 km rural haze only |
| | 3 | -clear plus selectable attenuation |
| LCSMODEL | | -model type to compute LCS |
| | 1 | -spherical model |
| | 2 | -flying brick model |
| REFLECT | % | -percentage of in band power reflected |
| SATRAK | degrees | -true heading of satellite ground track |
| TGTHDG | degrss | -true heading of target aircraft |
| OFFSET | km | -distance, target to sat ground track |

63

The next segment that requires additional data entry is atmosphere selection option, ATMOS. For atmosphere model three, the user is cued to enter an additional amount of attenuation ( in dB) for the zero degree zenith angle geometry. At all other zenith angles, the OATS model computes the additional attenuation to add to the clear atmosphere model (discussed previously under Transmittance).

The next data field requiring further data is LCSMODEL. If the spherical model is chosen, the OATS model cues the modeler for the radius of the sphere. If the flying brick model is chosen the model cues the modeler for the area of the three sides of the brick. These areas are entered in square meters. The top area should represent the projected area of the target from a top-down perspective. The frontal area (also the rear view area) is the area from a front-on perspective. The side area is likewise the area of the target as perceived from a side perspective.


## The Output Data and Calculations

The OATS model provides a variety of output data forms for the modeler to use for analysis. The method of output data selection is through the DATASLCT field. Three options are currently available for data selection:

1) the no-offset zenith angle where the S/N level first meets the previously entered required S/N

2) the no-offset zenith angle where the minimum detectable signal is first met

3) the signal power and S/N for a variation in one of the nine selectable variable.

The first of the three options outputs a no-offset zenith angle. This angle represents the point in the satellite's orbit at which the satellite can distinguish the signal return from the shot noise. Distinguishability is established by the SNdB (required S/N) field in the input. For example, if the SNdB is 3 dB and DATASLCT is set to 1, then OATS model will determine the angle at which the signal power is twice the noise power (3 dB). This is actually accomplished using a halving algorithm (7,403). Essentially, the algorithm establishes the bounds for the no-offset zenith angle and cuts the bounds in half until it converges on the actual angle. A flag is set in the OATS model if the routine does not converge. This will result in a warning being printed to the screen. The warning does not fully define the problem but just tells the modeler that the halving routine has reached 40 iterations without converging to the answer within the established accuracy limits. The modeler must decide why the convergence did not occur. Frequently, the convergence may fail because the angle is either larger than 80 degrees or the SNR will not be achieved at any angle.

Option two of the DATASLCT field will calculate the
no-offset zenith angle at which the minimum threshold for
detectability is reached.  It uses the same halving
algorithm as the SNR computations described above.  However,
the routine further goes on to calculate the time of track
for the lidar tracker.  This time of track algorithm is
built on multiple assumptions.  These are

1) the satellite is in a stable circular orbit

2) the pointing mechanism is precise enough to keep the
   beam on the target

3) there is no interrupt of tracking through the
   doppler null

4) there are no track interruptions for any atmospheric
   anomalies  (such as clouds, dust storms etc.)

5) there are no interruptions for system anomalies
   (such as noise)

6) the geometry of track is symmetrical (a zenith angle
   of 30 degrees is equivalent to a zenith angle of -30
   degrees)

7) the target aircraft remains straight and level and
   free from terrain masking

With these assumptions, option two returns the time of
possible track (i.e., the signal level is above minimum
detectable signal power requirements) in minutes.

An important note here is necessary to show the major
limitation in the first option.  Option one will return the
zenith angle that meets the SNdB threshold but does not
consider the signal level at that angle.  The modeler must
be careful to check the power threshold (minimum detectable

signal) when using option one so as to avoid finding an angle where the SNdB threshold is met but the power threshold is not.

The final option in the data selection process is designed for data generation. It gives the modeler the option of designating one of nine variables as the variable to increment and outputs the signal power and signal-to-noise ratio for each increment of the selected variable. For example, the modeler could select to increment the pulse power from 1 to 10 joules (step size of 1) while holding all other variables constant. For each incremental value of the pulse power, a data line is printed. Each data line contains the pulse power, the receiver power and the signal-to-noise ratio for that incremental run. The nine options to increment are:

1 - no-offset zenith angle
2 - satellite altitude
3 - laser pulse power
4 - laser pulse width
5 - receiver threshold sensitivity
6 - required signal-to-noise ratio for detection
7 - diameter of the receiver collection optics
8 - reflectivity of the target's skin
9 - target offset distance from satellite ground track

For the modeler's convenience, the data output for this option is sent to a file called "D.DAT" which is written to an output disk for later use. This output is then readily accessible for data plotting or storage.

An additional limitation of the OATS model is that it does not consider probability of detection nor probability of false alarm. The data output and comparisons throughout the model are done on power thresholds *only*. The modeler has no automated probability of detection capability.

The OATS model has many limitations formed by the assumptions made during its construction. These limitations, however, are soft and can easily be altered by a few lines of code. The core of the model is the lidar range equation (Equation 1) and is supported by subfunctions that can be manipulated to modify the program for additional analysis.

# IV.  RESULTS

The basic question that this thesis set about to
answer is whether or not a lidar system on a satellite could
be used to track aircraft.  The OATS model was built to do
this analysis with a wide range of options available for
analytical comparisons.  If the OATS model methodology is
accepted as valid, realistic lidar parameters must be es-
tablished for input data.  For example, if the OATS model
were run using a pulse power of 10 joules for the laser,
before the results can be claimed as acceptable the entering
arguments (e.g., 10 joule pulse) must be accepted as valid,
reasonable and realistic.

Because the OATS model contains so many variables for
analyzing aircraft trackability from space, a set of ac-
cepted constants was established.  For the analysis that
follows, the following variables are set up as constants.

| | | |
|---|---|---|
| Pulsewidth | PW | 0.1 microseconds |
| Rx Sensitivity | RxSens | 0.001 microwatts |
| Required S/N | SNR | 14 dB |
| Processing Gain | PG | 3 dB |
| Satellite Track | SATRAK | 0 degrees |
| Target Heading | TGTHDG | 40 degrees |
| Beam Divergence | BMDVG | model # 3 |
| Target | LCSMODEL | model # 2 (brick) |
| Target size | ------ | 5  sq meters front<br>21 sq meters top<br>12 sq meters side |

Once the above variables were established as constants, another set of variables was baselined for comparison. These baseline variables are listed below with their base-line values.

| | | |
|---|---|---|
| Atmosphere | ATMOS | model #2 (5 km haze) |
| Zenith Angle (no-offset) | DNOZANG | 30 degrees |
| Satellite Altitude | SATALT | 700 km |
| Pulse Power | Joule | 1 joule |
| Diameter of Optics | RXD | 0.8 meters |
| Tgt Reflectance | REFLECT | 21 % |
| Tgt Offset | OFFSET | 100 km |

With the above set of constants and baseline values, the OATS model was run for all four types of lasers listed in the program. For each laser type, a curve plotting the receiver power vs. no offset zenith angle was developed. These curves are shown in Figure 12 for the atmosphere with haze and in Figure 13 for the atmosphere without haze.

From Figure 12, one can conclude that holmium yields the best return for the same system conditions. In reality however, many considerations go into a determination of "best" such as cost, weight, size, efficiencies etc. For the sake of limiting the scope of this thesis, holmium was chosen as the optimum laser medium for aircraft tracking strictly on its performance diagrammed in Figure 12. All further analysis is based on holmium, in a 5 km haze atmosphere.

70

# RX POWER vs ZENITH ANGLE

(5 km HAZE)
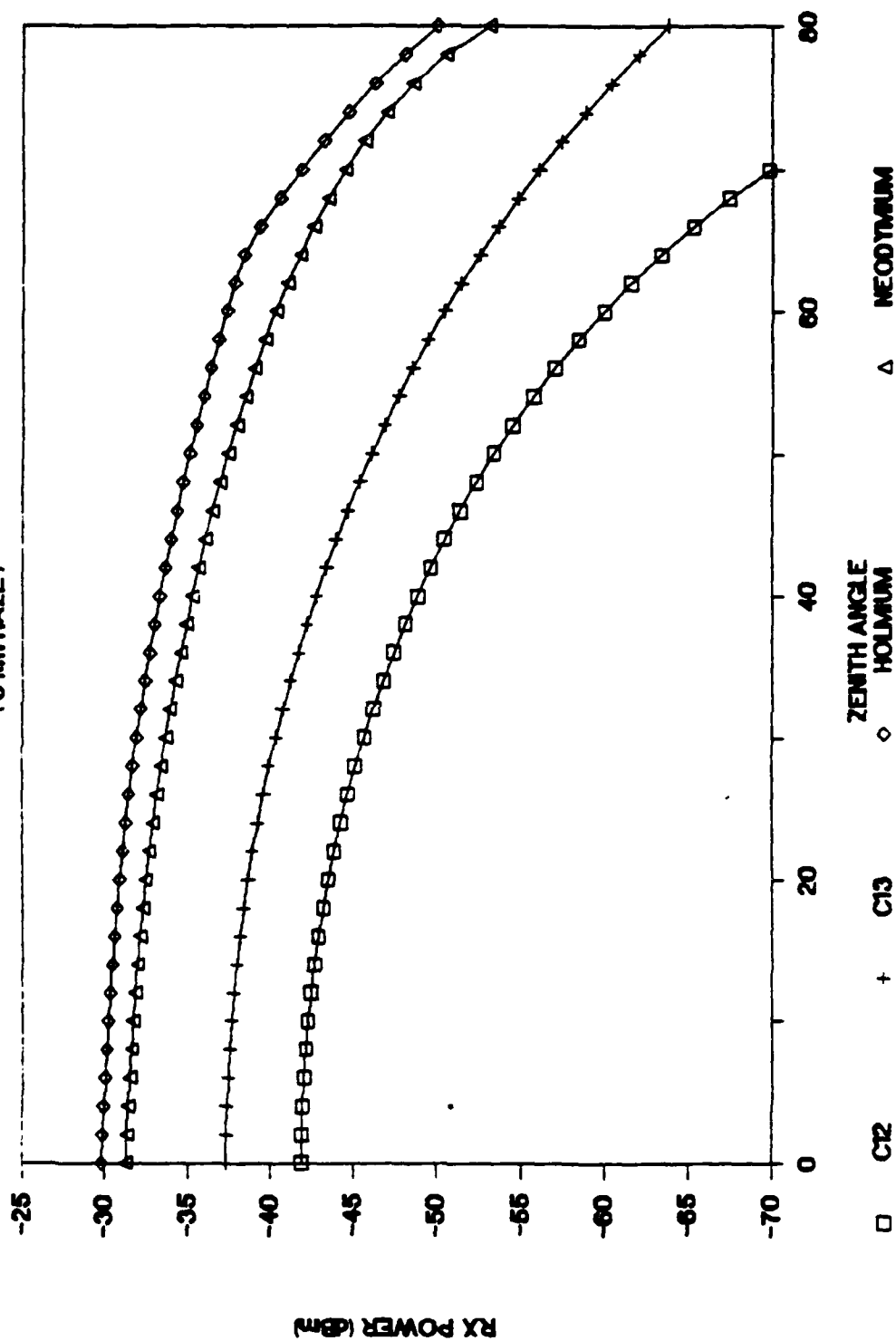


FIGURE 12 LASER COMPARISON (with Haze)

# RX POWER vs ZENITH ANGLE
**(clear atmosphere)**
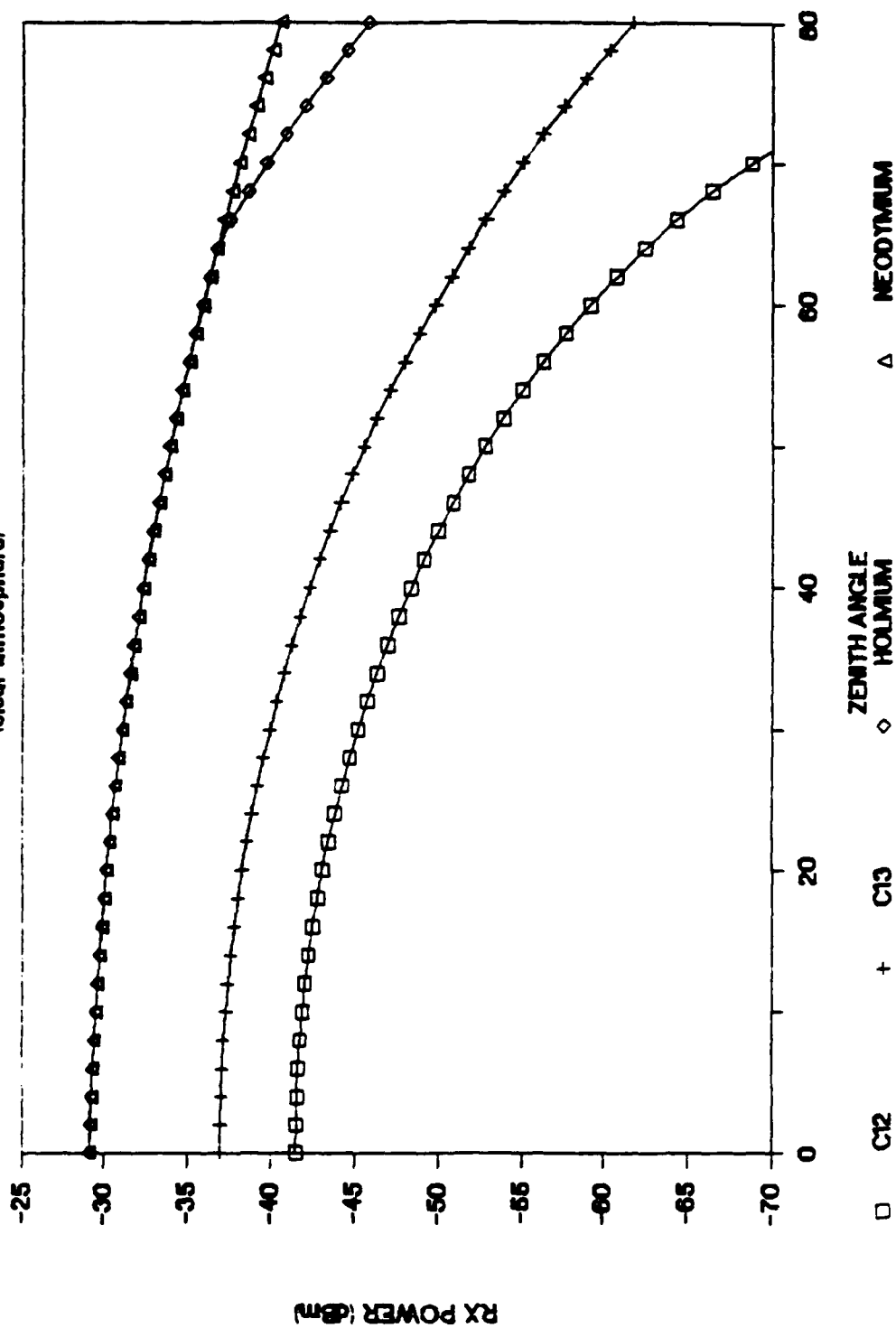


FIGURE 13 LASER COMPARISON (no Haze)

72

Various baseline parameters are changed in the next series of tests to determine the range of feasibility for a holmium laser in the 5 km atmosphere.

The first parameter to be varied was the no offset zenith angle. Although this was accomplished to form the holmium curve in Figure 12, Figure 14 shows this curve standing alone. Notice in Figure 14 the "dogleg" at the 64 degree point on the curve. This change in the curve is a result of the spotsize algorithm. From 0 degrees to approximately 64 degrees, the spot size of the laser was smaller than the projected area of the target. This is reasonable since an aircraft (or brick) has a larger projected area from a top perspective than a frontal/rearward perspective. After 64 degrees, the target's projected area is dominated by the smaller frontal/rearward surface. The spot size to projected area ratio, $\chi$, becomes one and no longer limits the LCS equations in the model. The OATS model lists the value for $\chi$ as the program is executing and therefore gives the modeler an insight on the occurrence of "doglegs" prior to plotting data.

During the next set of OATS model runs, the satellite altitude was allowed to vary. By cueing on available tracking time (TRAKTIME), the optimum satellite altitude was computed. This is graphically shown in Figure 15. Recall that track time is the time during a single satellite orbit that the target is trackable (within minimum detectable

73

# RX POWER vs ZENITH ANGLE

## ( HOLMIUM in 5 km HAZE )
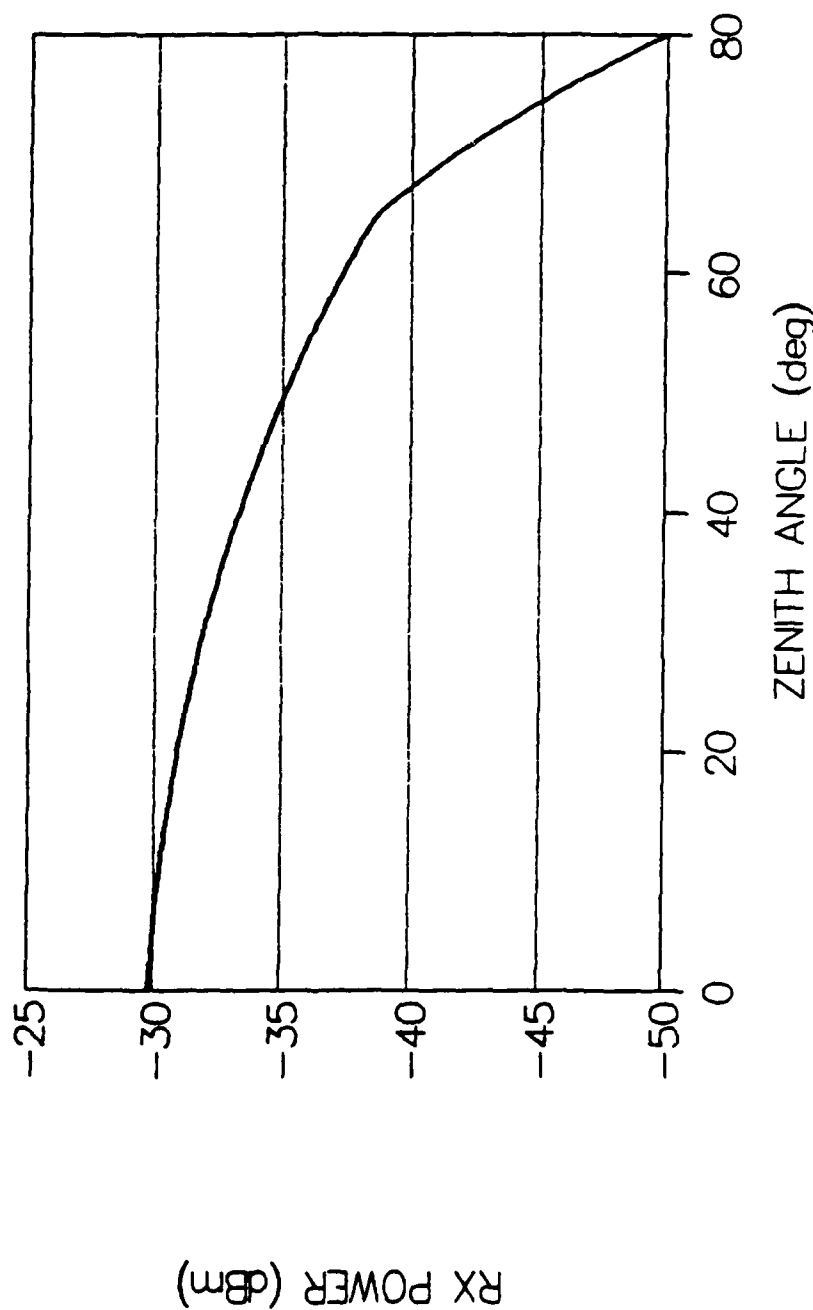


**FIGURE 14  Rx POWER  vs  ZENITH ANGLE**

# TRAKTIME vs SATALT

## ( HOLMIUM in 5 km HAZE )
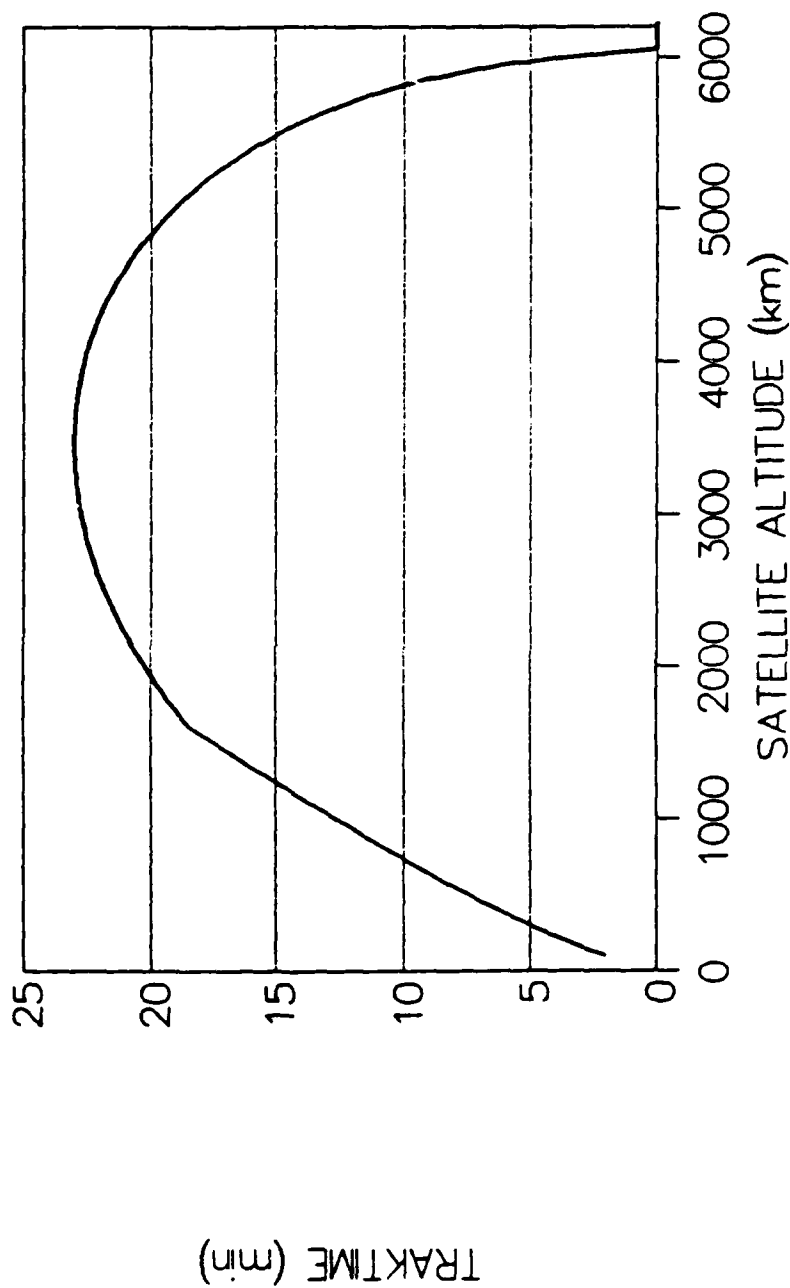


**FIGURE 15 TRAKTIME vs SATALT**

signal thresholds). For the baseline that was previously established, the maximum available single orbit track time is approximately 23 minutes for a satellite at approximately 3500 km altitude.

The plot of satellite altitude vs. receiver power is shown in Figure 16. As is predictable, the receiver power drops off as the distance increases. Again, however, one can see an apparent anomaly at approximately 1600 km on the plot. This discontinuity in the curve is attributable again to the spotsize correction algorithm. As the spot size grows beyond the projected area of the target, the power received at the satellite changes at a different rate also. Beyond approximately 1600 km, the beam becomes a "flood light", totally illuminating the target's silhouette. Before 1600 km, the beam was smaller that the target's silhouette and, therefore, only illuminated a "patch" on the target.

The next set of data shows the change in receiver power as the offset distance increases. Recall that the offset distance is the distance from the satellite's ground track to the target, always a perpendicular projection from the satellite's ground track line. This is the smallest distance from the target to the satellite's ground track. From the plot, Figure 17, one can see that the change appears linear. The relationship is not linear since the vertical axis is logarithmic. Establishing a minimum detection level

# RX POWER vs SAT ALTITUDE
## ( HOLMIUM in 5 km HAZE )
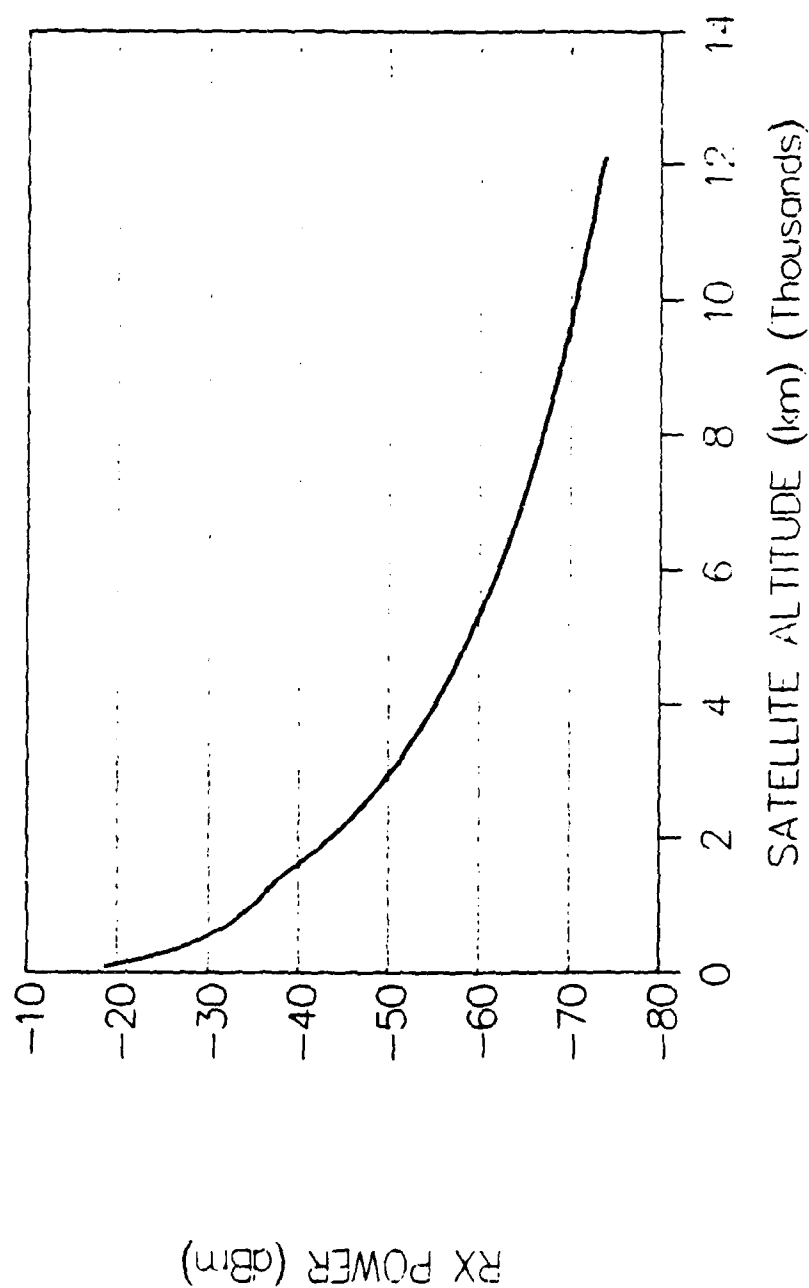


**FIGURE 16 Rx POWER vs SATALT**

77

# RX POWER vs OFFSET

## ( HOLMIUM in 5 km HAZE )
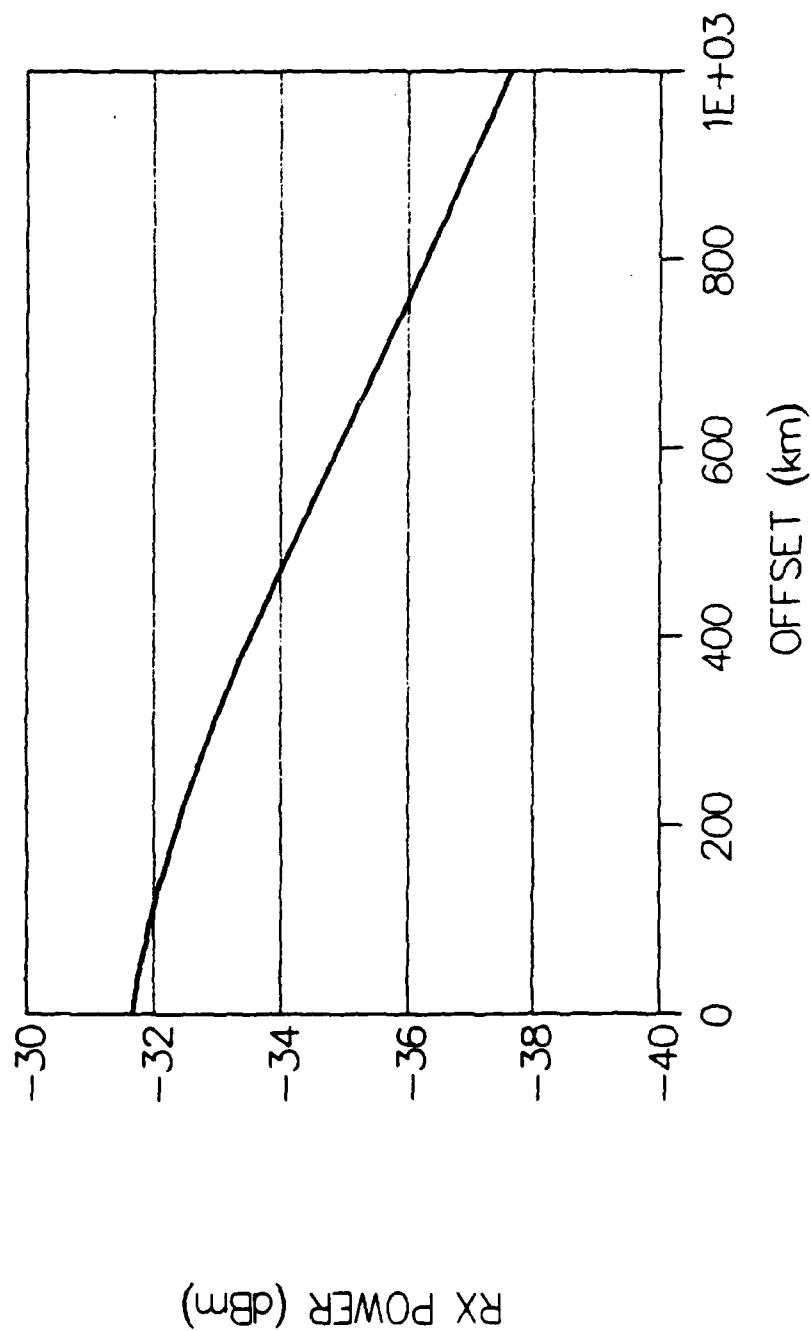


FIGURE 17 Rx POWER vs OFFSET

78

at 0.001 microwatts (-60 dBm on the scale), it appears that the lidar tracking system could easily track targets of this size out as far as 1000 km from the satellite's ground position. This does, however, assume a very clean atmosphere.

The next parameter of variation is target reflectance. Measured as a percentage of power reflected, this parameter is a function of the target's skin, whether paint or bare skin material. This is graphically displayed in Figure 18. Notice that the rate of change of the curve in the lower reflectance region (under 20% reflectance) is very large while the rate of change beyond 50% is relatively constant. This curve reveals two significant points to consider if such a lidar tracking system were to be built. The first is that targets that purposely wanted to be tracked should use a paint that is highly reflective at the wavelength in question. If a paint with a reflectance value of 80% were available, the target could have a receiver power 30 dB above the minimum detectable signal level (using these optimistic baseline values). This produces a large trackability domain for the target. The other point to consider is that targets that do not want to be tracked, could greatly complicate the tracking problem by using a highly absorptive paint. Each small increase in absorptivity below 10% yields a great decrease in the amount of reflected power. Note, however, that even at a reflectivity of 0.04%, the defined target is still trackable at a no-offset zenith

# RX POWER vs REFLECTANCE
## (WITH 5 km HAZE)
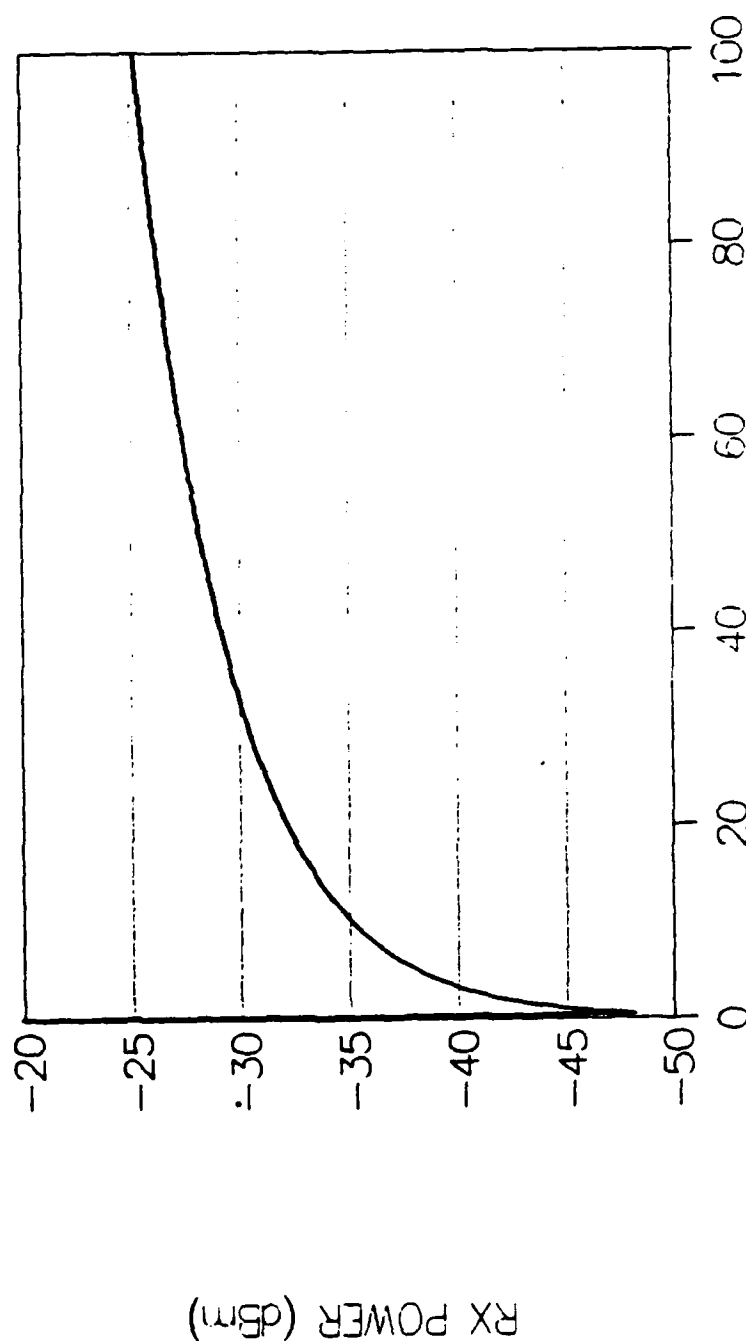


FIGURE 18  Rx POWER vs Reflectance

angle of 30 degrees and an offset of 100 km. *This shows that the window of trackability is still relatively large. A 30 degree no offset zenith angle results in a track time of approximately 1.8 minutes, more than enough to establish a target's position, heading, and speed.*

The next two variables that were changed for analysis are functions of the lidar system itself. These parameters are the laser pulse power or pulse energy and the diameter of the optics.

The pulse energy was varied over two orders of magnitude. This range shows a very significant result in the under-2 joules region. In this region, small changes in pulse energy resulted in dramatic change in receiver power. Above 4 joules, the small increases in pulse power yield relatively smaller increases in receiver power. Again, notice that even at small pulse energy values, the track-ability of the target is large. The receiver power is more than 10 dB above the minimum detectable threshold for pulse energy values as low as 0.1 joules. The receiver power is plotted against the pulse energy in Figure 19.

Figure 20 plots the diameter of the optics, whether mirrors or lenses, against the receiver power. As opposed to the other plots, this plot shows a very large change in receiver power for small changes in diameter of the optical system. The plot shows that certain diameters yield re-ceiver powers below the minimum detectable threshold (set to

# RX POWER vs PULSE ENERGY

## ( HOLMIUM in 5 km HAZE )
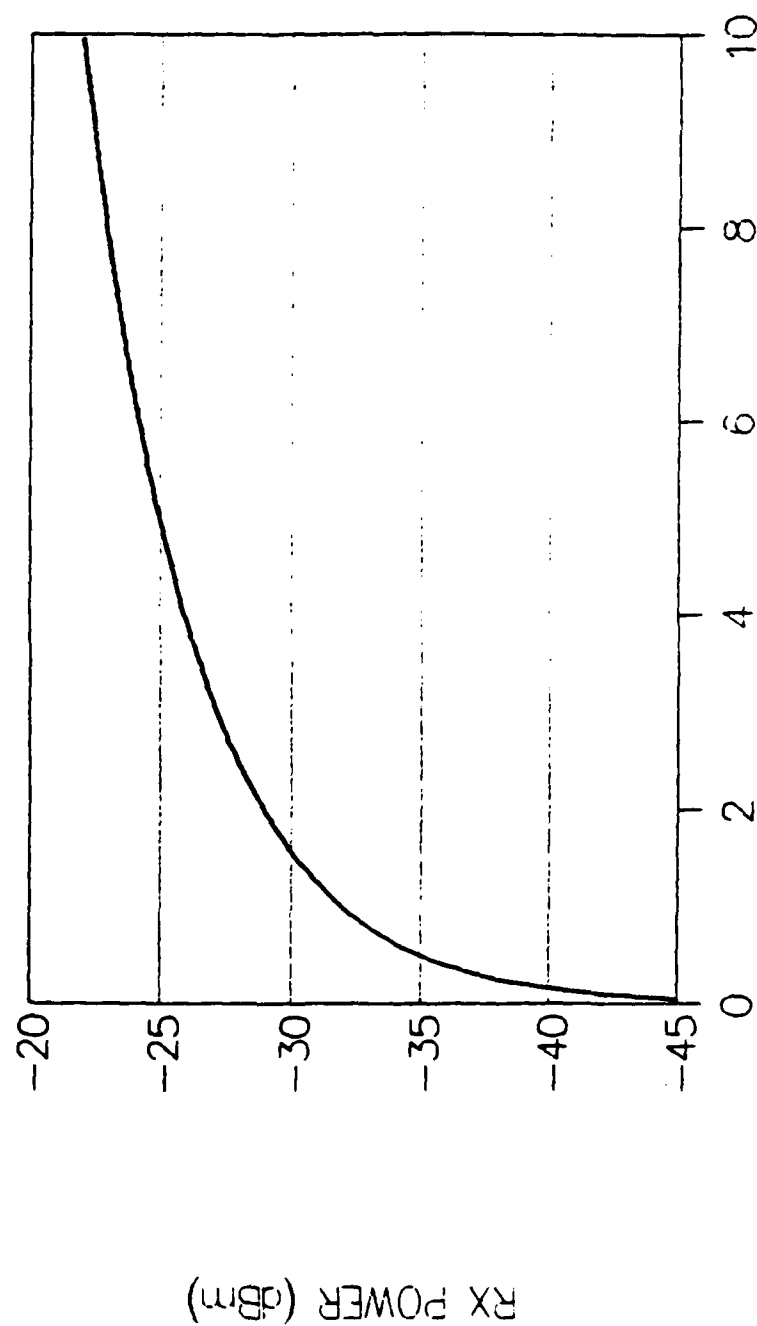


FIGURE 19 Rx POWER vs Pulse Energy

82

# RX POWER vs OPTIC DIAMETER

## ( HOLMIUM in 5 km HAZE )
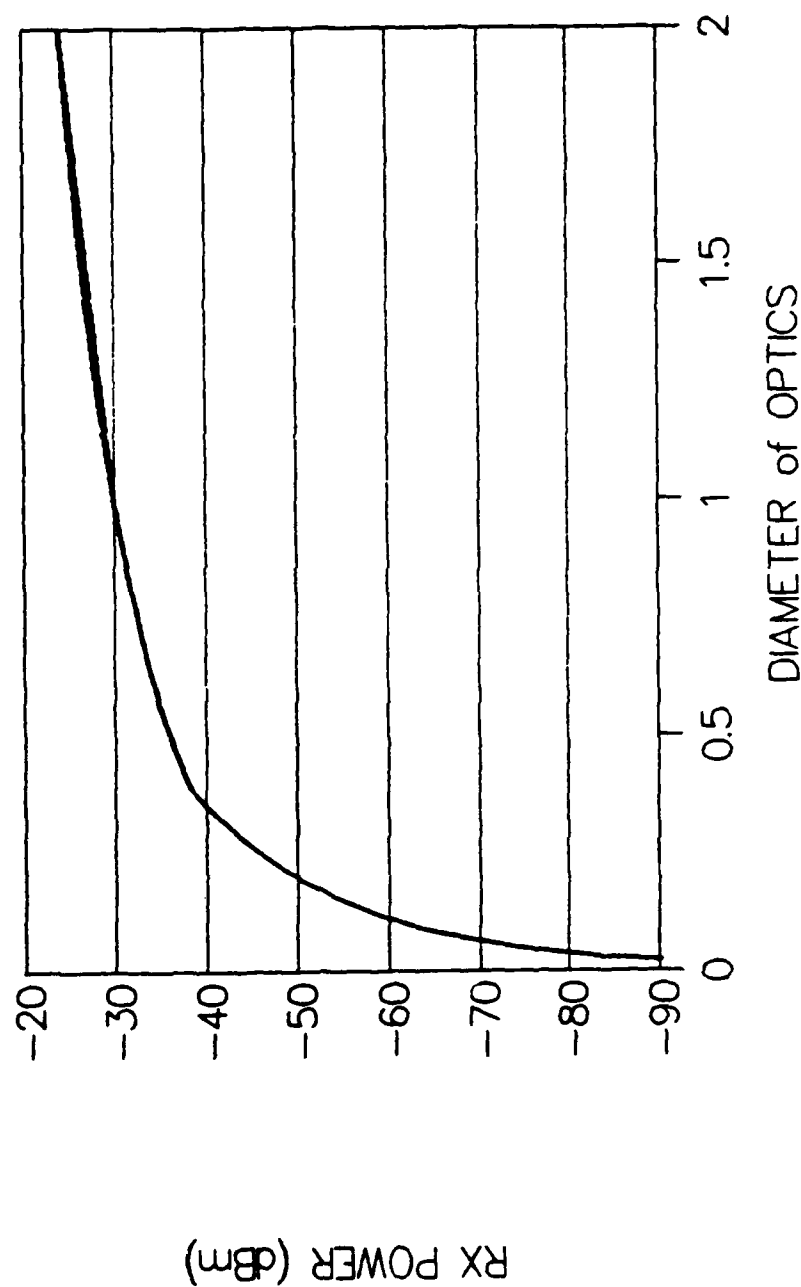


FIGURE 20 Rx POWER vs Optic Diameter

83

-60 dBm). The curve levels off after about 1 meter diameter with a slope showing approximately 3 dB of gain for each 50 cm in the diameter. Small diameter optics *do not appear to be practical* since the receiver power drops rapidly under 0.5 meters diameter. For spaceborne lidar systems however, size and weight are extremely important and very large diameter systems are also constrained by the space vehicle constraints.

## CONCLUSIONS AND RECOMMENDATIONS

From the results, one could hastily conclude that holmium lidar tracking of aircraft is easy and applicable over a wide range of system and target characteristics. However, the results must be viewed from a proper perspective. The assumptions upon which the OATS model is built are crucial and directly determine the results of the model. The assumptions must therefore always be included in any discussion of the results.

In general, the assumptions which were made in constructing the OATS model are "optimistic", resulting in better detectivity than can be expected in actual use. However, even with the optimism, this study does show that under relatively ideal conditions, lidar tracking of aircraft from space may be feasible. Further study is required to fully develop the feasibility envelope for such a system.

The areas of further study in this field can be clustered into three main categories. These areas are:

    1 -the satellite system itself, which includes such
       areas as the laser, receiver, orbital control,
       tracking and processing algorithms, etc.

    2 -the environment, which includes further atmospheric
       attenuation analysis for more types of atmospheres

    3 -the target, which includes further study of aircraft
       reflection characteristics.

Some specific area of improvement are therefore presented for future study and/or improvement for the OATS model.

The first recommended improvement to the OATS model is to obtain FASCODE atmospheric attenuation coefficients commensurate with an atmosphere containing some clouds. This improvement could be used to estimate how often a target could be expected to be trackable. For now, the results show excellent results for cooperative atmospheres only, the noncooperative atmospheres need to be examined.

The next improvement, alluded to earlier, is to correct the ranging algorithm for optical path length instead of the direct path length assumption used within. The maximum error for this approximation in the far IR wavelengths is approximately 2% ($\theta = 90°$). The quickest method to achieve better ranging would be to use the range value already established in FASCODE. These values, taken when the attenuation values are taken, can be fit to a curve (just as the transmittance values are) and incorporated into the OATS model as a fifth-order polynomial (just like transmittance).

The next improvement is the addition of doppler considerations. The structure in the OATS model already establishes the geometry for doppler calculations. A window defining doppler tracking requirements (i.e. amount of doppler shift necessary for tracking) could be added to show

where the doppler null would preclude tracking and define where tracking would be re-established.

To maintain the realism of the model, further noise sources should be added. In doing this, one may decide to include actual receiver configurations, materials and circuitry so as to get a better noise figure. Different configurations could be added as options into the model just as different lasers at specific resonances are currently incorporated.

Another consideration that should be considered for further work in this area is to re-establish the coordinate system for the geometry to a geocentric reference frame. This reference frame would provide an opportunity to model several satellites, several targets and do more complex multi-target and multi-satellite analysis. More exact analysis could be performed with offset targets. Currently, the OATS model is limited in its accuracy as the offset distances grow larger. Precise spherical geometry could be used to compute accurate geometries for large offset distances.

One of the possible, albeit difficult to obtain, improvements to the OATS model would be to add actual aircraft lidar cross section data along with actual skin paint reflectance values. If this data were available, the applicability of the model to actual aircraft would be

greatly enhanced. It would also tend to validate or refute the flying brick model. It may even reveal a potential improvement for the flying brick model that would increase its applicability.

The next bundle of recommendations relate to side investigations and are not necessarily improvements to OATS. The first of these investigations would be the study of the potential use of this lidar system in a bistatic scenario. Bistatic geometries could add another dimension to the system capabilities that were lost from clouds or non-diffuse reflections.

This proposed orbital lidar system would need very fine beam steering capabilities to accomplish its assigned tasks. Analysis of precision high power beam steering could be the "green light" or the "red light" for an entire program like an orbital lidar. If no technology exists to steer the beam in the directions required, then the system is impractical. Along with beam steering, one would need to develop scan algorithms for searching, acquiring and/or tracking. A simulation model would be an excellent search, acquisition and track evaluation tool and could use the OATS model as a subroutine to the main simulation program.

Another potential simulation for system design would be to design a model to test different satellite constellations for multiple orbital lidars. One would establish a certain

criterion for coverage and proceed to build up constellation configurations to meet the coverage requirements. Again, this one study could show the tracking from space concept as infeasible due to sheer number of satellites required. Then again, it may show that orbital lidar systems are maximized for certain satellite configurations.

The final and least precise study that must be accomplished is a cost analysis. This would follow the configuration study. Once the configuration study revealed the number of satellites required, then a cost for a space-based tracking system could be assessed.

A final recommendation here is from an idea that Dr. Paul McManamon had during a discussion. A space-based lidar system that was built as a sensor for the Strategic Defense Initiative could potentially be used for tracking aircraft as well (18). Expanding on the multi-use idea, one can easily find scores of uses for a lidar in space. Once in an established orbit, it could be used to track shuttle missions, track satellites, and even space debris. The same system could be used for atmospheric and environmental study. For example, an·orbital lidar could potentially track migrating Canadian geese and use the data for aircraft avoidance or biological studies.

# APPENDIX A    OATS MODEL CODE

```
'*****************************************************************
'  OPTICAL AIRCRAFT TRACKING SYSTEM (OATS)  MODEL          ****
'_____
DECLARE SUB MENU ()
DECLARE SUB CHGMENU ()
DECLARE SUB CALC ()
DECLARE FUNCTION BETA! ()
DECLARE FUNCTION dBm! (PWX)
DECLARE FUNCTION LCS (ZANG)
DECLARE FUNCTION TRANSMIT! ()
DECLARE FUNCTION RANGE! (SATALT)
DECLARE FUNCTION SPOTSZ! (BMDVG, RNG)
DECLARE FUNCTION TRAKTIME! ()
DECLARE FUNCTION TPAREA! ()
COMMON SHARED ATTEN, ATMOS, NOZANG, ZORNG, R, A1, A3, A2, X1, OFFSET, SATALT,
--ZANG
COMMON SHARED JOULES, DNOZANG, T, RNG, TLCS, SZ, BMDVG, RXAREA, LCSMODEL,
--RADSPHR
COMMON SHARED C1#, C2#, C3#, C4#, C5#, CI#, PW, WL, PWX, S, PG, Z, LASER,
--BEAMOD
COMMON SHARED SNdB, DATASLCT, SATRAK, TGTHOG, PWI, RXmicro, PGdB, RXD, REFLECT
COMMON SHARED SLCTR, RA1, RA2, RA3, RXSENS, SNR, CHKR1, CHKR2, CHI
OPEN "D.DAT" FOR OUTPUT AS #1
CLS
LOCATE 4, 1
COLOR 2
PRINT "  WELCOME TO THE OPTICAL AIRCRAFT TRACKING SYSTEM MODEL  (OATS) "
PRINT
PRINT "-------------------VERSION 1.1   21 NOV 1988------------------"
PRINT
PRINT "OATS is a computer model of a laser radar (LIDAR) system used to track"
PRINT "aircraft.  It offers a wide range of options for engineering and "
PRINT "scientific use with a variety of output options.  Specific assumptions"
PRINT "imbedded in this model are explained in the thesis document that goes"
PRINT "with this program.  "
COLOR 3
PRINT
PRINT
PRINT "-----------------------------CAUTION----------------------------------"
PRINT "    Use of this program without understanding the assumptions"
PRINT "    upon which it is built may cause undo embarassment & harm"
PRINT "                    YOU WERE WARNED !"
PRINT "----------------------------------------------------------------------"
COLOR 2
PRINT
PRINT
PRINT
```

```
PRINT "  This version of OATS is specifically designed for space-based
--applications"
PRINT "  It assumes a target at low altitude (10 meters) and offers four
--different "
PRINT "  laser types to chose from."
LOCATE 25, 21
INPUT "PRESS RETURN TO CONTINUE"; PR$
CLS
INPUT "ENTER SATELLITE ALTITUDE IN KILOMETERS"; SATALT
        SELECT CASE SATALT
          CASE IS < 120
            CLS
            PRINT "---------WARNING   WARNING    WARNING----------------
            PRINT "------------- THIS IS PRETTY LOW -------------------- "
            PRINT
          CASE IS > 30000
            CLS
            PRINT "---------WARNING              WARNING
--WARNING--------"
            PRINT "------------ THIS IS VERY HIGH FOR A TRACKING SATELLITE
--------"
            PRINT
          CASE ELSE
            PRINT
        END SELECT

CHOSELASER: PRINT
PRINT "ENTER THE NUMBER FOR THE TYPE OF LASER THAT YOU DESIRE TO TEST"
PRINT "        1 -  CO2 with normal Carbon 12 molecules"
PRINT "        2 -  CO2 with Carbon 13 (isotope) molecules"
PRINT "        3 -  HOLMIUM/YLF centered at 2.06 micrometers"
PRINT "        4 -  NEODYNIUM in silicate glass"'
----------------------------------------------
'Wavelength data from the following sources
'CO2 wavelengths from "The CO2 Laser" by W.J.Witteman
'                    Berlin:Springer-Verlag, 1987
'                    P20 line for C-12----page 24
'                    P20 line for C-13----page 27
'Holmium wavelength from Ken Schepler, AFWAL
'                    telephone conversation 13 Oct 1988
'Neodymium wavelength from "CRC Handbook of Laser Science &
'                    Technology Volume V: Optical
'                    Materials Part 3: Applications,
'                    Coatings and Fabrication"
'                    Editor Marvin J. Weber
'                    Boca Raton Florida:CRC Press Inc.
'                    1987 ---page 363,
'                    TYPE- Silicate glass
'                    Glass Designation - LG-660
'                    Manufacturer - Schott
INPUT LASER
```

```
          SELECT CASE LASER
                CASE 1
                   WL = 10.59104 / 1000000
                         PRINT
                CASE 2
                   WL = 11.1494 / 1000000
                         PRINT
                CASE 3
                   WL = 2.06 / 1000000
                         PRINT
                CASE 4
                   WL = 1.057 / 1000000
                         PRINT
                CASE ELSE
                   PRINT
                   PRINT "INPUT ERROR ----TRY AGAIN WITH A GOOD VALUE"
                   GOTO CHOSELASER
                END SELECT
                PRINT
INPUT "ENTER LASER PULSE ENERGY (in Joules)"; JOULES
PRINT
INPUT "ENTER PULSEWIDTH OF EACH LASER PULSE (in microseconds)"; PWI
PW = PWI / 1000000
PRINT
PRINT
"==================================================================="
PRINT "NOTE: Model assumes a Bandwidth-pulsewidth product of 1 for S/N
--calculations"
PRINT
"==================================================================="
PRINT
INPUT "ENTER REQUIRED S/N VALUE(in dB)"; SNdB
SNR = 10 ^ (SNdB / 10)
PRINT
INPUT "ENTER THE RECEIVER SENSITIVITY (in Microwatts)"; RXmicro
RXSENS = RXmicro / 1000000
PRINT
INPUT "ENTER PROCESSING GAIN (in dB)"; PGdB
PG = 10 ^ (PGdB / 10)
PRINT
INPUT "ENTER EFFECTIVE DIAMETER OF THE RECEIVING OPTICS (in meters)"; RXO
RXAREA = (3.14159265# * (RXD ^ 2)) / 4
DIVG:
PRINT
PRINT "ENTER LASER BEAM MODEL FOR THE BEAM DIVERGENCE"
PRINT "                    1 - SPECIFY 3dB BEAM DIVERGENCE MANUALLY"
PRINT "                    2 - USE RCVR DIAMETER & 3dB DIFFRACTION LIMIT"
PRINT "                    3 - USE RCVR DIAMETER & WORST THAN DIFFRACTION LIMIT"
INPUT BEAMOD
          SELECT CASE BEAMOD
             CASE 1
```

```
                    INPUT "ENTER BEAM DIVERGENCE (in Radians)"; BMDVG
                CASE 2
                    BMDVG = 1.08 * WL / RXD
                CASE 3
                    BMDVG = 1.3 * WL / RXD
                CASE ELSE
                    PRINT "TRY AGAIN,   INPUT VALUE WAS IN ERROR  "
                    GOTO DIVG
            END SELECT
GainTX = 12.56637062# / (BMDVG ^ 2)


CHOSEATMOS: PRINT "    "
PRINT
PRINT "ENTER NUMBER FOR THE ATMOSPHERIC MODEL DESIRED"
PRINT "          1 - CLEAR, no aerosols"
PRINT "          2 - HAZE, 5 km visibility rural type aerosol"
PRINT "          3 - SELECTED ATTENUATION, manually entered attenuation"
INPUT ATMOS
        SELECT CASE ATMOS
                CASE 1, 2
                   PRINT
                CASE 3
        PRINT " ENTER THE ATTENUATION TO ADD TO THE ALREADY EXISTING"
        PRINT " ATTENUATION FROM THE MOLECULAR ABSORPTION (in dB)"
        PRINT " i.e. 50 % attenuation from an aerosol would be 3dB"
        PRINT " entry is for ONE-WAY passage through the atmosphere"
        PRINT " at a zenith angle of ZERO (straight up through the
--atmosphere)"
        PRINT " --an exponential curve (trans vs range) is used for all"
        PRINT "    zenith angles other than zero."
        INPUT ATTENdB
        ATTEN = 10 ^ (ATTENdB / 10)
                CASE ELSE
                    PRINT
                    PRINT "INPUT ERROR ----TRY AGAIN WITH A GOOD VALUE"
                    GOTO CHOSEATMOS
        END SELECT


CHOSEMODEL: PRINT
PRINT "ENTER TARGET CROSS SECTION MODEL"
PRINT "          1 - TARGET IS A SPHERE"
PRINT "          2 - TARGET IS A BRICK"
INPUT LCSMODEL
        SELECT CASE LCSMODEL
            CASE 1
                INPUT "WHAT IS THE RADIUS OF THE SPHERE IN METERS"; RADSPHR
                PRINT "WHAT IS THE REFLECTANCE OF THE SPHERE ?"
                PRINT "reflectance is that percentage of energy at the "
                PRINT "wavelength of interest that is reflected (between 0 TO
--100)"
                INPUT REFLECT
```

```
                        R = REFLECT / 100
                   CASE 2
                     PRINT "THE FLYING BRICK MODEL IS A THREE DIMENSIONAL MODEL"
                     PRINT "OF AN OBJECT SIMPLIFYING THE TARGET TO THREE ORTHOGONAL"
                     PRINT "PLANES LIKE THREE SIDES OF A BRICK.  THEREFORE, THE THREE"
                     PRINT "FACES OF THE SYMETRICAL BRICK REPRESENT THE PROJECTED
--AREA"
                     PRINT "OF THE TARGET FROM A FRONTAL/REAR VIEW, FROM A TOP VIEW
--AND"
                     PRINT "FROM A SIDE VIEW ... essentially the target's silhouette "
                     INPUT "ENTER THE  FRONT / REAR  PROJECTED AREA (sqr meters)"; RA1
                     INPUT "ENTER THE TOP PROJECTED AREA (sqr meters)"; RA2
                     INPUT "ENTER THE SIDE PROJECTED AREA (sqr meters)"; RA3
                     PRINT "WHAT IS THE REFLECTANCE OF THE SKIN OF THE TARGET ?"
                     PRINT "reflectance is that percentage of energy at the "
                     PRINT "wavelength of interest that is reflected (between 0 to
--100)"
                     INPUT REFLECT
                        R = REFLECT / 100
                   CASE ELSE
                     PRINT "*********************************************************"
                     PRINT
                     PRINT "   -----   INPUT MUST BE 1 or 2.....TRY AGAIN  -----"
                     PRINT
                     PRINT "*********************************************************"
                     GOTO CHOSEMODEL
                 END SELECT

        '------------------------------------------'


HDGINPUT: PRINT
INPUT "ENTER SATELLITE GROUND TRACK HEADING REFERENCING TRUE NORTH (degrees)";
SATRAK
INPUT "ENTER TARGET HEADING REFERNCING TRUE NORTH (degrees)"; TGTHDG
XXXX = BETA
IF CHKR1 = 1 GOTO HDGINPUT
IF CHKR2 = 1 GOTO HDGINPUT
'---------------------------------------------------------------------
PRINT "The offset distance is the smallest distance from the target to the
--satellite's"
PRINT "ground track.  It therefore scribes a line that is orthogonal with the"
PRINT "satellites ground track"
INPUT "ENTER OFFSET DISTANCE (in kilometers)"; OFFSET
PRINT
PRINT "ENTER TYPE OF DATA DESIRED"
PRINT "   1 - Calculate the NOZANG where the S/N meets required level"
PRINT "   2 - Calculate the NOZANG where the minimum detectible pwr is met"
PRINT "   3 - Make one parameter vary and calculate min pwr & S/N over a
--range"
INPUT DATASLCT
ALPHA:
```

```
A1 = ABS(RA1 * (COS(BETA)) ^ 2) + (RA3 * (SIN(BETA)) ^ 2)
A2 = RA2
A3 = ABS(RA3 * (COS(BETA)) ^ 2) + (RA1 * (SIN(BETA)) ^ 2)


'----------------------------------------------------------------
SELECT CASE DATASLCT
   CASE 1
      RIGHT = 80: LEFT = 0: MID = 40
      COUNT = 0
LAP1: COUNT = COUNT + 1: DNOZANG = MID: NOZANG = DNOZANG / 57.29577951#
      IF COUNT = 40 THEN
         CLS
         PRINT "-----------------------------------------------------"
         PRINT "                         *** WARNING ***   "
         PRINT " count has reached 40 without converging to an answer "
         PRINT
"-----------------------------------------------------------------"
         GOTO QUIT1
      END IF
      CALC
      delta = S - SNR
      SELECT CASE delta
         CASE IS > .0001
            LEFT = MID
            MID = (LEFT + RIGHT) / 2
            GOTO LAP1
         CASE IS < -.0001
            RIGHT = MID
            MID = (LEFT + RIGHT) / 2
            GOTO LAP1
         CASE ELSE
            PRINT "+++++++++++++++++    BINGO YOGI    ++++++++++++++++++++++++"
         END SELECT
QUIT1: PRINT
      PRINT
"                                                                "
      PRINT
      PRINT "NO OFFSET ZENITH ANGLE FOR THE REQUIRED SIGNAL TO NOISE RATIO IS"
      PRINT "                        ", MID
      PRINT
"                                                                "
'----------------------------------------------------------------


      CASE 2
'----------------------------------------------------------------
      RIGHT = 80: LEFT = 0: MID = 40
      COUNT = 0
LAP2: COUNT = COUNT + 1: DNOZANG = MID: NOZANG = DNOZANG / 57.29577951#
      IF COUNT = 40 THEN
         CLS
```

```basic
        PRINT
        PRINT "----------------------------------------------------------------"
        PRINT "                        *** WARNING ***    "
        PRINT " count has reached 40 without converging to an answer "
        PRINT
"----------------------------------------------------------------"
      GOTO QUIT2
    END IF
    CALC
    delta = PWX - RXSENS
PRINT #1, USING "##.####^^^^"; DNOZANG, NOZANG, PWX, RXSENS, delta
PRINT delta
    SELECT CASE delta
        CASE IS > .00000000000001#
          LEFT = MID
          MID = (LEFT + RIGHT) / 2
          GOTO LAP2
        CASE IS < -.00000000000001#
          RIGHT = MID
          MID = (LEFT + RIGHT) / 2
          GOTO LAP2
        CASE ELSE
          CLS
          PRINT
          PRINT "+++++++++++++++++    BINGO - CONVERGENCE COMPLETE !
--+++++++++++++++++++++++++"
        END SELECT
QUIT2: PRINT
        IF S > SNR THEN
      PRINT
"_____"
      PRINT
      PRINT "NO OFFSET ZENITH ANGLE WHERE SIGNAL POWER IS DETECTIBLE IS"
      PRINT "                       ", MID, "Degrees"
      PRINT
"_____"
      PRINT
      PRINT " The track time available with this zenith angle and satellite
--altitude"
      PRINT "                       ", TRAKTIME, "Minutes"
      PRINT
"_____"
        ELSE
          CLS
          PRINT
          PRINT
          PRINT "SIGNAL TO NOISE RATIO IS INSUFFICIENT FOR TARGET TRACKING"
        END IF
'-----------------------------------------------------------------

    CASE 3
```

```
PRINT "THE VARIABLES THAT YOU ARE ALLOWED TO VARY ARE"
PRINT "          1 - DNOZANG  (the No Offset Zenith Angle in Degrees)"
PRINT "          2 - SATALT   (SATellite ALTitude in kilometers)"
PRINT "          3 - JOULES   (the laser pulse power in JOULES)"
PRINT "          4 - PW       (the Pulse Width in microseconds)"
PRINT "          5 - RXSENS   (RX minimum detectible signal level in
--microwatts)"
PRINT "          6 - SNR      (the required S/N to declare a target)"
PRINT "          7 - RXD      (the Diameter of the Receiver collection optics)"
PRINT "          8 - REFLECT  (the REFLECTivity of the target's skin in
--percent)"
PRINT "          9 - OFFSET   (distance from satellite's ground track to
--target)'"
PRINT
INPUT "ENTER THE OPTION YOU WISH TO VARY"; DCHOICE
PRINT
INPUT "ENTER LOW BOUND FOR YOUR CHOICE"; BOTTOM
PRINT
INPUT "ENTER UPPER BOUND FOR YOUR CHOICE"; TOP
PRINT
INPUT "ENTER STEP SIZE"; INCR
SELECT CASE DCHOICE
        CASE 2, 3, 4, 5, 6, 7, 8, 9
          INPUT "AT WHAT NO OFFSET ZENITH ANGLE DO YOU DESIRE THE DATA
--(degrees)"; DNOZANG
        CASE ELSE
          PRINT
     END SELECT
SELECT CASE DCHOICE
        CASE 1
          FOR DNOZANG = BOTTOM TO TOP STEP INCR
          CALC
          PRINT #1, USING "##.####^^^^"; DNOZANG, PWX, dBm(PWA), S
          PRINT USING "##.####^^^^"; DNOZANG, RNG, PWX, dBm(PWX), S
          NEXT
        CASE 2
          FOR SATALT = BOTTOM TO TOP STEP INCR
          CALC
          PRINT USING "##.####^^^^"; SATALT, PWX, dBm(PWX), S
          PRINT #1, USING "##.####^^^^"; SATALT, PWX, dBm(PWX), S
          NEXT
        CASE 3
          FOR JOULES = BOTTOM TO TOP STEP INCR
          CALC
          PRINT USING "##.####^^^^"; JOULES, PWX, dBm(PWX), S
          PRINT #1, USING "##.####^^^^"; JOULES, PWX, dBm(PWX), S
          NEXT
        CASE 4
          FOR PWI = BOTTOM TO TOP STEP INCR
          PW = PWI / 1000000
          CALC
```

```
                   PRINT USING "##.####^^^^"; PWI, PWX, dBm(PWX), S
                   PRINT #1, USING "##.####^^^^"; PWI, PWX, dBm(PWX), S
                   NEXT
               CASE 5
                 FOR RXmicro = BOTTOM TO TOP STEP INCR
                 RXSENS = RXmicro / 1000000
                 CALC
                 PRINT USING "##.####^^^^"; RXmicro, PWX, dBm(PWX), S
                 PRINT #1, USING "##.####^^^^"; RXmicro, PWX, dBm(PWX), S
                 NEXT
               CASE 6
                 FOR SNdB = BOTTOM TO TOP STEP INCR
                 SNR = 10 ^ (SNdB / 10)
                 CALC
                 PRINT USING "##.####^^^^"; SNdB, PWX, dBm(PWX), S
                 PRINT #1, USING "##.####^^^^"; SNdB, PWX, dBm(PWX), S
                 NEXT
               CASE 7
                 FOR RXD = BOTTOM TO TOP STEP INCR
                 RXAREA = (3.14159265# * (RXD ^ 2)) / 4
                 SELECT CASE BEAMOD
                 CASE 2
                   BMDVG = 1.08 * WL / RXD
                 CASE 3
                   BMDVG = 1.3 * WL / RXD
                 CASE ELSE
                   PRINT "CHECK THE VARIATION IN YOUR BEAM DIVERGENCE AS RXD CHANGES"
                 END SELECT
                 CALC
                 PRINT USING "##.####^^^^"; RXD, PWX, dBm(PWX), S
                 PRINT #1, USING "##.####^^^^"; RXD, CHI, dBm(PWX), S
                 NEXT
               CASE 8
                 FOR REFLECT = BOTTOM TO TOP STEP INCR
                 R = REFLECT / 100
                 CALC
                 PRINT USING "##.####^^^^"; REFLECT, PWX, dBm(PWX), S
                 PRINT #1, USING "##.####^^^^"; REFLECT, PWX, dBm(PWX), S
                 NEXT
               CASE 9
                 FOR OFFSET = BOTTOM TO TOP STEP INCR
                 CALC
                 PRINT USING "##.####^^^^"; OFFSET, PWX, dBm(PWX), S
                 PRINT #1, USING "##.####^^^^"; OFFSET, PWX, dBm(PWX), S
                 NEXT
               CASE ELSE
                 PRINT "CHOICE WAS IMPROPERLY ENTERED...DATA IS QUESTIONABLE"
             END SELECT
         CASE ELSE
           PRINT "SELECTION OF DATA WAS IMPROPERLY ENTERED...DATA IS QUESTIONABLE"
       END SELECT
```

```
COLOR 17, 7
LOCATE 25, 12
INPUT "   +++++++++++++    PRESS RETURN TO CONTINUE     +++++++++++++"; PR$
COLOR 2, 0
MENU
IF SLCTR = 0 GOTO ALPHA
CLS
LOCATE 14, 12
COLOR 0, 2
PRINT "THAT COMPLETES THE OATS MODEL FOR NOW-----i.e.  THE END"

END

FUNCTION BETA
        SELECT CASE SATRAK
                CASE IS < 0
                  CLS
                  LOCATE 12, 1
                  PRINT "**************************************************"
                  PRINT "ERROR    ERROR    ERROR    ----  DATA IS OUT OFF RANGE"
                  PRINT "---------------Re-enter satellite track-----------"
                  PRINT "---------------Re-enter target heading-----------"
                  PRINT "**************************************************"
                  CHKR1 = 1
                CASE IS <= 180
                  CHKR1 = 0
                CASE IS > 360
                  CLS
                  LOCATE 12, 1
                  PRINT "**************************************************"
                  PRINT "ERROR    ERROR    ERROR    ----  DATA IS OUT OFF RANGE"
                  PRINT "---------------Re-enter satellite track-----------"
                  PRINT "---------------Re-enter target heading-----------"
                  PRINT "**************************************************"
                  CHKR1 = 1
                CASE IS > 180
                  CHKR1 = 0
                  SATRAK = SATRAK - 180
        END SELECT
        SELECT CASE TGTHDG
                CASE IS < 0
                  CLS
                  LOCATE 12, 1
                  PRINT "**************************************************"
                  PRINT "ERROR    ERROR    ERROR    ----  DATA IS OUT OFF RANGE"
                  PRINT "-------------Re-enter satellite track-------------"
                  PRINT "-------------Re-enter target heading-------------"
                  PRINT "**************************************************"
                  CHKR2 = 1
                CASE IS <= 180
                  CHKR2 = 0
```

```basic
                     CASE IS > 360
                        CLS
                        LOCATE 12, 1
                        PRINT "******************************************************"
                        PRINT "ERROR    ERROR    ERROR    ----  DATA IS OUT OFF RANGE"
                        PRINT "----------------Re-enter satellite track------------"
                        PRINT "----------------Re-enter target heading------------"
                        PRINT "******************************************************"
                        CHKR2 = 1
                     CASE IS > 180
                        CHKR2 = 0
                        TGTHDG = TGTHDG - 180
               END SELECT
          BETA = ABS(SATRAK - TGTHDG) / 57.29577951#
     END FUNCTION

     SUB CALC
          NOZANG = DNOZANG / 57.29577951#
          RNG = (RANGE(SATALT)) * 1000
          T = TRANSMIT
          SZ = SPOTSZ(RNG, BMDVG)
             IF TPAREA > SZ THEN
                CHI = SZ / TPAREA
                PRINT "CHI IS CURRENTLY AT------------------", CHI
             ELSE CHI = 1
             END IF
          TLCS = LCS(NOZANG)
          CCT = (PG * JOULES * TLCS * RXAREA * (T ^ 2) * CHI)
          CCB = (BMDVG ^ 2) * (RNG ^ 4)
          PWX = CCT / (PW * CCB * 9.869604404#)
          S = (CCT * WL) / (CCB * 1.96058E-23)
     '        PRINT "******************************************************************"
     '        PRINT "proc gain-----"; PG
     '        PRINT "joules--------"; JOULES
     '        PRINT "rxarea--------"; RXAREA
     '        PRINT "transmittance-"; T
     '        PRINT "chi-----------"; chi
     '        PRINT "beam divergence"; BMDVG
     '        PRINT "RANGE----------"; RNG
     '        PRINT "pulse width----"; PW
     '      PRINT PWX, S
     END SUB
     '++++++++++++++++++++++++++++++++++++++++++++++++++++++++++++++
     'Significant portions of this program were structured after
     ' interfaces designs built or described by Steven Spence.
     ' AFIT/GST 89J
     '++++++++++++++++++++++++++++++++++++++++++++++++++++++++++++++
     SUB CHGMENU
     'This subroutine changes the input values displayed in the menu
     SELECT CASE SLCTR
          CASE 1
```

```
          LOCATE 1, 33
          PRINT "xxxxxxxx"
          LOCATE 1, 33
          INPUT SATALT
          SELECT CASE SATALT
            CASE IS < 120
               CLS
               PRINT "---------WARNING   WARNING   WARNING--------------- "
               PRINT "------------- THIS IS PRETTY LOW ----------------- "
               PRINT
            CASE IS > 30000
               CLS
               PRINT "---------WARNING              WARNING
--WARNING--------"
               PRINT "------------- THIS IS VERY HIGH FOR A TRACKING SATELLITE
--------"
               PRINT
            CASE ELSE
               PRINT
          END SELECT

      CASE 2
          LOCATE 2, 33
          PRINT "xxxxxxxx"
          LOCATE 2, 33
          INPUT LASER
          SELECT CASE LASER
                  CASE 1
                    WL = 10.59104 / 1000000
                         PRINT
                  CASE 2
                    WL = 11.1494 / 1000000
                         PRINT
                  CASE 3
                    WL = 2.06 / 1000000
                         PRINT
                  CASE 4
                    WL = 1.057 / 1000000
                         PRINT
                  CASE ELSE
                    CLS
                    COLOR 0, 2
                    LOCATE 12, 28
                    PRINT "INPUT ERROR"
                    COLOR 2, 0
                    LOCATE 24, 9
                    INPUT "HIT RETURN TO CONTINUE - THEN FIX YOUR ERROR"; PR$
          END SELECT

      CASE 3
          LOCATE 3, 33
```

```
                    PRINT "xxxxxxxx"
                    LOCATE 3, 33
                    INPUT JOULES
               CASE 4
                    LOCATE 4, 33
                    PRINT "xxxxxxxx"
                    LOCATE 4, 33
                    INPUT PWI
                    PW = PWI / 1000000

               CASE 5
                    LOCATE 5, 33
                    PRINT "xxxxxxxx"
                    LOCATE 5, 33
                    INPUT SNdB
                    SNR = 10 ^ (SNdB / 10)

               CASE 6
                    LOCATE 6, 33
                    PRINT "xxxxxxxx"
                    LOCATE 6, 33
                    INPUT RXmicro
                    RXSENS = RXmicro / 1000000

               CASE 7
                    LOCATE 7, 33
                    PRINT "xxxxxxxx"
                    LOCATE 7, 33
                    INPUT PGdB
                    PG = 10 ^ (PGdB / 10)

          CASE 8
                    LOCATE 8, 33
                    PRINT "xxxxxxxx"
                    LOCATE 8, 33
                    INPUT RXD
                    RXAREA = (3.14159265# * (RXD ^ 2)) / 4

               CASE 9
                    LOCATE 9, 33
                    PRINT "xxxxxxxx"
                    LOCATE 9, 33
                    INPUT BEAMOD
                    SELECT CASE BEAMOD
                      CASE 1
                        CLS
                        LOCATE 12, 12
                        INPUT "ENTER BEAM DIVERGENCE (in Radians)"; BMDVG
                        CLS
                      CASE 2
                        BMDVG = 1.08 * WL / RXD
```

```
        CASE 3
          BMDVG = 1.3 * WL / RXD
        CASE ELSE
                CLS
                COLOR 0, 2
                LOCATE 12, 28
                PRINT "INPUT ERROR"
                COLOR 2, 0
                LOCATE 24, 9
                INPUT "HIT RETURN TO CONTINUE - THEN FIX YOUR ERROR"; PR$
            END SELECT
     GainTX = 12.56637062# / (BMDVG ^ 2)

 CASE 10
      LOCATE 10, 33
      PRINT "xxxxxxxx"
      LOCATE 10, 33
      INPUT ATMOS
      SELECT CASE ATMOS
              CASE 1, 2

              CASE 3
              CLS
              LOCATE 7, 1
     PRINT " ENTER THE ATTENUATION TO ADD TO THE ALREADY EXISTING"
     PRINT " ATTENUATION FROM THE MOLECULAR ABSORPTION (in dB)"
     PRINT " i.e. 50 % attenuation from an aerosol would be 3dB"
     PRINT " entry is for ONE-WAY passage through the atmosphere"
     PRINT " at a zenith angle of ZERO (straight up through the
--atmosphere)"
     PRINT " --an exponential curve (trans vs range) is used for all"
     PRINT "    zenith angles other than zero."
     INPUT ATTENdB
     ATTEN = 10 ^ (ATTENdB / 10)
              CASE ELSE
                 CLS
                 COLOR 0, 2
                 LOCATE 12, 28
                 PRINT "INPUT ERROR"
                 COLOR 2, 0  .
                 LOCATE 24, 9
                 INPUT "HIT RETURN TO CONTINUE - THEN FIX YOUR ERROR"; PR$
            END SELECT

 CASE 11
      LOCATE 11, 33
      PRINT "xxxxxxxx"
      LOCATE 11, 33
      INPUT LCSMODEL
      CLS
      SELECT CASE LCSMODEL
```

```
            CASE 1
              LOCATE 12, 5
              INPUT "WHAT IS THE RADIUS OF THE SPHERE IN METERS"; RADSPHR
            CASE 2
              LOCATE 9, 4
              PRINT "THE FLYING BRICK MODEL IS A THREE DIMENSIONAL MODEL"
              PRINT "OF AN OBJECT SIMPLIFYING THE TARGET TO THREE ORTHOGONAL"
              PRINT "PLANES LIKE THREE SIDES OF A BRICK.  THEREFORE, THE THREE"
              PRINT "FACES OF THE SYMETRICAL BRICK REPRESENT THE PROJECTED
--AREA"
              PRINT "OF THE TARGET FROM A FRONTAL/REAR VIEW, FROM A TOP VIEW
--AND"
              PRINT "FROM A SIDE VIEW ... essentially the target's silhouette "
              INPUT "ENTER THE  FRONT / REAR  PROJECTED AREA (sqr meters)"; RA1
              INPUT "ENTER THE TOP PROJECTED AREA (sqr meters)"; RA2
              INPUT "ENTER THE SIDE PROJECTED AREA (sqr meters)"; RA3
            CASE ELSE
                    CLS
                    COLOR 0, 2
                    LOCATE 12, 28
                    PRINT "INPUT ERROR"
                    COLOR 2, 0
                    LOCATE 24, 9
                    INPUT "HIT RETURN TO CONTINUE - THEN FIX YOUR ERROR"; PR$
            END SELECT

        CASE 12
            LOCATE 12, 33
            PRINT "xxxxxxxx"
            LOCATE 12, 33
            INPUT REFLECT
            R = REFLECT / 100

        CASE 13
            LOCATE 13, 33
            PRINT "xxxxxxxx"
            LOCATE 13, 33
            INPUT SATRAK
            XXXX = BETA
                IF CHKR1 = 1 THEN
                        COLOR 2, 0
                        LOCATE 24, 9
                        INPUT "HIT RETURN TO CONTINUE - THEN FIX YOUR ERROR"; PR$
                END IF
        CASE 14
            LOCATE 14, 33
            PRINT "xxxxxxxx"
            LOCATE 14, 33
            INPUT TGTHDG
            XXXX = BETA
                IF CHKR2 = 1 THEN
```

```
                    COLOR 2, 0
                    LOCATE 24, 9
                    INPUT "HIT RETURN TO CONTINUE - THEN FIX YOUR ERROR"; PR$
            END IF
        CASE 15
            LOCATE 15, 33
            PRINT "xxxxxxxx"
            LOCATE 15, 33
            INPUT OFFSET
        CASE 16
            LOCATE 16, 33
            PRINT "xxxxxxxx"
            LOCATE 16, 33
            INPUT DATASLCT


END SELECT
MENU
END SUB

FUNCTION dBm (PWX)                              'X is in watts
  . V = PWX * 1000
    IF V < 1E-09 THEN
    dBm = 0
    GOTO SKIPPER
    END IF                                      'convert to milliwatts
    dBm = 10 * (LOG(V) / LOG(10#))              'take log10 of V and mutiply by
--10
'                                               -----------------------------------
'                                               Log10 function from Microsoft
'                                               QuickBASIC 4.0 BASIC Language
'                                               Reference, 1987
SKIPPER:
END FUNCTION

FUNCTION LCS (NOZANG)
    SELECT CASE LCSMODEL
      CASE 1
        LCS = R * (RADSPHR ^ 2) * 8.37758041#    'pi*(8/3)
      CASE 2
        VLO# = RANGE(SATALT)
        VL1# = X1 / VLO#
        sig1# = 4 * R * A1 * ((VL1#) ^ 2)
        Z = ZORNG * COS(NOZANG)
        VL2# = Z / VLO#
        sig2# = 4 * R * A2 * ((VL2#) ^ 2)
        VL3# = OFFSET / VLO#
        sig3# = 4 * R * A3 * ((VL3#) ^ 2)
        LCS = sig1# + sig2# + sig3#
      CASE ELSE
        PRINT "--------*******   ERROR IN FUNCTION LCS      *******--------"
    END SELECT
```

105

```
END FUNCTION

SUB MENU
TRYAGAIN:
 CLS
 LOCATE 1, 1
 PRINT "1.  SATELLITE ALTITUDE"
 LOCATE 2, 1
 PRINT "2.  LASER TYPE "
 LOCATE 3, 1
 PRINT "3.  PULSE ENERGY"
 LOCATE 4, 1
 PRINT "4.  PULSE WIDTH"
 LOCATE 5, 1
 PRINT "5.  REQUIRED S/N"
 LOCATE 6, 1
 PRINT "6.  MIN DETECTABLE SIGNAL"
 LOCATE 7, 1
 PRINT "7.  PROCESSING GAIN"
 LOCATE 8, 1
 PRINT "8.  DIAMETER OF OPTICS"
 LOCATE 9, 1
 PRINT "9.  BEAM DIVERGENCE MODEL"
 LOCATE 10, 1
 PRINT "10. ATMOSPHERE MODEL"
 LOCATE 11, 1
 PRINT "11. TARGET MODEL"
 LOCATE 12, 1
 PRINT "12. TARGET REFLECTANCE"
 LOCATE 13, 1
 PRINT "13. SATELLITE HEADING"
 LOCATE 14, 1
 PRINT "14. TARGET HEADING"
 LOCATE 15, 1
 PRINT "15. OFFSET DISTANCE"
 LOCATE 16, 1
 PRINT "16. DATA OUTPUT REQUEST"

 LOCATE 1, 33
 PRINT SATALT
 LOCATE 2, 33
 PRINT LASER
 LOCATE 3, 33
 PRINT JOULES
 LOCATE 4, 33
 PRINT PWI
 LOCATE 5, 33
 PRINT SNdB
 LOCATE 6, 33
 PRINT RXmicro
 LOCATE 7, 33
```

```
        PRINT PGdB
        LOCATE 8, 33
        PRINT RXD
        LOCATE 9, 33
        PRINT BEAMOD
        LOCATE 10, 33
        PRINT ATMOS
        LOCATE 11, 33
        PRINT LCSMODEL
        LOCATE 12, 33
        PRINT REFLECT
        LOCATE 13, 33
        PRINT SATRAK
        LOCATE 14, 33
        PRINT TGTHDG
        LOCATE 15, 33
        PRINT OFFSET
        LOCATE 16, 33
        PRINT DATASLCT
        LOCATE 19, 1
        COLOR 0, 2
        PRINT "YOU MAY CHANGE ANY OF THE ABOVE VALUES SIMPLY BY ENTERING ITS NUMBER"
        COLOR 2, 0
        PRINT
        PRINT "ENTER 0 TO CALCULATE AGAIN WITH THE ABOVE DATA SET"
        PRINT "ENTER 21 IF YOU HAVE HAD ENOUGH AND WISH TO RETURN TO DOS"
        INPUT SLCTR
        SELECT CASE SLCTR
                CASE 0
                        EXIT SUB
                CASE 21
                        EXIT SUB
                CASE 1 TO 16
                        CHGMENU
                CASE ELSE
                        GOTO TRYAGAIN
        END SELECT

END SUB

FUNCTION RANGE (SATALT)
        VR1# = 6371.23 + .01          'ASSUMES TARGET ALTITUDE OF 10 METERS
        VR2# = 6371.23 + SATALT
        VR3# = (2 * VR1#) * COS(3.14159265# - NOZANG)
        VR4# = (VR2# ^ 2) - (VR1# ^ 2)
        VR5# = SQR((VR3# ^ 2) + (4 * VR4#))
' ZORNG is the Zero Offset RaNGe (i.e. the range when OFFSET = 0)
        ZORNG = (VR5# + VR3#) / 2
        X1 = ZORNG * SIN(NOZANG)
        Z = ZORNG * COS(NOZANG)
        RNGSQR# = OFFSET ^ 2 + X1 ^ 2 + Z ^ 2
```

```
            RANGE = SQR(RNGSQR#)
            VR6# = SQR(RNGSQR# - (Z ^ 2))
            VR7# = VR6# / Z
            ZANG = ATN(VR7#)
END FUNCTION

FUNCTION SPOTSZ (BMDVG, RNG)
            SPOTSZ = .78539816# * (RNG ^ 2) * (BMDVG ^ 2)
END FUNCTION

FUNCTION TPAREA
'_____
'This function computes the total projected area of the brick model
'The total is a sum of the parts (top,side and front)
'................................................................
'
IF LCSMODEL = 2 THEN
    D = RANGE(SATALT)
    AP1 = X1 * A1
    AP2 = Z * A2
    AP3 = OFFSET * A3
    SUM = AP1 + AP2 + AP3
    TPAREA = SUM / D
    END IF
IF LCSMODEL = 1 THEN
    TPAREA = (RADSPHR ^ 2 * 3.14159265#)
    END IF
END FUNCTION

FUNCTION TRAKTIME

            VR1# = 6371.23 + .01         'ASSUMES TARGET ALTITUDE OF 10 METERS
            VR2# = 6371.23 + SATALT
            VR3# = (2 * VR1#) * COS(3.14159265# - NOZANG)
            VR4# = (VR2# ^ 2) - (VR1# ^ 2)
            VR5# = SQR((VR3# ^ 2) + (4 * VR4#))
' ZORNG is the Zero Offset RaNGe (i.e. the range when OFFSET = 0)
            ZORNG = (VR5# + VR3#) / 2

            TREV = (.009952 * (VR2# ^ 1.5)) / 60   '  REV Time in minutes
            OMEGA = 6.28318531# / TREV
            VK1 = ZORNG / VR2#
            VK2 = SIN(3.14159265# - NOZANG)
            VK3 = VK1 * VK2
' Calculate the ARCSIN of VK3                      'This relationship is from
            VK4 = SQR(1 - (VK3 ^ 2))               'CRC Standard Mathematical
--Tables
            BHALF = ATN(VK3 / VK4)                 '21st edition, page 233
            TRAKTIME = (2 * BHALF) / OMEGA
END FUNCTION
```

```
FUNCTION TRANSMIT      'Computes transmittance of the
'                       atmosphere
SELECT CASE LASER
    CASE 1                          'CO2 using C12
        SELECT CASE ATMOS
            CASE 1, 3                       'Clear atmosphere
                C1# = -.26438815#           'Molecular absorption only
                C2# = 4.57337687#
                C3# = -8.2907455#
                C4# = 6.42929668#
                C5# = -1.88496131#
                CI# = -.01635833#
            CASE 2
                C1# = -.31883222#           'HAZE with 5 km visibilty
                C2# = 4.27150562#
                C3# = -7.28951884#
                C4# = 5.38389615#
                C5# = -1.51345106#
                CI# = -.0098359#
        END SELECT
    CASE 2                          'CO2 with C13
        SELECT CASE ATMOS
            CASE 1, 3
                C1# = 1.9240306#            'Clear atmosphere
                C2# = -4.72236837#          'Molecular absorption only
                C3# = 6.25641659#
                C4# = -4.24200153#
                C5# = 1.15335803#
                CI# = .59438551#
            CASE 2
                C1# = 3.57172183#
                C2# = -8.747844260000001#        'HAZE with 5 km visibilty
                C3# = 11.56313808#
                C4# = -7.80928598#
                C5# = 2.11201757#
                CI# = .23738812#
        END SELECT
    CASE 3                          'Holmium
        SELECT CASE ATMOS
            CASE 1, 3
                C1# = .76297032#
                C2# = -1.96013817#          'Clear atmosphere
                C3# = 2.66230004#           'Molecular absorption only
                C4# = -1.82902376#
                C5# = .50041431#
                CI# = .85239347#
            CASE 2
                C1# = 3.98595311#
                C2# = -9.59816461#
                C3# = 12.56345419#          'HAZE with 5 km visibilty
                C4# = -8.43270371#
```

109

```
                   C5# = 2.27119836#
                   CI# = .12015229#
          END SELECT
CASE 4                                    'Neodynium
     SELECT CASE ATMOS
        CASE 1, 3
             C1# = .8226326#
             C2# = -2.09733802#
             C3# = 2.83434822#            'Clear atmosphere
             C4# = -1.93997169#           'Molecular absorption only
             C5# = .52917037#
             CI# = .83868596#
        CASE 2
             C1# = 3.67542735#
             C2# = -6.6265573#
             C3# = 7.09392008#
             C4# = -4.1192832#            'HAZE with 5 km visibilty
             C5# = .99615146#
             CI# = -.25207037#
     END SELECT
END SELECT

     VT1# = COS(ZANG)
     Q1 = C1# * (VT1#)
     Q2 = C2# * (VT1# ^ 2)
     Q3 = C3# * (VT1# ^ 3)
     Q4 = C4# * (VT1# ^ 4)
     Q5 = C5# * (VT1# ^ 5)
     IF ATMOS = 3 THEN
             TRANS = 1 / ATTEN
             ALPHA = ((LOG(TRANS)) / 120)
             L = RANGE(120)
             TRANSA = EXP(ALPHA * L)
         ELSE
             TRANSA = 1
     END IF
     TRANSMIT = (CI# + Q1 + Q2 + Q3 + Q4 + Q5) * TRANSA
     PRINT ZANG, VT1#
END FUNCTION
```

# APPENDIX B --- ROSETTA STONE FOR OATS MODEL

| OATS MODEL VARIABLE | VARIABLE IN THESIS | VARIABLE DESCRIPTION |
|---|---|---|
| A1 | $A_1$ | transformed area of the frontal surface of the brick |
| A2 | $A_2$ | transformed area of the top surface of the brick |
| A3 | $A_3$ | transformed area of the side surface of the brick |
| ALPHA | $\alpha$ | attenuation coefficient for additional loss mechanisms |
| AP1 | | frontal component of the target's total projected area |
| AP2 | | top component of the target's total projected area |
| AP3 | | side component of the target's total projected area |
| ATMOS | na | number that defines the atmosphere type to be applied to the model |
| ATTEN | na | additional atmospheric attenuation at a zenith angle of 0 used in atmosphere #3 |
| ATTENdB | $\delta$ | the variable ATTEN in dB |
| BEAMOD | na | number that defines the beam divergence type to be applied in the model |
| BETA | $\beta$ | angle between the satellite ground track direction and the target heading |
| BHALF | na | geocentric angle between the target position and the satellite at the point that the satellite is first trackable |
| BMDVG | $\theta_B$ | beam divergence angle of the transmitted laser beam (full angle in radians) |
| BOTTOM | na | beginning value for the variable that is to be incremented when using DATASLCT 3 |
| C1 | na | first coefficient of the fifth order polynomial that defines atmospheric attenuation for the model |
| C2 | na | second coefficient of the fifth order polynomial that defines atmospheric attenuation for the model |
| C3 | na | third coefficient of the fifth order polynomial that defines atmospheric attenuation for the model |
| C4 | na | fourth coefficient of the fifth order polynomial that defines atmospheric attenuation for the model |
| C5 | na | fifth coefficient of the fifth order polynomial that defines atmospheric attenuation for the model |

| | | |
|---|---|---|
| CI | na | attenuation when zenith angle is zero, used as the constant in the fifth order polynomial defining attenuation |
| CCB | na | calculation factor in subroutine CALC is denominator of range equation |
| CCT | na | calculation factor in subroutine CALC is numerator of range equation |
| CHI | $\chi$ | ratio of laser spot size to target's projected area |
| COUNT | na | the count on a counter in the routine to find the zenith angle that meets the pre-establised criterion |
| D | d | the value in function TPAREA that defines the range from target to satellite |
| DATASLCT | na | number designating type of data to be output when the model is run |
| DCHOICE | na | number designating the variable to increment for DATASLCT = 3 |
| DELTA | na | the difference between required S/N and the actual system S/N     OR the difference between detectable signal power and actual power |
| DNOZANG | na | the no offset zenith angle measured in degrees |
| GainTX | $G_{Tx}$ | the gain in the system from the laser beam directionality |
| INCR | na | the value by which the variable of study is incremented when DATASLCT = 3 |
| JOULES | $P_{Tx}$ | the energy in a single laser pulse measured in joules |
| L | L | length of atmosphere through which a laser beam travels -used in function transmit |
| LASER | na | number designating type of laser to be used in the model |
| LCSMODEL | na | number designating type of target to be tracked  1 for sphere    2 for brick |
| LEFT | na | left bound for the halving algorithm used to find required zenith angle |
| MID | na | mid value for the nalving algorithm used to find required zenith angle |
| NOZANG | $\theta_N$ | no offset zenith angle (in radians) |
| OFFSET | y | distance from the target to the satellite ground track |
| OMEGA | $\omega$ | revolution rate of the satellite |
| PG | $\mathbb{G}$ | processing gain of the receiver system |
| PGdB | na | processing gain in dB |
| PW | PW | pulse width of the laser pulse in seconds |
| PWI | na | pulse width of the laser pulse in $\mu s$ |
| PWX | $P_{Rx}$ | available power for the receiver to process (after processing gain is added) |
| R | $\rho$ | reflectance of the target skin |
| RA1 | $A_1$ | raw frontal area of the target |
| RA2 | $A_2$ | raw top area of the target |

| | | |
|---|---|---|
| RA3 | A3 | raw side area of the target |
| RADSPHR | na | radius of the target sphere (in meters) |
| REFLECT | na | reflectance of the target skin in percent |
| RIGHT | na | right bound of halving algorithm used to find the required zenith angle |
| RNG | d or R | range of the target from the satellite (in meters) |
| RNGSQR | na | RNG squared (intermediate calculation) |
| RXAREA | na | effective receiving area of optics (in square meters) |
| RXD | D | diameter of receiving optics (meters) |
| RXmicro | na | minimum detectable signal in $\mu$-watts |
| RXSENS | na | RXmicro in watts |
| S | S/N | actual S/N at the receiver |
| SATALT | h | satellite altitude above the earth (km) |
| SATRAK | na | direction of satellite ground track |
| SIG1 | $\sigma_1$ | component of total LCS due to the transformed frontal area |
| SIG2 | $\sigma_2$ | component of total LCS due to the top area |
| SIG3 | $\sigma_3$ | component of total LCS due to the transformed side area |
| SLCTR | na | |
| SNdB | na | required S/N for target declaration in dB |
| SNR | na | required S/N for target declaration |
| SUM | na | sum of area components for projected area computations |
| SZ | na | spot size of laser beam at the target |
| T | $\tau$ | transmittance of the atmosphere |
| TGTHDG | na | target's heading oriented from true north |
| TLCS | $\sigma_t$ | target's laser cross section |
| TOP | na | upper bound of incremental data computation routine when DATASLCT = 3 |
| TRANS | na | transmittance factor of the atmosphere when using additional attenuation |
| TRANSA | $\tau_a$ | transmittance factor which modifies the atmospheric attenuation when additional attenuation is requested |
| TREV | P | time of a single satellite revolution |
| VK1 | na | intermediate calculation variable in the TRAKTIME function |
| VK2 | na | intermediate calculation variable in the TRAKTIME function |
| VK3 | na | intermediate calculation variable in the TRAKTIME function |
| VK4 | na | intermediate calculation variable in the TRAKTIME function |
| VL0 | na | intermediate calculation variable in the LCS function |
| VL1 | na | intermediate calculation variable in the LCS function |
| VL2 | na | intermediate calculation variable in the LCS function |

| | | |
|---|---|---|
| VL3 | na | intermediate calculation variable in the LCS function |
| VR1 | na | intermediate calculation variable in the RANGE function |
| VR2 | na | intermediate calculation variable in the RANGE function |
| VR3 | na | intermediate calculation variable in the RANGE function |
| VR4 | na | intermediate calculation variable in the RANGE function |
| VR5 | na | intermediate calculation variable in the RANGE function |
| VR6 | na | intermediate calculation variable in the RANGE function |
| VR7 | na | intermediate calculation variable in the RANGE function |
| VT1 | na | intermediate calculation variable in the TRANSMIT function |
| WL | $\lambda$ | wavelength of the laser |
| X1 | $x$ | x component of distance from satellite to the target |
| Z | $z$ | z component of distance from satellite to the target |
| ZANG | $\theta$ | zenith angle from target to the satellite |
| ZORNG | $d^{\kappa}$ | range from satellite to target if OFFSET is set to zero |

114

## APPENDIX C    INPUT DATA FROM FASCODE

### INPUT DATA FOR C12 WITH NO HAZE

| $\theta$ | $\cos \theta$ | $\tau(\theta)$ |
|---|---|---|
| 0.000000 | 1.000000 | 0.5465100 |
| 3.000000 | 0.9986295 | 0.5460600 |
| 5.000000 | 0.9961947 | 0.5452600 |
| 8.000000 | 0.9902681 | 0.5432900 |
| 10.00000 | 0.9848077 | 0.5414600 |
| 12.00000 | 0.9781476 | 0.5392200 |
| 15.00000 | 0.9659258 | 0.5350400 |
| 17.00000 | 0.9563047 | 0.5317000 |
| 20.00000 | 0.9396926 | 0.5258300 |
| 23.00000 | 0.9205049 | 0.5188700 |
| 25.00000 | 0.9063078 | 0.5136000 |
| 28.00000 | 0.8829476 | 0.5046700 |
| 30.00000 | 0.8660254 | 0.4980200 |
| 33.00000 | 0.8386706 | 0.4868900 |
| 35.00000 | 0.8191521 | 0.4786700 |
| 37.00000 | 0.7986355 | 0.4697600 |
| 40.00000 | 0.7660444 | 0.4550200 |
| 43.00000 | 0.7313537 | 0.4384800 |
| 45.00000 | 0.7071068 | 0.4263700 |
| 47.00000 | 0.6819984 | 0.4133300 |
| 50.00000 | 0.6427876 | 0.3918700 |
| 53.00000 | 0.6018150 | 0.3679500 |
| 55.00000 | 0.5735765 | 0.3505200 |
| 57.00000 | 0.5446391 | 0.3318100 |
| 60.00000 | 0.5000000 | 0.3012100 |
| 63.00000 | 0.4539905 | 0.2674100 |
| 65.00000 | 0.4226182 | 0.2430500 |
| 67.00000 | 0.3907312 | 0.2172600 |
| 70.00000 | 0.3420202 | 0.1761600 |
| 73.00000 | 0.2923718 | 0.1329800 |
| 75.00000 | 0.2588191 | 0.1039500 |
| 77.00000 | 0.2249510 | $7.5797997 \times 10^{-2}$ |
| 80.00000 | 0.1736482 | $3.8364001 \times 10^{-2}$ |

### SELECTED PORTIONS OF SAS OUTPUT

#### R-SQUARE

0.999995

| PARAMETER | ESTIMATE |
|---|---|
| INTERCEPT | -0.01635833 |
| A | -0.26438815 |
| ASQ | 4.57337687 |
| ACU | -8.29074550 |
| AQUAD | 6.42929668 |
| AQUIN | -1.88496131 |

115

# INPUT DATA FOR C12 WITH HAZE

| $\theta$ | $\cos \theta$ | $\tau (\theta)$ |
|---|---|---|
| 0.00000 | 1.000000 | 0.5238700 |
| 10.00000 | 0.9848077 | 0.5186900 |
| 20.00000 | 0.9396926 | 0.5026800 |
| 30.00000 | 0.8660254 | 0.4742700 |
| 40.00000 | 0.7660444 | 0.4305700 |
| 50.00000 | 0.6427876 | 0.3669200 |
| 60.00000 | 0.5000000 | 0.2767900 |
| 70.00000 | 0.3420202 | 0.1556800 |
| 80.00000 | 0.1736482 | $3.0096000E-02$ |

## SELECTED PORTIONS OF SAS OUTPUT

### R-SQUARE
0.999999

| PARAMETER | ESTIMATE |
|---|---|
| INTERCEPT | -0.00983590 |
| A | -0.31883222 |
| ASQ | 4.27150562 |
| ACU | -7.28951884 |
| AQUAD | 5.38389615 |
| AQUIN | -1.51345106 |

# INPUT DATA FOR C13 WITH NO HAZE

| $\theta$ | $\cos \theta$ | $\tau (\theta)$ |
|---|---|---|
| 0.000000 | 1.000000 | 0.9637000 |
| 3.000000 | 0.9986295 | 0.9636500 |
| 5.000000 | 0.9961947 | 0.9635600 |
| 8.000000 | 0.9902681 | 0.9633500 |
| 10.00000 | 0.9848077 | 0.9631500 |
| 12.00000 | 0.9781476 | 0.9629000 |
| 15.00000 | 0.9659258 | 0.9624400 |
| 17.00000 | 0.9563047 | 0.9620700 |
| 20.00000 | 0.9396926 | 0.9614100 |
| 23.00000 | 0.9205049 | 0.9606300 |
| 25.00000 | 0.9063078 | 0.9600200 |
| 28.00000 | 0.8829476 | 0.9589900 |
| 30.00000 | 0.8660254 | 0.9582000 |
| 33.00000 | 0.8386706 | 0.9568700 |
| 35.00000 | 0.8191521 | 0.9558700 |
| 37.00000 | 0.7986355 | 0.9547600 |
| 40.00000 | 0.7660444 | 0.9528800 |
| 43.00000 | 0.7313537 | 0.9507000 |
| 45.00000 | 0.7071068 | 0.9490600 |
| 47.00000 | 0.6819984 | 0.9472300 |
| 50.00000 | 0.6427876 | 0.9441100 |
| 53.00000 | 0.6018150 | 0.9404200 |
| 55.00000 | 0.5735765 | 0.9375900 |
| 57.00000 | 0.5446391 | 0.9343900 |
| 60.00000 | 0.5000000 | 0.9287500 |
| 63.00000 | 0.4539905 | 0.9218300 |
| 65.00000 | 0.4226182 | 0.9162900 |
| 68.00000 | 0.3746066 | 0.9061000 |
| 70.00000 | 0.3420202 | 0.8976600 |
| 73.00000 | 0.2923718 | 0.8814100 |
| 75.00000 | 0.2588191 | 0.8671800 |
| 77.00000 | 0.2249510 | 0.8488900 |

## SELECTED PORTIONS OF SAS OUTPUT

R-SQUARE

0.999971

| PARAMETER | ESTIMATE |
|---|---|
| INTERCEPT | 0.59438551 |
| A | 1.92403060 |
| ASQ | -4.72236837 |
| ACU | 6.25641659 |
| AQUAD | -4.2420\`153 |
| AQUIN | 1.15335803 |

# INPUT DATA FOR C13 WITH HAZE

| $\theta$ | $\cos \theta$ | $\tau (\theta)$ |
|---|---|---|
| 0.00000 | 1.000000 | 0.9269900 |
| 10.00000 | 0.9848077 | 0.9259100 |
| 20.00000 | 0.9396926 | 0.9224900 |
| 30.00000 | 0.8660254 | 0.9161800 |
| 40.00000 | 0.7660444 | 0.9057800 |
| 50.00000 | 0.6427876 | 0.8887700 |
| 60.00000 | 0.5000000 | 0.8593800 |
| 70.00000 | 0.3420202 | 0.8014100 |
| 80.00000 | 0.1736482 | 0.6476000 |

## SELECTED PORTIONS OF SAS OUTPUT

R-SQUARE

0.999996

| PARAMETER | ESTIMATE |
|---|---|
| INTERCEPT | 0.23738812 |
| A | 3.57172183 |
| ASQ | -8.74784426 |
| ACU | 11.56313808 |
| AQUAD | -7.80928598 |
| AQUIN | 2.11201757 |

# INPUT DATA FOR HOLMIUM WITH NO HAZE

| $\theta$ | $\cos \theta$ | $\tau (\theta)$ |
|---|---|---|
| 0.00000 | 1.000000 | 0.9888800 |
| 10.00000 | 0.9848077 | 0.9887100 |
| 20.00000 | 0.9396926 | 0.9881700 |
| 30.00000 | 0.8660254 | 0.9871700 |
| 40.00000 | 0.7660444 | 0.9855100 |
| 50.00000 | 0.6427876 | 0.9827600 |
| 60.00000 | 0.5000000 | 0.9779000 |
| 70.00000 | 0.3420202 | 0.9679000 |
| 80.00000 | 0.1736482 | 0.9381300 |

### SELECTED PORTIONS OF SAS OUTPUT

R-SQUARE

0.999992

| PARAMETER | ESTIMATE |
|---|---|
| INTERCEPT | 0.85239347 |
| A | 0.76297032 |
| ASQ | -1.96013817 |
| ACU | 2.66230004 |
| AQUAD | -1.82902376 |
| AQUIN | 0.50041431 |

# INPUT DATA FOR HOLMIUM WITH HAZE

| $\theta$ | $\cos \theta$ | $\tau (\theta)$ |
|----------|---------------|-----------------|
| 0.000000 | 1.000000 | 0.9097400 |
| 10.00000 | 0.9848077 | 0.9084100 |
| 20.00000 | 0.9396926 | 0.9042300 |
| 30.00000 | 0.8660254 | 0.8965300 |
| 40.00000 | 0.7660444 | 0.8838500 |
| 50.00000 | 0.6427876 | 0.8631900 |
| 60.00000 | 0.5000000 | 0.8277200 |
| 70.00000 | 0.3420202 | 0.7586200 |
| 80.00000 | 0.1736482 | 0.5813500 |

## SELECTED PORTIONS OF SAS OUTPUT

### R-SQUARE
0.999997

| PARAMETER | ESTIMATE |
|-----------|----------|
| INTERCEPT | 0.12015229 |
| A | 3.98595311 |
| ASQ | -9.59816461 |
| ACU | 12.56345419 |
| AQUAD | -8.43270371 |
| AQUIN | 2.27119836 |

# INPUT DATA FOR NEODYMIUM WITH NO HAZE

| $\theta$ | $\cos \theta$ | $\tau(\theta)$ |
|---|---|---|
| 0.000000 | 1.000000 | 0.9874900 |
| 10.00000 | 0.9848077 | 0.9873000 |
| 20.00000 | 0.9396926 | 0.9867000 |
| 30.00000 | 0.8660254 | 0.9855800 |
| 40.00000 | 0.7660444 | 0.9837100 |
| 50.00000 | 0.6427876 | 0.9806300 |
| 60.00000 | 0.5000000 | 0.9751900 |
| 70.00000 | 0.3420202 | 0.9640500 |
| 80.00000 | 0.1736482 | 0.9314500 |

## SELECTED PORTIONS OF SAS OUTPUT

R-SQUARE

0.999992

| PARAMETER | ESTIMATE |
|---|---|
| INTERCEPT | 0.83868596 |
| A | 0.82263260 |
| ASQ | -2.09733802 |
| ACU | 2.83434822 |
| AQUAD | -1.93997169 |
| AQUIN | 0.52917037 |

# INPUT DATA FOR NEODYMIUM WITH HAZE

| $\theta$ | $\cos \theta$ | $\tau (\theta)$ |
|---|---|---|
| 0.00000 | 1.000000 | 0.7675500 |
| 10.00000 | 0.9848077 | 0.7644300 |
| 20.00000 | 0.9396926 | 0.7546400 |
| 30.00000 | 0.8660254 | 0.7367900 |
| 40.00000 | 0.7660444 | 0.7080200 |
| 50.00000 | 0.6427876 | 0.6627100 |
| 60.00000 | 0.5000000 | 0.5893700 |
| 70.00000 | 0.3420202 | 0.4619700 |
| 80.00000 | 0.1736482 | 0.2199000 |

## SELECTED PORTIONS OF SAS OUTPUT

R–SQUARE

1.000000

| PARAMETER | ESTIMATE |
|---|---|
| INTERCEPT | -0.25207037 |
| A | 3.67542735 |
| ASQ | -6.62655730 |
| ACU | 7.09392008 |
| AQUAD | -4.11928320 |
| AQUIN | 0.99615146 |

# APPENDIX D

```
*************************************
*   SAMPLE FASCODE INPUT DATA FILES   *
*************************************
```

C12-at 40 degrees zenith angle
_____

CO2/nohaze/MIDLATWINTER/40DEG
```
HI=1 F4=1 CN=1 AE=1 EM=1 SC=0 FI=0 PL=0 TS=0 AT=1 MG=0 LS=1         0      0    0
   944.194     944.194      0.000      0.000      0.000      0.000      0.000      0.000
     0.000       0.000
     3     3     0     1     1    28     0          0.000    120.000    944.194
     0.010       0.000    40.000     0.000      0.000      0
     0.000       0.000     0.000     0.000      0.000
     0     0     0     3     0     0      0.000      0.000      0.000      0.000      0.000
```

C13-at 40 degrees zenith angle
_____

BIG13CO2/NOHAZE/MIDLATWINTER/40DEGREES
```
HI=1 F4=1 CN=1 AE=1 EM=1 SC=0 FI=0 PL=0 TS=0 AT=1 MG=0 LS=1         0      0    0
   896.909     896.909      0.000      0.000      0.000      0.000      0.000      0.000
     0.000       0.000
     3     3     0     1     1    28     0          0.000    120.000    896.909
     0.010       0.000    40.000     0.000      0.000      0
     0.000       0.000     0.000     0.000      0.000
     0     0     0     3     0     0      0.000      0.000      0.000      0.000      0.000
```

HOLMIUM-at 40 degrees zenith angle
_____

HOLMIUM IN YLF/NOHAZE/MIDLATWINTER/40DEGREES
```
HI=1 F4=1 CN=1 AE=1 EM=1 SC=0 FI=0 PL=0 TS=0 AT=1 MG=0 LS=1         0      0    0
  4854.369    4854.369      0.000      0.000      0.000      0.000      0.000      0.000
     0.000       0.000
     3     3     0     1     1    28     0          0.000    120.000   4854.369
     0.010       0.000    40.000     0.000      0.000      0
     0.000       0.000     0.000     0.000      0.000
     0     0     0     3     0     0      0.000      0.000      0.000      0.000      0.000
```

NEODYNIUM-at 40 degrees zenith angle
_____

--NEODYNIUM/NO HAZE/MIDLATITUDE WINTER/40DEG--
```
HI=1 F4=1 CN=1 AE=1 EM=1 SC=0 FI=0 PL=0 TS=0 AT=1 MG=0 LS=1         0      0    0
  9460.738       0.000      0.000      0.000      0.000      0.000      0.000      0.000
     0.000       0.000
     3     3     0     0     1    28     0          0.000    120.000   9460.738
     0.010       0.000    40.000     0.000      0.000      0
     0.000       0.000     0.000     0.000      0.000
     0     0     0     3     0     0      0.000      0.000      0.000      0.000      0.000
```

# BIBLIOGRAPHY

1. Anderson, G.P. and others. AFGL Atmospheric Constituents Profile (0-120km). AFGL-TR-86-0110 Hanscom AFB, Massachusetts: Air Force Geophysics Laboratory, 15 May 1986.

2. Bachman, Christian G. Laser Radar Systems and Techniques. Dedham, Massachusetts: Artech House, Inc., 1979.

3. Bate, Roger R. and others. Fundamentals of Astrodynamics. New York: Dover Publications, 1971.

4. Boyd, Robert W. Radiometry and the Detection of Optical Radiation. New York: John Wiley & Sons, 1983.

5. Canan, James W. "Our Blind Spots in Space," Air Force Magazine: 44-47 (February 1988).

6. Clough, S.A. and others. "Atmospheric Radiance and Transmittance: FASCODE2," Handout # 12 from the 1987 Conference on LOWTRAN and FASCODE held at Wright-Patterson AFB OH by Mr. Ron Rodney, AFWAL Staff Meteorologist, a photocopy of a paper presented at the Sixth Conference on Atmospheric Radiation, May 1986, Williamsburg VA.

7. Etter, D.M. Structured FORTRAN 77 for Engineers and Scientists, second edition. Menlo Park, California: Benjamin/Cummings Publishing Company Inc., 1987.

8. Evans, LtCol Howard. Class lectures in Physics 621, Electro-Optical Space Systems Technology. School of Engineering, Air Force Institute of Technology (AU), Wright-Patterson AFB OH, February and March 1988.

9. Eves, Howard. "Analytical Geometry," CRC Standard Mathematical Tables, 21st edition, edited by Samuel M. Selby. Cleveland: The Chemical Rubber Company, 1973.

10. Fluckiger, D.U. and others. "Optical Autodyne Detection Theory and Experiment," Applied Optics, 26: 318-325 (15 January 1987).

11. Holland, Donald. AFIT/GSO-88D. Technical Discussions Wright-Patterson AFB OH 1988.

12. Jenks, Frank, Aeronautical Systems Division Staff Meteorologist. Telephone conversation. Wright-Patterson AFB OH, April 1988.

13. Kane, Thomas J. and others. "Potential for coherent Doppler Wind Velocity Lidar Using Neodymium Lasers," Applied Optics, 23: 2477-2481 (1 August 1984).

14. Kniezys, F.X. and others. Atmospheric Transmittance/ Radiance: Computer Code LOWTRAN 6. AFGL-TR-83-0187 Hanscom AFB, Massachusetts: Air Force Geophysics Laboratory. 1 August 1983.

15. Lawder, Timothy J. Specification for an Infrared Satellite Surveillance System for the Detection of Aircraft. MS thesis, AFIT/GSO/ENP/87D-1. School of Engineering, Air Force Institute of Technology (AU), Wright-Patterson AFB OH, November 1987.

16. Luke, Dr. Theodore E. Professor of Physics. Personal interview. Air Force Institute of Technology, Wright-Patterson AFB OH, April 1988.

17. McManamon, Dr. Paul. "Light Weight Laser Radar." Memorandum for Record. AFWAL Wright-Patterson AFB OH, 6 January 1988.

18. McManamon, Dr. Paul, AFWAL/AARI-2. Personal Interview. Wright-Patterson AFB OH 6 May 1988.

19. Preliminary User Instructions for FASCOD2 Handout # 11 from the 1987 Conference on LOWTRAN and FASCODE held at Wright-Patterson AFB OH by Mr. Ron Rodney, AFWAL Staff Meteorologist 1 October 1985.

20. Rodney, Ronald, AFWAL Staff Meteorologist. Telephone conversation Wright-Patterson AFB OH 21 Nov 1988.

21. SAS® Introductory Guide, third edition. Cary, NC: SAS Institute Inc., 1985.

22. Seyrafi, Khalil. Electro-Optical Systems Analysis, third edition. Los Angeles: Electro-Optical Research Company, 1985.

23. Skolnik, Merrill I. Introduction to Radar Systems. New York: McGraw-Hill Book Company, 1962.

24. Slater, Philip N. Remote Sensing Optics and Optical Systems. Reading, Massachusetts: Addison-Wesley Publishing Company, 1980.

25. Sliney, David and Myron Wolbarsht. Safety with Lasers and Other Optical Sources. New York:Plenum Press, 1980.

26. Stimson, George W. _Introduction to Airborne Radar_.
    Hughes Aircraft Company  El Segundo,California, 1983.

27. Weigand, Kirk and Jim Blake, Lt.   AFWAL/AAWP-3
    Personal Interview. Wright-Patterson AFB  25 Oct 1988.

## VITA

Captain Scott P. Simmons was born in Darby, Pennsylvania on 3 September 1957. He lived in Springfield, Pennsylvania until 1975, when he graduated from high school and entered the United States Air Force Academy. He received a Bachelor of Science degree in Electrical Engineering and obtained his commission in 1979. He subsequently entered Undergraduate Navigator Training at Mather AFB, California and received his wings in 1980. Captain Simmons was assigned to the 55th Strategic Reconnaissance Wing, Offutt AFB, Nebraska were he served as an instructor and evaluator in RC-135s. In 1984, Captain Simmons was assigned to Headquarters Strategic Air Command, also at Offutt AFB, where he worked on the B-1B program as an avionics engineer. In 1987, he entered the School of Engineering, Air Force Institute of Technology for graduate studies in Space Operations.

# REPORT DOCUMENTATION PAGE

Form Approved
OMB No. 0704-0188

| 1a. REPORT SECURITY CLASSIFICATION | 1b. RESTRICTIVE MARKINGS |
|---|---|
| UNCLASSIFIED | |

| 2a. SECURITY CLASSIFICATION AUTHORITY | 3. DISTRIBUTION / AVAILABILITY OF REPORT |
|---|---|
| 2b. DECLASSIFICATION / DOWNGRADING SCHEDULE | Approved for public release; Distribution unlimited |

| 4. PERFORMING ORGANIZATION REPORT NUMBER(S) | 5. MONITORING ORGANIZATION REPORT NUMBER(S) |
|---|---|
| AFIT/GSO/ENP/88D-5 | |

| 6a. NAME OF PERFORMING ORGANIZATION | 6b. OFFICE SYMBOL (If applicable) | 7a. NAME OF MONITORING ORGANIZATION |
|---|---|---|
| School of Engineering | AFIT/ENP | |

| 6c. ADDRESS (City, State, and ZIP Code) | 7b. ADDRESS (City, State, and ZIP Code) |
|---|---|
| Air Force Institute of Technology Wright-Patterson AFB OH 45433-6583 | |

| 8a. NAME OF FUNDING / SPONSORING ORGANIZATION | 8b. OFFICE SYMBOL (If applicable) | 9. PROCUREMENT INSTRUMENT IDENTIFICATION NUMBER |
|---|---|---|
| | | |

| 8c. ADDRESS (City, State, and ZIP Code) | 10. SOURCE OF FUNDING NUMBERS | | | |
|---|---|---|---|---|
| | PROGRAM ELEMENT NO. | PROJECT NO. | TASK NO | WORK UNIT ACCESSION NO. |
| | | | | |

11. TITLE (Include Security Classification)

ANALYSIS OF SPACE-BASED LIDAR FOR AIRCRAFT TRACKING

12. PERSONAL AUTHOR(S)
Scott P. Simmons, Capt, USAF

| 13a. TYPE OF REPORT | 13b. TIME COVERED | 14. DATE OF REPORT (Year, Month, Day) | 15. PAGE COUNT |
|---|---|---|---|
| MS Thesis | FROM _____ TO _____ | 1988 December | 135 |

16. SUPPLEMENTARY NOTATION

| 17. | COSATI CODES | | 18. SUBJECT TERMS (Continue on reverse if necessary and identify by block number) |
|---|---|---|---|
| FIELD | GROUP | SUB-GROUP | Optical Detection |
| 17 | 05 | 01 | Optical Radar |
| | | | Laser Tracking |

19. ABSTRACT (Continue on reverse if necessary and identify by block number)

Thesis Advisor: Major David Stone
Department of Physics

Approved for release in
Accordance with AFR 190-1
12 Jan 1989

| 20. DISTRIBUTION / AVAILABILITY OF ABSTRACT | 21. ABSTRACT SECURITY CLASSIFICATION |
|---|---|
| ☒ UNCLASSIFIED/UNLIMITED ☐ SAME AS RPT. ☐ DTIC USERS | UNCLASSIFIED |

| 22a. NAME OF RESPONSIBLE INDIVIDUAL | 22b. TELEPHONE (Include Area Code) | 22c. OFFICE SYMBOL |
|---|---|---|
| David Stone, Major, USAF | (513) 255-2012 | ENP |

DD Form 1473, JUN 86     Previous editions are obsolete.     SECURITY CLASSIFICATION OF THIS PAGE